NASA CR-159757

EXHAUST EMISSION REDUCTION

For

INTERMITTENT COMBUSTION

AIRCRAFT ENGINES

(NASA-CR-159757) EXHAUST EMISSION REDUCTION FOR INTERMITTENT COMBUSTION AIRCRAFT ENGINES (Avco Lycoming Div.) 114 p HC A06/MF A01 CSCL 21E
N80-14130
Unclas
G3/07 46489

By: R.N. Moffett

AVCO CORPORATION
AVCO LYCOMING WILLIAMSPORT DIVISION

prepared for

NATIONAL AERONAUTICS AND SPACE ADMINISTRATION

NASA LEWIS RESEARCH CENTER
CONTRACT NAS-19754

October 1979

FOREWARD

AVCO Lycoming conducted the research described in this report under NASA Contract NAS3-19754. The NASA Project Manager was Mr. P. Meng of the Lewis Research Center.

The program, aimed at improving fuel economy and exhaust emissions in piston aircraft engines, consisted of three main study areas: Advanced Ignition Concepts, Ultrasonic Fuel Atomization, Variable Valve Timing. AVCO Lycoming was assisted by two subcontractors: Bendix Electrical Components Division, which was responsible for providing both hardware and technical assistance during the ignition concepts study, and Autotronics Controls Corporation, which provided the Post Carburetion Atomization unit employed during the ultrasonic fuel atomization study.

This report was originally issued as AVCO Lycoming Report Number 3538.

TABLE OF CONTENTS

LIST OF TABLES

LIST OF FIGURES

LIST OF FIGURES - (Contd.)

LIST OF FIGURES - (Contd.)

BACKGROUND

Optimum performance and fuel economy with minimum exhaust emissions are necessary and desirable characteristics of the modern piston aircraft engine. The ongoing development of new or improved technology constantly alters the limiting parameters affecting these goals. A continuous process of re-examination and updating is required to maintain stride with this progress. To this purpose, AVCO Lycoming was contracted by NASA to conduct a major research program aimed at the application of improved technology in this area.

Contributing to the need for this program was the establishment of exhaust emission standards for newly manufactured piston aircraft engines. The requirements were published in the Federal Register (Volume 38, No. 136, July 17, 1973), by the U. S. Environmental Protection Agency and were proposed to become effective December 31, 1979.

In view of the established exhaust emission standards the investigation of possible techniques to reduce the quantity of pollutants in the nature of carbon monoxide (CO), unburned hydrocarbons (HC), and oxides of nitrogen (NO_x), emitted from piston aircraft engines was initiated. These first attempts at pollutant reductions were aimed at variations in engine controllable parameters such as fuel-air ratio and ignition timing. However, drawing on the automotive experience gained from the late 1960's, excessive leaning of piston engines can produce engine stumble and hesitation, not to mention decreasing fuel economy. Adding the concern for diminishing fuel reserves, the importance of investigating new engine concepts that utilize radically different operating parameters became important if the standard were to be met. Specifically it was proposed that new concepts of piston aircraft engines or their operation beyond simple leaning or ignition timing changes be investigated as a method to reduce exhaust pollutant emissions. In addition, these studies were to be directed so as to retain or improve the fuel consumption, flight safety, etc., at the levels of engines of current design.

The scope of this contract was to design and test modifications to an AVCO Lycoming aircooled, reciprocating piston aircraft engine(s) and its components to determine their effects on exhaust gas emissions and fuel consumption, as well as cost, weight, performance and safety of flight aspects. This work encompassed one major and two minor changes to the selected engine(s).

Specifically, the objectives of this investigation were:

a) To document the pollutant yields, namely total unburned hydrocarbons, carbon monoxide and oxides of nitrogen, generated by AVCO Lycoming aircraft engines. Test engines were both current production models utilizing modified accessories and components and a prototype engine incorporating a major variation from current design practices.

b) To determine the effectiveness of each modification with respect to specific fuel consumption and engine exhaust emissions.

c) To further relate the effectiveness of each pollutant reduction modification in terms of safety, cost, weight, and any other significant factors that may be detrimental to the operation and maintenance of general aviation aircraft.

The programs, as outlined, involved the design and procurement of experimental hardware, and the testing and further development of each respective concept. The results of the primary development process were then to be evaluated as to their effectiveness at satisfying the initial concept selection criteria and whether further effort toward developing the experimental hardware into certified production items was justified.

Three specific concepts were chosen, based on their potential benefit at improving one or more of the designated criteria. The areas selected, as well as the rationale which was employed to determine their selection, are as follows:

1) Variable Valve Timing - To produce a specified power output at high engine speed, increased valve overlap is utilized with the result that at low engine speeds, high pollutant levels and BSFC's may be experienced. A system which would permit the optimization of valve overlap at both high and low speed conditions should provide a benefit in engine performance, economy and exhaust emissions.

2) Ultrasonic Fuel Vaporization - Liquid fuel droplets in the intake charge can lead to poor cylinder to cylinder fuel distribution and uneven combustion. Improved fuel vaporization should reduce pollutants and improve brake specific fuel consumption.

3) <u>High Energy - Multiple Spark Discharge and Spark Plug Tip Penetration</u> - The leaner mixtures required for reduced emissions and improved specific fuel consumption impose greater demands on the ignition system. Positive ignition of the intake charge is required to satisfy these requirements.

The following report covers the activities conducted under NASA Contract Number NAS3-19754. For clarity, it has been divided into three major subsections representing the respective study areas.

IGNITION CONCEPTS

INTRODUCTION

Acceptable operation at progressively leaner fuel/air mixtures is the major vehicle for both reducing exhaust pollutant concentrations and improving fuel economy in a spark ignited internal combustion, piston aircraft engine. Since it is more difficult to initiate and sustain combustion with leaner mixture ratios, a positive ignition of the intake charge is necessary. This may also reduce cycle to cycle combustion variations and extend the lean misfire limit. Positive ignition of leaner mixtures conceptually requires an increased spark plug demand voltage (potential necessary to ionize gases between electrodes with subsequent spark discharge) and can be affected by the location and propogation of the initial spark in the combustion chamber. An improvement in ignition quality which benefits or extends engine operation at leaner mixtures should provide a reduction in engine exhaust emissions and/or engine specific fuel consumption.

The five basic ignition systems which were investigated for their sole or combined effect on pollutant emissions and fuel economy were:

1) Standard ignition (magneto) system.
2) Extended electrode spark plugs.
3) Staggered spark timing.
4) Texaco multiple spark system.
5) Capacitive discharge ignition system.

Using the standard ignition system as a baseline, comparative surveys (both emissions and performance) were conducted to identify possible and significant improvements with other ignition system configurations. Where applicable, and in addition to monitoring emissions and performance parameters, oscilloscope traces of spark plug demand voltages versus crankshaft rotation angle were recorded to compare the operational characteristics of the various systems. The operational modes examined corresponded to those specified for the proposed Federal Exhaust Emissions Cycle for Piston Aircraft Engines.

TEST EQUIPMENT

Engine: The AVCO Lycoming aircraft engine model TIGO-541-D1BD is a horizontally opposed, turbocharged, fuel injected, air cooled aircraft engine with a gear driven propeller shaft, top side induction and down exhaust. The engine crankcase is designed to incorporate side mounted accessory drives and accessories. Each of the six cylinders has a bore of 13.02 cm (5.125 inches) and a piston stroke of 11.11 cm (4.375 inches), which yields a total piston displacement of 8875.19 cu cm (541.5 cubic inches). The specified compression ratio is 7.3:1 and standard ignition timing is 20° BTC. Minimum recommended grade fuel is 100 LL aviation gasoline. The fuel is metered through a Bendix servo regulator, continuous flow type, RSA-10DB2 fuel injector. The proposed engine rating for this model is 335.3 Kw (450 BHP) at 3200 RPM at 163.4 KPa (48.4 In. Hg) manifold pressure and .458 Kg/Kw-Hr (.750 Lbs/BHP-Hr) BSFC at sea level conditions. However, for these comparative tests 152.0 KPa (45 In. Hg) manifold pressure at .427 Kg/KW-Hr (.700 Lbs/BHP-Hr) BSFC producing 316.6 Kw (426 HP) was used to simulate the most commonly utilized production configuration.

Ignition Systems: The standard ignition system, as tested, consisted of a Bendix D6RN-2230 magneto, P/N L-17627-216. This unit was modified so that the low side of the secondary winding of the output coil was grounded externally in order to use a current probe to measure the secondary winding current. This was a single drive dual magneto, which energized two spark plugs per cylinder through a shielded harness. One of the recommended spark plugs for this engine, the Champion RHB-36W, a fine wire electrode type plug utilizing iridium alloy materials, was selected as the standard or baseline spark plug. The RHB-36W spark plug electrode gap was specified to be .46 mm (.018 inch) to .51 mm (.020 inch) and was set to a nominal .48 mm (.019 inch) for the baseline tests. The standard ignition system was also tested with used standard spark plugs. These were also Champion RHB-36W spark plugs, which were returned from service after 107 hours of operation. The used spark plugs had moderately rounded edges on the electrodes and the gap was .64 mm (.025 inch), which was considered typical of used spark plugs.

The standard spark plug and the two configurations of extended electrode spark plugs which were tested are shown on Figure 1, page 61. The fine wire electrodes of the standard spark plug are approximately flush with the face of the spark plug. The extended electrode spark plugs were of the massive electrode type with the two ground electrodes and the center electrode extended into the combustion chamber 6.4 mm and 12.7 mm (¼ and ½ inches) respectively, over the standard plug. The chosen gap for the extended electrodes was .46 mm to .51 mm (.018 to .020 inch). Except for the extended spark plugs, the remainder of the ignition system was held in the standard configuration for these studies. The 6.4 mm (¼ inch) extended tip plugs were also tested a second time as simulated used spark plugs after the gap had been adjusted to .64 cm (.025 inch).

Piston aircraft engines have two spark plugs per cylinder located in the top and bottom of the combustion chamber usually timed to fire at the same time. However, three purposely staggered ignition timings were investigated. For this portion of the testing the same standard magneto unit energized a special harness which fired all the top spark plugs with the right magneto and all the bottom spark plugs with the left magneto. To obtain a staggered timing with the top plug firing at 25° BTC and the bottom plug firing at 20° BTC, one set of breaker contacts was adjusted to open 5° earlier (more advanced) than the standard (20°). This configuration was then reversed to obtain a staggered firing with the top plug at 20° BTC and the bottom plug at 25° BTC. In the same manner, additional staggered firings of 15° and 25° BTC were evaluated. This procedure maintained electrode coverage in the distributor and the magneto still had ample output voltage.

Three capacitive discharge (C-D) ignition systems were tested. These systems consisted of a Bendix S-1800 magneto which is a breakerless type magneto normally used on industrial engines, with the timing controlled by a rotor with vanes passing an electro-magnetic pickup coil. The magneto was modified to allow the value of the tank capacitance and tank capacitor voltage to be varied in discrete increments from 0.5 to 4.0 microfarads and 50 to 300 volts, respectively. The C-D magneto was used with two different output coils. The first coil tested (Bendix 10-57460) provided a long spark duration of about 100 micro seconds. The long duration coil was tested with an initial capacitance and voltage of 4 microfarads with 300 volts and a follow-on combination of 4 microfarads with 200 volts. The second coil tested (Bendix 10-372385) produced a short spark duration of 10 micro-seconds. The test program with the short duration coil was accomplished with a capacitance and voltage of 4 microfarads and 250 volts. When the tank capacitance and capacitor voltage were less than these minimum values, misfires were found to occur.

The multiple spark ignition system was provided in cooperation with Texaco and consisted of two Texaco units - a model 015-19 control unit and a model 010-6 power unit. These units required 24 volt DC power, which was supplied by a battery and a high capacity charger. This system employed a Bendix D-2000 magneto housing which was modified to serve as a distributor and timing device. The system was essentially a high voltage oscillator which was turned on by the breaker points in the magneto housing and then turned off after oscillating for a predetermined number of crankshaft degrees. The duration of oscillation was adjustable from 20° to 35°. The frequency of the oscillations (multiple sparks) was approximately 1100 sparks per second. The system was tested at two spark durations; 20° and 35° (crankshaft degrees).

METHOD OF TEST

The TIGO-541-D1BD engine, S/N L-806-X, included the following special instrumentation:

a) The crankshaft gear spline was strain gaged to enable engine torque to be measured. This torquemeter arrangement had been previously calibrated on a dynamometer. The signal from the strain gages was relayed from the engine through a set of internal slip rings and was read-out on a Bean strain indicator.

b) A special three tooth gear was mounted on the rear of the crankshaft to trigger a magnetic pickup inside the crankcase and generate an electrical pulse at 15° BTC for each cylinder. This timing signal was used to calculate the dynamic spark timing of the engine by measuring the interval between the spark occurence and the crankshaft pulse on a two channel memory oscilloscope.

c) An exhaust system was installed which permitted the measurement of exhaust emissions. The turbocharger and wastegate outlets were ducted into a common collector to permit total engine exhaust flow sampling. An exhaust emissions sampling probe was inserted into this collector which routed combustion gases via a heated sample line to the exhaust analysis console. The sample probe was a 3.2 mm (1/8 inch) ID tube with one end closed and was positioned to extend almost completely across the 10.2 cm (4.0 inch) collector pipe diameter. The sample probe had five 1.6 mm (1/16 inch) holes equally spaced along its length aligned into the exhaust flow to admit gases into the sample system. The tailpipe extended approximately .61 m (two feet) beyond the location of the sample probe. A thermocouple was also inserted into the exhaust gas near the sample probe so that the temperature could be monitored at that point.

The spark plug demand voltages were measured throughout the tests on a storage oscilloscope. The characteristic waveform of each ignition system was determined and it was evident when a positive spark was not produced. In addition, the dynamic spark timing could be measured. To account for temperature variations within the engine, the four spark plugs in cylinders 4 and 6 were the sites chosen for this investigation. The demand voltage was recorded by photographing the wave form on a storage oscilloscope. A current probe was used to attempt to calculate spark energy, but due to the restrike wave form during the system discharge, the spark energy could not be accurately determined.

To insure that the spark plugs were the correct heat range for the various ignition systems, the spark plug electrode temperatures were measured on all the ignition systems. The temperatures were measured using special spark plugs which had a thermocouple imbedded in the insulator around the center electrode. The four thermocoupled spark plugs were located in cylinders 3 and 5.

The emissions console used by AVCO Lycoming to analyze the engine exhaust was fabricated by Beckman Instruments. It consists of a pump located inside the console which draws exhaust from the sample probe through a heated transfer line. From the pump the exhaust is distributed to the following five separate analyzers:

a) Carbon monoxide, Beckman Model 864, NDIR Type.

b) Carbon dioxide, Beckman Model 865, NDIR Type.

c) Oxides of nitrogen, Beckman Model 951-H, Chemiluminescent Type.

d) Hydrocarbons, Beckman Model 402, FID Type.

e) Oxygen, Beckman Model F3, Magnetic Susceptibility Type.

The analyzers were calibrated daily using reference gases. To provide for instrument and engine stabilization the exhaust was sampled and monitored for about three minutes at each point. A schematic of the emissions console is shown on Figure 2, page 62.

The testing was conducted on a propeller test stand. The engine was given a 1½ hour run-in following approximate theoretical propeller load power settings. Table I lists the 13 ignition system variations tested.

For each ignition configuration tested, constant speed, leanout runs were made at the five nominal power settings listed in Table II. Within the propeller test stand limitations, these settings correspond to the five modes specified in the Federal Cycle for piston aircraft emissions. The fuel mixture was leaned from full rich through stoichiometric fuel-air ratio in approximately equal fuel flow decrements to give four or five data points per leanout and the manifold pressure was held constant throughout the leanout except for idle and taxi modes. The cylinder head temperature was limited to

260°C (500°F) maximum and, although the specified limit for the turbine inlet temperature is 899°C (1650°F), this limit was waived in order to allow leaning through stoichiometric fuel-air ratios. Turbine inlet temperatures of up to 982°C (1800°F) were encountered.

RESULTS:

Figures Number 3 through 7, pages 63 through 67, show the emissions data for the five modes tested and include data for each of the five ignition systems examined. It should be noted that there were no correction factors supplied to these data to compensate for variations of ambient conditions, or to adjust pollutant mass rates for differences in observed power output. Therefore, some scatter within the data may not be a result of the system under test, but more a function of the actual ambient conditions encountered. The range of data on each curve is shown as a band. No single ignition system configuration tested resulted in a consistent or significant improvement in either emissions or fuel economy over the standard magneto system.

At the Approach Mode, the range and relative accuracy of the airflow meter were such that errors were induced into the fuel/air ratio measurements. These discrepancies caused a shifting of the curves, left and right, on the X-axis, resulting in a wide data band. To resolve this condition, as shown on Figure 5, page 65, the results have been plotted using the calculated fuel/air ratio (determined by an adaptation of the Spindt calculation) rather than the measured value. With the data plotted in this manner, the CO emissions results from all of the ignition system configurations tested falls into a narrow band. Some significant variations were apparent in HC emissions, however, these differences were not consistent at other modes.

The measured exhaust emissions at the idle and taxi modes tended to form wider data bands. The low fuel and airflows which dictated precise measurement coupled with unstable engine operation resulted in an increase in potential experimental error. Again, however, none of the ignition systems evaluated resulted in a consistent improvement over the standard system.

Table I summarizes the spark duration and voltage trends for all the ignition configurations tested at each of the five power modes. The data lists the maximum spark plug demand voltage at each condition and the total time of the spark duration, including any restrikes.

Details of the demand voltage for the various ignition systems are provided on Figures 8 through 13, pages 68 through 73. The demand voltage trace patterns of the 6.4 mm (¼ inch) extended electrode spark plugs were similar to the standard electrode plug, and are shown on Figures 8 through 10, pages 68 through 70. The figures are labelled for run number, mode, position and ignition system configuration. The near vertical trace lines show the measured spark plug electrode voltage rising until sufficient energy was available to ionize the gas between the spark plug electrodes, thereby causing the discharge, or spark, to occur. The voltage discharge occurred so rapidly that no restoration trace was shown to the zero voltage line. Subsequent restrikes were generally at lower voltages, although occassionally a higher voltage restrike was observed. When a gradual decay of the voltage was found, such as the final voltage rise and decay shown in most of the photographs, no restrike spark had occurred. At certain conditions, as many as 25 restrikes were noted, resulting in spark duration of up to 35° crankshaft angle.

Demand voltages with the 6.4 and 12.7 mm (¼ and ½ inch) extended electrode plugs were slightly lower than with the standard plugs (see Table I). It was felt that this was due to the sharper edge on the extended ground electrodes; the voltages would probably be equal when the sharp edges had eroded. With the staggered spark timing system, the second spark plug to fire required a higher demand voltage, most likely due to the increased cylinder pressure. Photographs taken of the demand voltage traces of both spark plugs in the same cylinder (Figure 11 page 71) indicated up to 35° continuous spark available for ignition with the staggered timing configuration.

The typical demand voltage pattern for the capacitive discharge system is shown on Figure 12, page 72. As illustrated, the C-D systems characteristically delivered predominantly a single spark with only infrequent restrikes. The demand voltages were not significantly different from the standard system, but the spark duration was significantly less (see Table I, page 53) With the long duration coils (10-57460) the spark duration was approximately one tenth of the standard system. The spark duration with the short duration coils (10-372385) was about one hundredth that of the standard system. Lower energy values for the C-D system than those tested would not provide sufficient output voltage to meet the spark plug demands for producing a dependable spark.

The waveform of the multiple spark system is shown on Figure 13, page 73. Since the system was essentially a high voltage oscillator, the breakdown voltage alternated polarity for each spark. Random restrikes were unusual, as evidenced by the periodic waveform depicted on the photograph. It was noted that the spark duration was erratic due to open circuiting of some of the output pulses. (At higher speeds and loads, the voltage supplied to the spark plug appeared marginal in that some misfiring occurred.) The Texaco ignition system was not designed to operate with the capacitance load that the shielded ignition harness imposed upon it. However, sufficient data was obtained to determine that for up to 35° spark duration, no effect upon engine performance or emissions was apparent at any mode. The 35° duration was only tested at the Approach, Taxi and Idle modes, where the most benefit of the increased duration was expected.

Spark plug tip temperatures were recorded throughout the tests. Spark plug temperatures increased and peaked during a leanout similar to the trends defined by cylinder head temperatures. The standard spark plugs had a suitable heat range for all of the ignition systems. From experience, at approximately 816°C (1500°F) the electrodes begin to burn and preignition may occur. This temperature was rarely reached during these tests. Below 260°C (500°F) lead deposits and oil fouling may occur. During idle the spark plug temperatures were often below 260°C (500°F), but the engine was not operated at this condition for extended periods. The 6.4 and 12.7 mm (¼ and ½ inch) extended electrode spark plugs operated within similar temperature values.

DISCUSSION

Various configurations of ignition systems were evaluated which supplied the required demand voltage to the spark plugs at several timings and rates of voltage rise. The magnitude and trend of the voltage characteristics were dependent on the spark plug requirement (i.e. gap) and the prevailing conditions inside the combustion chamber. For example, demand voltage increases with an increase in charge density within the combustion chamber. Therefore, an increase in manifold pressure, or a retardation of spark timing tends to increase demand voltage. In addition, as the fuel/air mixture is leaned beyond approximately best power mixtures, the demand voltage also increases. Spark plug electrodes with reduced gap or sharp edges also decrease demand voltage. Table III, page 54, shows a summary of these trends and is derived from Table I.

The restrike phenomena observed with the standard magneto ignition system may be attributed to, in part, the turbulence within the combustion chamber repeatedly interrupting, or extinguishing, the spark. After the initial spark, the gases in the vicinity of the spark plug electrodes are ionized, which permits restrikes to occur at lower demand voltages. Bench testing, conducted at Bendix with simulated combustion chambers where no turbulence or combustible mixture was present, have not shown this restrike phenomena. Under those conditions, the voltage discharge at the electrodes occurred only once, resulting in a longer continuous spark from which it was possible to measure spark energy. The rapid restrike phenomena encountered during the AVCO Lycoming testing precluded this measurement of spark energy.

The 6.4 and 12.7 mm (¼ and ½ inch) extended electrode spark plugs had the potential benefit of locating the spark further from the boundary effects of the combustion wall for more positive ignition. Due to their location, the electrodes of these extended spark plugs were subjected to two possible opposing conditions, possibly of different magnitudes than the standard plugs. The extended electrodes were:

a) exposed to a cooling effect from the incoming fresh intake charge; and

b) exposed to a heating effect from the heating gases during the combustion process.

Overall, these two factors appeared to cancel each other in this particular cylinder head configuration. A determination as to what detrimental effect that this heating and cooling cycle, if it existed, would have on spark plug life or electrode erosion was not made.

The concept of staggered spark timing was to lengthen the interval of actual spark plug firing over the combustion cycle. A direct consequence would be a lengthening of the combustion duration since the flame front from the first spark would travel further. This could reduce the rate of pressure rise and peak pressures in the combustion chamber reducing both the torsional vibrations of the rotating system and possibly exhaust emissions, especially HC, because of higher exhaust gas temperatures. With the second spark plug firing a few degrees later, the safety feature of the dual ignition system was essentially retained. However, as evidenced by the emissions data depicted, the influence of the staggered spark timing was not recognizable as a definite improvement in engine parameters. The torsional aspect of staggered timing was therefore not investigated.

The capacitive discharge systems tested displayed a much more rapid rise of the demand voltage than the standard magneto system. The more sudden rise in voltage theoretically would fire a fouled spark plug when the standard system would not. After the initial spark the capacitor system did not contain enough energy to support restrikes as was common of the other systems. The total spark duration with long duration coils was 1/10 that of the standard system, and the short duration coil system was only 1/100 as long. The demand voltages were approximately equal to that of the standard system. The C-D systems tested produced a reliable spark and positive ignition, provided adequate energy levels were maintained.

The Texaco multiple spark ignition system provided a series of sparks throughout a fixed crankshaft rotation angle regardless of speed. The duration was adjustable from 20° to 35° (crankshaft degrees). During engine operation that required high demand voltage, many of the oscillations displayed an open circuit condition which caused the duration to vary. The open circuit was caused by lack of sufficient energy to charge the capacitance load that the shielded harness imposed. Texaco personnel stated that through appropriate design the system could be modified to correct this problem in the future. The potential advantage of the multiple spark system was simply that a positive spark existing over a longer period of time allowed a greater opportunity to ignite a mixture in the combustion chamber.

The 35° spark duration was only tested at the idle, taxi and approach modes, since the lower engine speeds would show the most benefit of prolonged duration, and because the Texaco ignition system may not have had the capacity to supply the demand voltage at high power settings.

CONCLUSIONS

None of the ignition systems configurations tested yielded an improvement in engine performance, fuel economy, or exhaust emissions when compared with the standard magneto ignition system. From these data the performance, economy and emissions of the AVCO Lycoming TIGO-541-D1BD engine do not appear to be limited by the ignition spark duration or energy.

The standard magneto proved capable of supplying the highest demand voltages required with no apparent indication of marginal performance for all modes tested. The standard system spark duration, due to the restrike phenomena, was comparable to the multiple spark system with 20° duration. This was one of the ignition system characteristics which, at the outset of the program, was thought to have been desirable. However, since the capacitive discharge system with its very short, single spark duration, showed the same data trends as other systems with long spark durations of many crankshaft degrees, it was concluded that the fuel mixture usually ignited upon the initial spark, making many of the restrikes unnecessary. If a delay in the charge ignition existed, it was too small or inconsistent to be detected by variations of the standard engine monitors (primarily performance and emissions). The effectiveness of the standard ignition system (as well as the other systems evaluated) in obtaining satisfactory charge ignition was probably aided by the two spark plugs per cylinder typical of the aircraft piston engine.

ULTRASNOIC FUEL VAPORIZATION

INTRODUCTION

An important factor in the fueling of a carburetted engine is the extent of fuel atomization in the intake manifold. Poor breakup of fuel in the intake charge can lead to excessive cylinder to cylinder mixture distribution variations which are manifested as unsatisfactory engine performance, economy, acceleration and/or emissions. The requirement for leaner mixtures to promote emissions control and fuel economy dictates the need for good mixture distribution to maintain satisfactory engine performance characteristics.

Horizontally opposed piston aircraft engines with their exposed intake pipes are conceptually more sensitive to induction system fuel condensation than their automotive counterparts. Such alternatives as heating the intake charge and/or the induction system have been historically disregarded for piston aircraft engines due to the inherent loss in the maximum power output.

As an alternative to induction system heating it was proposed to investigate an ultrasonic fuel atomizer or post carburetor atomizer (PCA) on a carburetted piston aircraft engine to determine if:

1) vaporizing fuel droplets in the intake charge could measurably improve mixture distribution; and
2) such an improvement in mixture distribution could permit operation at leaner mixtures, thereby improving fuel economy and exhaust emissions.

The program was established to include engine performance, fuel economy and exhaust emissions considerations as criteria in the evaluation of this concept. The PCA unit was developed and provided by Autotronic Controls Manufacturer.

DEFINITION OF TERMS

Definition of the following engine configuration terms are provided since they are used frequently in the text:

a) Standard engine - Engine without the PCA.

b) PCA installed - The PCA was installed, but the unit was not electrically activated and the atomizer tube was not vibrating.

c) PCA operating - The PCA was installed and electrically activated.

d) PCA rotated - This describes the PCA mounted in other than the standard position. This position was recommended by Autotronic Controls, based on their preceding testing. Alternate positions were obtained by rotations of 90° increments clockwise when viewed from the top of the engine.

e) Carburetor S/N X03 - Pepperbox fuel nozzle (multiple orifices), Marvel Schebler Model MA-4SPA, Setting No. ACX-2579.

f) Carburetor S/N A-40-20036 - straight fuel nozzle, Marvel Schebler Model MA-4SPA, Setting No. 10-3678-32.

DESCRIPTION

The AVCO Lycoming Model O-320-E2D is a four cylinder, horizontally opposed, air cooled, direct drive, normally aspirated aircraft engine. The bore and stroke are 13.02 cm and 9.84 cm (5.125 and 3.875 inches) respectively, resulting in a displacement of 5241.5 cu cm (319.8 cubic inches). The carburetor is an updraft type, Marvel Schebler Model MA-4SPA mounted below the oil sump. The spark timing is 25° BTC and the compression ratio is 7.0:1. The minimum grade aviation fuel specified for this engine model is 80/87 octane. The engine has a full throttle rating of 111.8 Kw (150 BHP) at 2700 RPM, .336 Kg/Kw-Hr (.55 Lb/BHP-Hr) BSFC, at standard day, sea level conditions.

The post carburetor atomizer (PCA) consisted of a venturi flow nozzle formed by two inserts positioned to produce directional flow in a plane perpendicular to the axis of the atomizer tube. The external dimensions of the PCA formed a cube approximately 8 cm (3 inches) on a side with a flange on the top and bottom providing "bolt on" installation between the carburetor and intake manifold. The incorporation of the PCA lengthened the intake manifold by approximately 9 cm (3½ inches). A photograph and a cross sectional schematic of the PCA are shown in Figures 14 and 15, page 74.

The PCA was designed to utilize ultrasonic vibrations to atomize liquid fuel drops downstream of the carburetor into droplets of 20 microns or less in diameter. The PCA and the electronic driving and control units were developed and supplied by Autotronic Controls Corporation. This development included optimizing the venturi for maximum directional control of the fuel-air mixture flow with minimum wall "wetting" and designing the atomizer tube to resonate at maximum effective frequencies. The basic PCA operating frequency was approximately 64,000 Hz. A plexiglass window located at the end of the atomizer tube allowed observation of the atomization process during testing.

For characterization of the individual cylinder combustion parameters an exhaust sampling system was used which consisted of a 46 cm (18 inch) straight exhaust pipe for each cylinder with a provision for an individual emissions sample probe. A schematic of the system is shown in Figure 16, page 75. The four sample lines then ran to individual solenoid valves, into a common heated sample line, and then to the emissions console. The exhaust emissions from each cylinder, or the total engine, could be analyzed by activating the appropriate selected solenoid valves.

METHOD OF TEST

Testing was conducted on both dynamometer and propeller test stands. Baseline engine performance and emissions data were obtained to characterize the standard engine. Two model carburetors with different fuel metering nozzles were tested. One unit employed a straight metering injection tube with a single orifice at its end. The other unit, designated a "pepperbox" nozzle configuration, had 18 small orifices located radially around the end of the tube. Depending on the engine model and induction system configuration, it has been found by AVCO Lycoming that the two units can produce distinct differences in mixture distribution quality. Since it was the intent of this program to determine the effect of the PCA on mixture distribution, the carburetor with the most diverse distribution was examined to afford a clear demonstration of the unit.

The PCA was evaluated in three installed configurations; atomizer tube parallel to throttle butterfly (standard orientation - see Figure 15) and rotated 90° and 180°, respectively. Testing was conducted with the PCA installed but not activated as well as with the unit operating.

The standard and PCA equipped engine configurations were evaluated at power conditions generally corresponding to those specified in the Federal Exhaust Emissions Cycle for Aircraft Piston Engines. Dynamometer testing at the idle mode was not conducted since mixture distribution and power output data at idle tend to be erratic. Taxi mode trends are normally very similar to idle, but due to a more favorable speed/inertia condition related to the dynamometer, the data quality is more repeatable.

The following listing summarizes the performance runs which were conducted to evaluate the three basic engine/fuel system configurations (standard engine, PCA installed but not activated, PCA operating):

a) Full Throttle Performance - Engine speed (RPM) was varied at a constant full throttle setting and best power fuel mixture.

b) Bare Carburetor Run - Engine speed (RPM) was varied at a constant full throttle setting with all ducts removed from the carburetor entrance and all blowers turned off to provide relatively stagnant air at the carburetor inlet. The purpose of this run was to obtain manifold pressure data for the basic engine, which was subsequently used to correct observed horsepower to standard conditions.

c) Mixture Distribution - The fuel flow was varied from full rich through best economy. Engine speed (RPM) and throttle setting were held constant. This type of run served as an indicator of fuel distribution to the cylinders by relating cylinder head temperature trends versus fuel/air ratio and served as the primary criterion used in evaluating the PCA.

d) Variable Manifold Pressure - The engine speed and the rated BSFC were held constant while the manifold pressure was varied. (NOTE: At low manifold pressures a best power mixture strength was used.)

e) Propeller Load Curve - The engine speed and power were varied in a proportion that simulated the power required to drive a fixed pitch propeller. The fuel mixture was held in full rich position, thereby demonstrating the fuel metering characteristics of the carburetor through a wide power range.

RESULTS

The results of the mixture distribution runs are summarized in Table IV, page 55. These runs were made with carburetor S/N X03, which was of the "pepperbox" nozzle configuration. For these data, the occurrence of the temperature maximum for each cylinder served as the indicator for mixture distribution. Ideally, for perfect mixture distribution, all cylinder head temperatures should peak at the same fuel flow. Table IV lists the difference in fuel flow between the richest and leanest cylinder as an indication of the mixture quality. The lower the magnitude of the value for Δ fuel flow, the better the relative distribution.

All of the part throttle runs were made by setting the throttle so that each engine configuration produced an equal power at .334 Kg/Kw-Hr. (.55 Lb/BHP/Hr) BSFC. The BHP's and BSFC's listed in Table IV for the part throttle settings are derived from the mixture distribution runs at the fuel flow specified in the "data type" column. This method compensated for changes in ambient conditions that affected the overall power developed by the engine. By setting the observed powers equal, the rate at which the power decreased when the mixture was leaned, provided a basis which could be used as a comparison. Theoretically an engine with good mixture distribution can be leaned with less loss in power than an engine with poor distribution, since none of the cylinders begin to misfire prematurely. It is shown in Table IV that only at 2430 RPM, 89.5 Kw (120 BHP), did the PCA significantly improve the mixture distribution; the BSFC and BHP were improved here also. At 2430 RPM, 78.3 Kw (105 BHP), the PCA did not improve the mixture distribution sufficiently to cause improved power or economy. At the two lowest power settings the PCA provided negligible difference in engine performance. At the full throttle power settings mixture distribution was slightly degraded with the PCA and the added intake airflow restriction of the PCA reduced the observed BHP. (Note that ambient conditions are not taken into account here.) There was generally no significant difference in any engine parameters between the PCA operating and PCA installed but not operating.

A similar summary of the results of the mixture distribution runs made with carburetor S/N A-40-20036 (straight nozzle) is shown in Table V, page 56. A comparison of Table IV and Table V shows that the overall mixture distribution was better with the "pepperbox" nozzle carburetor than the straight nozzle configuration. The comparison between the standard and PCA equipped engines was similar to that discussed for Table IV.

The full throttle performance run results are shown on Figure No. 17, page 76. This curve shows a 3-5% power loss due to the installation of the PCA. All the runs were made at the rated specific fuel consumption of .334 Kg/Kw-Hr (.55 Lb/BHP-Hr) BSFC, and the power data corrected to standard day, sea level conditions. The corrected manifold pressures are lower with the PCA installed, which accounts for the lower power.

Figure No. 18, page 77, shows the results of the propeller load run for the standard engine and the PCA operating. This curve shows that the PCA did not change the carburetor fuel metering schedule throughout the power range, as seen in the fuel/air ratio plot. As the airflow was restricted by the PCA, the carburetor compensated by decreasing fuel flow and maintaining approximately the same fuel/air ratio at each power setting.

Exhaust emissions measurements were made on individual cylinders and the total engine to establish any effect of the PCA. The variation in emissions from cylinder to cylinder reflects the differences in the fuel/air ratio of the mixture each cylinder receives. Commonly, carbon monoxide (CO) concentrations are surveyed since a nearly linear relationship exists with fuel/air ratios from rich conditions to near stoichiometric. A subsequent comparison of these indicated fuel/air ratios translates into the quality of the mixture distribution.

Figure No. 19, page 78, shows a summary of the results of the individual cylinder emission survey conducted at the take-off mode condition at a .075 fuel/air ratio. For comparative purposes, the data is shown as the difference between the maximum and minimum pollutant values for the four cylinders surveyed, divided by the full scale value of the range of the instrument. For example, Figure No. 19, page 78, shows that the total differential in CO emissions between the four cylinders was 36% of the full scale value. The installation of the PCA (non-operating) increased this spread to 64%; while activating the PCA resulted in a further increase to 96%. In this instance, the incorporation of the PCA resulted in an increase in the spread between the measured individual cylinder CO emissions with a related degradation in cylinder to cylinder mixture distribution.

Figure No. 20, page 79, summarizes the survey results from the climb mode at .075 fuel/air ratio. In this instance, the incorporation of the PCA resulted in decreased spreads between individual cylinder emissions levels and therefore improved cylinder to cylinder mixture distribution.

Similarly the results of the individual cylinder emissions survey conducted at the approach mode at a .075 fuel/air ratio are shown by Figure No. 21, page 80. Figure No. 22, page 81, shows the survey results from the taxi mode at a .090 fuel/air ratio. The incorporation of the PCA had negligible effect on the mixture distribution in these cases.

A comparison of the total engine emissions for the take-off mode is shown on Figure No. 23, page 82. The standard engine, PCA installed and PCA operating configurations are shown. All three configurations resulted in essentially the same overall emissions levels except near stoichiometric fuel/air (.067), where the standard engine demonstrated slightly lower CO emissions. The HC levels at the lean end of both PCA configurations rise off scale sharply. Individual cylinder emissions results showed that number 3 cylinder had experienced a high degree of misfiring at this point.

A comparison of the total engine emissions for the three configurations during the climb mode is given in Figure No. 24, page 83. No significant difference in total engine emissions was found. The PCA made the greatest improvement in mixture distribution at the climb mode; however, it can be seen that a net improvement in emissions was not accomplished. The measurement of overall engine emissions to compare the three configurations becomes equally important in determining any net benefit with the PCA concept.

The approach mode total engine emissions for the three configurations are compared on Figure No. 25, page 84. The difference between the three configurations appear inconsistent in that the standard engine fell between the PCA installed and PCA operating results.

Figure No. 26, page 85, compares the taxi mode total engine emissions of the three configurations. No significant difference is shown in engine emissions between the three configurations.

An evaluation was also made to determine PCA performance versus orientation of the vibrating tube (with respect to throttle shaft). Up to this point in the test program the vibrating tube had been aligned with the throttle shaft. The unit engine performance, etc. was then examined after rotating the PCA 90° and 180°, respectively, from its initial orientation. As expected, due to the near symmetry of the unit, the results from the initial and 180 degree orientations were similar. The 90 degree orientation showed some minor variations in mixture distribution when compared to the initial orientation. However, the only significant improvement in distribution for any of the PCA orientations was again found at the climb mode.

Figure No. 27, page 86, shows the total engine emissions at the climb mode condition for the standard engine, PCA on -rotated 90 degrees and PCA on -rotated 180 degrees. Again, despite the significant improvement in cylinder to cylinder distribution attributed to the PCA at this condition, little or no benefit in total engine emissions is shown over the normal operation range of the engine.

DISCUSSION:

The general performance trends of an internal combustion piston engine are dependent upon fuel/air ratio, as depicted in Figure No. 28, page 87. Power output, fuel economy, cylinder head temperature and other parameters attain their optimum or maximum values at different fuel/air ratios. The desired fuel/air ratio is influenced by the power mode selected. For example, best power would be desirous for take-off and best economy for cruise conditions. However, for whatever mixture strength is chosen, it is desirable to have all of the cylinders receiving a homogeneous intake charge or performance might be detrimentally affected. This becomes especially critical when operating near best economy (approximately stoichiometric fuel/air) or even leaner. Operation in this area is approaching the lean flammability limit and engine mixture leaning will be limited by the single leanest cylinder experiencing misfires at the flammability limit.

The function of the PCA was to provide a homogeneous mixture entering the induction manifold prior to being distributed to the individual cylinders. The incorporation of the PCA, while not ensuring equal quantity distribution of fuel would, it was hoped, break up large drops of fuel into microscopic size, thereby resulting in a more homogeneous mixture being distributed to the cylinders. These tests shows that distribution of intake charge was partly a function of the intake manifold configuration. At many of the conditions tested, cylinders 1 and 2 received a substantially richer mixture than cylinders 3 and 4. This was indicated in mixture distribution runs where numbers 1 and 2 cylinder head temperatures peaked at lower fuel flows. An example is shown on Figure No. 29, page 88.

Another major factor influencing mixture distribution of carburetted engines of this configuration is the throttle plate angle. The axis of the throttle butterfly plate is positioned such that the openings in the manifold for cylinders 1 and 2 are forward, while cylinders 3 and 4 are aft of it, as shown in Figure 30, page 89. Part throttle conditions, as shown in Figure 31, page 89, result in partial deflection of the intake charge, thereby degrading mixture distribution.

The results of the emissions and performance surveys indicated that the incorporation of the PCA unit into the induction system definitely affected mixture distribution. However, activating the PCA did not make a consistent or significant change in the parameters being monitored. The physical change to the intake manifold due to the incorporation of the PCA seemed to be the major contributor to the total effect on the system. Since the PCA was installed downstream of the carburetor, the PCA provided additional riser height, thereby reducing the throttle angle influence on mixture distribution.

The PCA was slightly more effective when installed with the vibrating tube at 90 degrees to the throttle shaft axis. With this orientation, more flow was apparently directed onto the atomizing tube.

The dynamometer tests demonstrated that the "pepperbox" nozzle carburetor substantially improved the mixture distribution over that of the standard nozzle carburetor. At the climb mode, the improvement with the "pepperbox" nozzle carburetor over the standard unit was of the same magnitude as the benefit found with the PCA. This condition, the 80% power range, was the operating condition at which the PCA improved the mixture distribution the most. At other power settings, the engine performance and distribution with the standard carburetor showed more improvement with the "pepperbox" nozzle carburetor than with the PCA.

CONCLUSIONS

The post-carburetor atomizer (PCA) was evaluated for its effect on engine power, economy and exhaust emissions. The intent of PCA was to promote performance improvements and leaner engine operation through improved mixture distribution. Testing on both dynamometer and propeller test stands was conducted with extensive engine performance and emissions data collected. The PCA was also evaluated when operated in three different orientations with respect to the carburetor and intake manifold. The conclusions of these tests were as follows:

1) A 3-5% power loss was experienced at full throttle, best power mixture, over the entire speed range with the PCA.

2) Little or no benefit in minimum brake specific fuel consumption was indicated for the use of the PCA over the standard carburetor system.

3) The PCA did not significantly alter the relationship of overall engine emissions with respect to fuel/air ratio.

4) Improvement in cylinder to cylinder mixture distribution was shown for the 80% power setting with the PCA, but at rated power and taxi the PCA degraded mixture distribution.

5) The PCA orientation with respect to the carburetor and induction manifold did effect the mixture distribution. Best results were obtained when the PCA tube was perpendicular to the throttle plate shaft.

6) The effect of the PCA on mixture distribution appears primarily due to its physical configuration, and added riser height since there was minimal change in engine performance between the atomizer vibrating or merely installed.

7) A "pepperbox" nozzle carburetor can promote mixture distribution equal in quality to that of the PCA equipped engine.

VARIABLE VALVE TIMING

INTRODUCTION

As piston engine rotational speed increases, intake and exhaust flow dynamics dictate that higher valve overlap is required to produce satisfactory performance. For piston aircraft engines, the valve timing and overlap is normally optimized to obtain maximum rated power at rated speed. Typically, at high speed and power, increased valve overlap (intake valve opening before exhaust valve closes) is required to insure sufficient aspiration. However, at lower powers and speeds, this high overlap valve timing can allow a short circuiting of the intake charge through the combustion chamber directly into the exhaust system, or possibly increased charge dilution with residual exhaust gas, either of which would result in degraded fuel economy and exhaust emissions.

The optimization of valve sequencing for each individual operating mode would, of course, improve engine performance over the entire flight profile. Conceptually, the ability to change valve timing during engine operation either requires that the camshaft have one or more sets of lobes (corresponding to the number of timings to be utilized during operation), or be adjustable (lobes be reindexed with respect to each other and/or the camshaft gear). The accommodation of such a system would substantially add to the complexity of the engine. The potential benefit in performance, fuel economy or emissions by incorporating such complexities must be determined by the limitations of the current design; in other words, how far from optimum is the performance of the standard, fixed timing camshaft over the operating profile of the engine?

Closely related with the valve sequencing is the optimization or tuning of the induction system to maximize engine performance. Performance improvements through induction system tuning are primarily limited to a certain range of engine speed or load. The tuning itself can be accomplished by varying the length and cross sectional area of the individual intake pipes.

DESCRIPTION OF TEST HARDWARE

The test bed used for the evaluation of the variable valve timing concept was the AVCO Lycoming IO-360 SPL engine. This engine is a direct drive, four cylinder, normally aspirated, horizontally opposed, air cooled, aircraft model. The cylinder bore and piston stroke of 13.02 cm (5.125 inches) and 11.11 cm (4.375 inches) respectively, result in a total piston displacement of 5916.8 cu cm (361 cubic inches). The compression ratio is 8.7:1 and the minimum recommended fuel grade is 100 LL aviation gasoline, or equivalent. The ignition timing is specified as 20° BTC.

The variable timing feature was incorporated into this engine by an adjustable camshaft (reference Figure 32, page 90) fabricated from two concentric shafts. The intake and exhaust lobes were attached independently to the inner and outer shafts. Adjustment of valve sequencing was accomplished by rotating the shafts relative to each other and securing this sequence by locking flanges located at the forward end of the shafts. A third flange, located at the rear of the camshaft, permitted rotation of the entire camshaft assembly with respect to the camshaft drive gear (and therefore the crankshaft). This adjustment advanced or retarded the overall valve sequence.

Due to physical design limitations the minimum adjustable increment was 2° 18' 28" camshaft degrees, which throughout this report will be referred to as one timing unit. For the remainder of this report, the valve sequencing currently employed by AVCO Lycoming in high speed engine applications will be referred to as standard or (0,0) timing. The numerical description refers to the timing units for the intake and exhaust valves respectively. For other valve timing settings, a positive value indicates an advanced timing and a negative denotes a retarded condition.

To aid in visualizing the valve timing synchronization, Figure 33, page 91, shows a grid presenting the various combinations obtainable. Standard timing (0,0) is located at the centroid of the grid. Moving horizontally from left to right along the X-axis corresponds to maintaining a constant exhaust valve timing, but increased valve overlap by advancing the initiation of the intake valve opening. Proceeding vertically from top to bottom along the Y-axis, maintains a constant intake valve opening but results in decreased overlap due to an advance of the exhaust valve opening. A 45° diagonal from upper left to bottom right represents a line of constant valve overlap.

A total of three camshafts, each with different cam lobe profiles, were evaluated. To establish baseline data, one camshaft had a production AVCO Lycoming "high speed" lobe configuration. The second profile configuration evaluated was fabricated to produce an 8° (camshaft angle) longer valve open duration than the standard. A 14° shorter duration lobe profile was evaluated for the third configuration.

Three (3) sets of intake pipes were tested during this program. The standard intake pipe specified for this engine is approximately 50.8 cm (20 inches) in length and 5.1 cm (2 inches) in diameter. To alter engine tuning, lengthened intake pipes, 71.1 cm (28 inches) long and 5.1 cm (2 inches) in diameter were assembled and tested. A third variation used decreased diameter 4.4 cm (1-3/4 inches) intake pipes of the same length as the standard pipes.

METHOD OF TEST

To minimize the testing to be conducted where exhaust emissions were to be measured, the performance evaluation was first conducted on a dynamometer. In this manner, it was possible to eliminate those valve timing settings which were least promising from the testing sequence.

The following performance runs were conducted with each of the three camshaft lobe configurations:

A) Two hour, full rich, shakedown run.

B) Full throttle performance survey at best power mixture strength from 3200, 3000, 2800, 2600, 2400, 2200 and 2000 RPM.

C) Bare injector run to obtain manifold pressure corrections for best power mixture at 3200, 3000, 2800, 2600, 2400, 2200 and 2000 RPM.

D) Variable manifold pressure tests at best power mixture for the following conditions:

1) Engine speeds - 3200, 3000, 2800 and 2600 RPM.

2) Manifold pressure - 60.8, 67.5, 74.3, 81.0, 87.8, 94.6 KPa (18, 20, 22, 24, 26, 28 In. Hg) absolute and full throttle.

E) Constant speed (variable fuel flow) mixture distribution surveys from full rich through best economy at the following conditions:

1) 1500 RPM, 50.6 KPa (15 In. Hg) manifold pressure.

2) 3200 RPM, full throttle.

3) 3030 RPM, 85% power.

4) 2620 RPM, 55% power.

The above tests were made at the standard valve timing. Items B, D, E-1 and E-2 were repeated at various valve timing combinations. While specific settings tested varied somewhat between the three camshafts, to provide a good individual performance characterization, a total of 23, 21 and 23 settings were tested with the standard lobe, the 14° shorter duration lobe and the 8° longer duration lobe camshafts, respectively.

Exhaust emissions surveys were subsequently conducted on a propeller test stand with the standard lobe and 14° shorter duration lobe camshafts. Exhaust concentrations of CO, CO_2, HC and NO_x were measured with the analysis instrumentation described in Section 2 of this report (Reference Figure No. 2). A description of the test conditions and engine power modes employed for these surveys is presented in Table No. VI. Inlet air pressure (99.6 KPa) 29.5 In.

Hg was maintained for all testing. Although this model engine was not a certificated production engine, a horsepower rating of 149.1 Kw (200 BHP) was assigned for this testing.

Locked throttle, mixture distribution runs (variable fuel flow) were conducted at each of the conditions shown in Table No. VI. The 78.3 Kw (105 BHP) power output for the simulated approach model condition exceeded the normal value of 40% (of rated power). This was due to the different low pitch stop requirements for propeller blade angle between actual flight and the static test stand condition. A total of eight valve timings were evaluated at each mode. Based on the dynamometer performance surveys, each of these timings was found to produce optimum or near optimum power output for one of the modes.

A brief investigation of the possible effect of induction system tuning on engine performance was made with the standard lobe camshaft configurations. To provide comparative data to the standard induction system, two other systems were tested. System number 1 consisted of intake pipes having the same 5.1 cm (2.0 inch) diameter as the standard units, but were increased in length from 50.8 cm (20 inch) to 71.1 cm (28 inch). System number 2 intake pipes were similar in length to the standard system, but were 4.4 cm (1-3/4 inch) diameter compared to 5.1 cm (2.0 inch) diameter for the standard system.

Full throttle performance, variable manifold pressure performance and constant speed (variable fuel flow) mixture distribution surveys were conducted with each system. Six different valve timings were evaluated with induction system number 1, while 14 timings were investigated with system number 2.

RESULTS

Figure No. 34, page 92, shows a performance map for the standard camshaft, 3200 RPM, full throttle, best power mixture, an indicated, optimum power occurred in the region of the grid controid (0,0), which corresponds to the standard AVCO Lycoming valve timing used in high speed engines. Isobars have been constructed delineating areas or settings of approximate equal power output. It should be noted that since the number of data points does not complete the grid, the line construction was accomplished somewhat subjectively.

Full throttle performance maps with the standard camshaft for 2800, 2400 and 2000 RPM engine speeds are shown on Figures Number 35, 36 and 37, pages 93, 94 and 95. These data depict that with decreasing speed and essentially fixed exhaust valve timing, optimum valve sequencing occurred with a progressively advanced intake valve opening. This corresponds to an increase in valve overlap. Similar timing trends were noted with the other two camshaft lobe configurations.

The results of the full throttle performance runs conducted with the three camshaft lobe configurations showed that with optimum valve sequencing, both the long and short duration camshaft lobe configurations provided better engine performance (power output) than the standard camshaft. Comparing power output at the seven engine speeds tested (3200, 3000, 2800, 2600, 2400, 2200 and 2000 RPM), the long duration lobe camshaft resulted in a slight increase (½ to 3%) in power when valve timing was optimized. With standard (0,0) timing, however, the long duration camshaft slightly degraded maximum power output at these conditions. A similar comparison at (0,0) standard valve timing with the short duration camshaft showed a 1-13% performance increase compared to the standard cam lobe camshaft. With optimum valve timings for both camshafts, performance increases of 1-9% were obtained.

Figure Numbers 38, 39 and 40, pages 96,97 and 98, respectively, show the performance maps for a constant speed (2800 RPM) variable manifold pressure 87.8, 74.3, 60.8 KPa (26, 22, 18 In. Hg) testing sequence. As manifold pressure decreased, optimum timing occurred with progressively retarded intake valve opening, which resulted in decreased valve overlap.

The performance map showing minimum obtainable brake specific fuel consumption versus valve timing for 1500 RPM, 50.6 KPa (15 In. Hg) manifold pressure with the standard lobe camshaft is shown on Figure No. 41, page 99. The cross hatched area shown corresponds to those valve setting combinations which were unobtainable due to camshaft construction. Optimum timing occurred with advanced intake and exhaust valve openings with decreased valve overlap. Figure No. 42, page 100, shows similar results for the longer valve open duration camshaft. The performance with this camshaft was very sensitive to changes in valve settings. Optimum timing occurred approximately in the same region as the standard lobe camshaft. The lowest minimum brake specific fuel consumption was obtained with the short duration camshaft, as shown on Figure No. 43, page 101. The results indicated that engine performance with this camshaft was less sensitive to valve timing combinations than the other camshaft lobe configuration. Optimum timing again occurred with slightly advanced valve sequencing.

The results of the full throttle performance surveys conducted with the two variations of the standard intake pipe configuration are shown on Figure No. 44, page 102. The increased length induction system (number 1) provided a performance increase of 3-11% over the engine speed range tested. Additionally, the 4.4 cm (1-3/4 inch) diameter induction system provided a performance increase over the standard system of 2-15% under similar conditions. The overall magnitude of increases attributed to these induction system revisions was greater than the improvement gained by valve timing changes.

The results of the emissions surveys conducted with the standard lobe (6 settings) and short duration (14 settings) lobe camshafts at the take-off mode conditions are shown on Figure No. 45, page 103. To clarify this summary several data trends from a relatively wide range of valve sequencings are shown by the various symbols. No significant difference in CO emissions between any of the valve sequences or lobe configurations is shown. Some small differences in hydrocarbon emissions were apparent with valve timing changes with the standard lobe. However, HC emissions were substantially reduced (up to approximately 50%) with the short duration lobe camshaft. These results, although shown for a limited number of settings, remained valid over the entire range of valve sequencings evaluated.

Figure No. 46, page 104, shows the results of the emissions survey conducted with the standard and short duration lobe camshafts at the Taxi Mode conditions. Although some scatter in data trends is apparent, no significant difference in CO emissions between any of the valve timing settings or lobe configurations is shown. Again, some difference in HC emission trends is apparent with respect to valve timing changes. Here however, in contrast to higher power conditions, the standard lobe camshaft appears to have slightly lower HC emission trends than the short duration camshaft. Again, although the data presented reflects a limited number of valve timing settings, the general results noted were valid over the entire range of sequences tested.

DISCUSSION

To provide a perspective view of the magnitude of valve open duration and timing, Figure No. 47, page 105, shows the relation between valve opening and crankshaft rotation. Two rotations of the crankshaft are made during each power cycle so that valve overlap occurs only near TDC (0°) between the exhaust and intake stroke. Figure No. 48, page 106, summarizes the optimum valve timing combinations for four selected power conditions. (Note that -14° implies short duration camshaft, etc.). It can be seen that the optimum valve timing becomes further advanced with increasing valve overlap at the lower RPM full throttle conditions, independent of lobe contour. As expected, very little valve overlap is required at the 1500 RPM part throttle conditions for optimum performance. It should be noted that the valve open sequence represented by the individual bars are representative of the opening and closing events of the camshaft. The effective flow through the valve port near the valve opening or closing point is relatively undefined. However, this condition does not alter the basic trends of the data obtained.

Table No. VII shows a summary of the optimum performance results obtained with valve timing variations for selected engine conditions. At 3200 RPM. full throttle, standard (0,0) valve timing produced the maximum power output of the three camshaft lobe configurations examined with the standard induction system. The short duration camshaft lobe provided a 1% increase in power output, but also required an increase in best power brake specific fuel consumption of 6%. The standard lobe camshaft/lengthened intake pipe configuration provided a 6% improvement in performance with a 2% benefit in best power BSFC. as compared to the standard lobe camshaft alone.

The greatest benefit in engine power output with respect to changes in valve timing and induction system occurred at the 2800 RPM, full throttle operating condition. Of the configurations where valve timing change was the sole variable, the long duration camshaft provided a 7% improvement in engine performance and an 8% benefit in best power BSFC at a (2, -1) valve sequencing, compared with the standard cam lobe and standard valve timing. Again, maximum power output was obtained with the standard camshaft/lengthened intake pipe configuration.

At the 2800 RPM, 81 KPa (24 In. Hg) manifold pressure condition, equal maximum power outputs were obtained with the short duration camshaft and the standard camshaft/lengthened induction system configurations. But when fuel consumption is considered, the short duration camshaft provided a 14% lower best power BSFC than the standard camshaft.

The standard camshaft/4.4 cm (1-3/4 inch) diameter intake pipe configuration provided maximum power output at the 2000 RPM, full throttle operating condition. Minimum best power BSFC for this power was provided by the short duration camshaft configuration.

The minimum BSFC was provided by the short duration camshaft at the 1500 RPM, 50.6 KPa (15 inch) manifold pressure condition; however, the modified induction system configurations were not evaluated at this condition.

A very simple, but somewhat effective method of comparing the potential benefits for each configuration is obtained by combining the percent improvement or loss of each engine condition into a total percentage performance improvement factor. These factors, shown on Table VII, reflect the overall benefit in both performance and BSFC for each of the configurations tested. The standard camshaft/smaller diameter intake pipe configuration provided the maximum total percentage performance improvement, although the lengthened intake pipe configuration provided nearly similar results. For the "valve sequencing only" configurations, the maximum performance improvement was provided by the short duration camshaft, however, more than half of this improvement was obtained at the 1500 RPM engine condition alone. On a specific fuel consumption basis, the maximum total percentage BSFC improvement was obtained with the short duration camshaft with standard length induction pipes.

The various configurations tested were in part or totally derived from three basic modifications to the standard engine; reindexed valve timing, revised camshaft lobe profile and/or modified induction system. By separating the effects attributable to each variable an approximation of the relative effectiveness of each modification may be obtained. Such an evaluation shows that these three main categories should be ranked in order of potential performance benefit as: induction system tuning, camshaft lobe profile, and valve sequencing. Based on the data from these selected engine conditions, induction system tuning provides substantially greater benefit than the other considerations. It must be noted however that these judgements are made relative to the standard camshaft/standard tuning configuration. This implies that for this particular engine, the greatest potential for performance improvement is in proper tuning of the induction system. Other engine models may respond differently to individual changes of these or other parameters.

At the engine conditions tested, no significant difference in CO exhaust emissions was found between any of the valve timing configurations. Carbon monoxide, primarily a product of an incomplete combustion process, is directly affected by the fuel/air ratio of the charge in the cylinder. Valve sequencing, or valve open duration, does not influence the mixture strength of the incoming charge. While it might b· ··ıoretically possible to induce incomplete combustion with a certain ve sequencing, it is expected that engine performance would be drastically affected. From these tests the degradation in power did not indicate complementary increases in exhaust concentrations of CO. Fuel air ratio remains to be the controlling parameter in these test configurations.

At certain operating conditions HC emissions were substantially influenced by changes in valve sequencing and valve open duration. Over the range of valve timings tested, the short duration camshaft provided 40% greater variations in HC emissions, as did the standard lobe camshaft. Certain retarded, high valve overlap settings with the short duration camshaft increased HC emissions by as much as 20% and at advanced low overlap timings, HC emissions decreased by up to 20%. A comparison of HC emissions between the two camshafts at standard timing is shown on Table VIII.

CONCLUSIONS

Extensive testing of a variable valve timing configuration camshaft on an experimental version of an Avco Lycoming IO-360 engine was conducted to evaluate the potential performance, fuel economy and emissions benefits with optimized valve sequencing for various engine conditions. A limited evaluation of modified induction systems was also made from these data. The following conclusions have been made:

1) The standard (0,0) valve timing employed by Avco Lycoming in high speed engine applications provided optimum performance at rated engine speed (3200 RPM), full throttle.

2) At full throttle, as engine speed decreased, optimum valve timing became increasingly more advanced with increased valve overlap.

3) At constant speed, as manifold pressure was decreased, optimum valve timing shifted from an advanced-increased overlap to a retarded-decreased overlap condition.

4) The short duration camshaft provided a 2-13% improvement in power over the standard camshaft comparing (0,0) valve indexing for the engine speeds tested at full throttle. The long duration camshaft provided no significant improvement at these conditions.

5) Carbon monoxide exhaust emissions were not significantly affected by valve timing changes over the ranges tested. Unburned hydrocarbon emissions, however, could be reduced by 20% at the take-off and climb modes and 50% at the idle and taxi modes by optimizing valve sequencing.

6) The incorporation of the lengthened (compared to standard) induction system provided a 5-12% improvement in power output at the conditions tested.

7) Although some areas of significant improvement could be isolated, no evidence or service testing was conducted to determine the potential extended life characteristics of the various camshaft lobe configurations.

OVERALL CONCLUSIONS

To determine if improved ignition quality would benefit engine exhaust emissions and/or specific fuel consumption, several ignition system configurations were evaluated. Capacitive discharge, multiple spark and staggered spark systems, as well as various spark plug configurations, were examined. The results of the tests showed that none of the configurations provided a consistent, significant improvement in the monitored parameters over the standard ignition system. Neither the spark duration nor spark plug tip location, which are currently employed in this model engine, are considered to be limiting factors for improving performance or emissions.

The effect of ultrasonic fuel atomization on piston aircraft engine performance fuel economy and exhaust emissions was evaluated for a range of operating conditions. A significant improvement in cylinder-to-cylinder mixture distribution was obtained at one engine condition. However, no improvement in total engine emissions fuel economy, or performance was obtained. The effect of the post carburetor atomizer, (PCA), on mixture distribution was almost entirely attributable to the added riser height with the unit installed. In Avco Lycoming engines, the induction system for the normally aspirated, carbureted configuration, is immersed in the oil sump. During normal engine operation, wall temperatures up to 120°C (250°F) might be encountered, which would substantially aid the fuel vaporization process. This arrangement apparently provides sufficient fuel mixture vaporization such that the operation of the ultrasonic unit made no additional significant improvement. A 3-5% loss in rated full throttle engine performance resulted from the additional manifold restriction of the ultrasonic unit.

For piston aircraft engines, valve sequencing has been traditionally determined by maximizing rated power output. At lower engine speeds and powers, less than optimum performance often results. Testing was conducted to qualify the potential performance and/or emissions benefits which would be provided to the overall operating profile with selected optimum valve timing sequences for each specific engine condition. The results showed that the standard high speed valve timing employed by Avco Lycoming provided the maximum power output at rated engine speed and was generally a good compromise at lower powers and speeds. Improvements in engine performance up to 13% at certain off rated conditions were obtained with optimized valve timing. Over the ranges tested and at constant fuel air ratio, valve timing did not influence CO emission levels. HC emissions showed considerable dependence on valve timing and substantial reductions up to 50% were obtained at optimum settings. Additional testing, conducted to evaluate the effect of induction system tuning on these results, showed that performance improvements of the same magnitude could be accomplished with standard valve timing and revised induction system. Considering the magnitudes of the overall improvements in performance which were found, and due to the greatly increased complexity of the variable valve timing system, induction system tuning is a more viable concept for improving overall engine performance.

TABLE I - MAXIMUM SPARK PLUG DEMAND VOLTAGE (KV PEAK) AND SPARK DURATION*

*MILLISEC UNLESS OTHERWISE NOTED

RUN NO	IGNITION SYSTEM	IDLE		TAXI		TAKE OFF		CLIMB		APPROACH	
		VOLT.	DUR.	VOLT.	DUR.	VOLT.	DUR.	VOLT.	DUR.	VOLT.	DUR.
24-70 170-194 499-520	Standard Magneto (Model D6RN-220, S/N L17627-216) Std Plugs, Champion RHB 36W New, .48 MM Gap	9	0.6-3.0	8	1.2-3.5	13	0.5-1.8	14.5	0.3-1.7	11	0.7-1.9
71-32 521-541	Standard Magneto 6.4 MM Extended Electrode Champion 0044065A Plugs New, .48 MM Gap	7	0.6-3.5	6.5	0.4-2.5	9.5	0.6-1.4	10	0.6-1.6	7.5	0.9-1.4
133-169	Standard Magneto 12.7 MM Extended Electrode Champion 044065B Plugs New .48 MM Gap	7.5	0.8-3.5	6.5	1.5-3.9	10.5	0.4-1.6	10.5	0.6-1.6	8	0.8-1.6
195-218	Standard Magneto Std Plugs, Champion RHB 36W Used, .64 MM Gap	10.5	0.5-3.0	7.5	1.0-3.0	15	0.2-1.2	16(1)	0.1-1.6	12.5	0.6-2.0
225-247	Standard Magneto 6.4 MM Extended Electrode Champion 0044065A Plugs Used, .64 MM Gap	9	0.9-3.5	7	1.2-3.5	12	0.3-1.3	12	0.4-1.4	9.5	0.7-1.6
272-296	Staggered Firing Standard Magneto Std Plugs, Champion RHB 36W New, .48 MM Gap										
	Top Plugs (25° BTC)	7	0.5-2.0	6	0.9-3.5	9	0.8-1.6	10	0.7-2.1	9	1.0-2.1
	Bottom Plugs (20° BTC)	8	1.0-3.0	7	1.5-4.0	10.5	0.6-1.2	12	0.6-1.6	10.5	1.0-1.9

(Continued)

TABLE 1.- MAXIMUM SPARK PLUG DEMAND VOLTAGE (KV PEAK) AND SPARK DURATION*

*MILLISEC UNLESS OTHERWISE NOTED

RUN NO	IGNITION SYSTEM	IDLE VOLT.	IDLE DUR.	TAXI VOLT.	TAXI DUR.	TAKE OFF VOLT.	TAKE OFF DUR.	CLIMB VOLT.	CLIMB DUR.	APPROACH VOLT.	APPROACH DUR.
297-319 353-370	Staggered Firing Standard Magneto Std Plugs, Champion RHB 36W New, .48 MM Gap Top Plugs (20° BTC) Bottom Plugs (25° BTC)	9 8.5	1.0-2.5 0.5-1.5	7 6.5	1.5-3.5 1.2-3.5	12 11.5	0.6-1.4 0.7-1.3	12 11.5	0.6-2.0 0.6-1.5	10.5 10.5	1.1-2.1 1.0-1.9
320-352	Staggered Firing Standard Magneto Std Plugs, Champion RHB-36W New, .48 MM Gap Top Plugs (15° BTC) Bottom Plugs (25° BTC)	5.5 5.5	1.6-3.0 1.5-2.5	6.5 5.5	1.5-3.5 1.2-3.5	12 11.5	0.4-1.6 0.4-1.2	14 12.5	0.2-1.6 0.3-1.2	11 10	1.0-2.0 1.0-1.8
371-410	Capacitive Discharge S-1800 Magneto, 300 V Supply Long Duration, 10-57460 Coils Std Plugs, Champion RHB-36W	7	.16-.18	7	.13-.15	14	.09-.14 (2)	14	.10-.14 (2)	11	.11-.14
411-419	Capacitive Discharge S-1800 Magneto, 200 V Supply Long Duration 10-57460 Coils Std Plugs, Champion RHB-36W	SAME AS PREVIOUS RESULTS									
420-466	Capacitive Discharge S-1800 Magneto, 250 V. Supply Short Duration Coils, 10-372385 Std Plugs, Champion RHB-36W	10	11-30 (3)	9	10-40 (3)	14	9-70 (3)	15	9-80 (3)	11	10-60 (3)
467-487	Multiple Spark (20° Duration) D-2000 Magneto Std Plugs, Champion RHB-36W	7	4.8-6.2	7	2.8-3.5	14	0.3-1.5 (1)	14	0.5-1.7	11	1.2-1.8
488-498	Multiple Spark (35° Duration) D-2000 Magneto Std Plugs, Champion RHB-36W	11	8.5-12.0 (1)	7	5.0-5.8 (1)	-	-	-	-	11	2.2-2.7 (1)

TABLE II

"TIGO-541-D1BD EMISSION LEANOUT TEST PARAMETERS"

MODE	ENGINE POWER % OF RATED	ENGINE SPEED RPM	MAN. PRESS. KPa (IN.HG)	COOLING AIR P KPa (IN. H_2O)	COMP. INLET PRESS. KPa (IN.HG)
Idle	-	600	As Required	None	99.6 (29.5)
Taxi	-	1200	As Required	None	99.6 (29.5)
Take-Off	100	3200	152 (45)	2 (8)	99.6 (29.5)
Climb	80	2880	135 (40)	2 (8)	99.6 (29.5)
Approach	40	2780	78 (23)	2 (8)	99.6 (29.5)

TABLE III

SPARK PLUG	ELECTRODE GAP mm (In.)	TEST MODE	FUEL/AIR MIXTURE	MAGNETO TIMING	DEMAND VOLTAGE
Standard	.48 (.020)	T.O.	Lean	20° BTC	13 kv
½ In. Extended (Sharp Edges)	.48 (.020)	T.O.	Lean	20° BTC	9-1/2
Standard	.64 (.025)	T.O.	Lean	20° BTC	15
Standard	.48 (.020)	Idle	Lean	20° BTC	9
Standard	.48 (.020)	T.O.	Rich	20° BTC	9
Standard	.48 (.020)	T.O.	Lean	25° BTC	11-1/2

TABLE IV

MIXTURE DISTRIBUTION RUNS COMPARISON, CARBURETOR S/N X03

NOMINAL SETTING	DATA TYPE	STANDARD ENGINE	PCA INSTALLED	PCA OPERATING
2700 RPM	Mixture Distribution Δ Fuel Flow Kg/Hr (Lb/Hr)	2.3 (5)	2.7 (6)	3.6 (8)
	BSFC (Minimum) $\frac{Kg}{Kw/Hr}$ $\left(\frac{Lb.}{BHP\text{-}Hr.}\right)$	.284 (.465)	.287 (.470)	.284 (.465)
	Observed Maximum Kw (HP)	102.3 (137.2)	98.4 (132.0)	98.5 (132.1)
2430 RPM	Mixture Distribution Δ Fuel Flow Kg/Hr (Lb/Hr)	4.5 (10)	2.2 (5)	1.4 (3)
	BSFC @ 23.6 Kg/Hr (52 Lb/Hr) F.F. $\frac{Kg}{Kw\text{-}Hr}$ $\left(\frac{Lb}{BHP\text{-}Hr}\right)$	.289 (.475)	.287 (.470)	.281 (.460)
89.5 (120) Kw (BHP)	Observed Kw (BHP) @ 23.6 Kg/Hr (52 Lb/Hr) F.F.	81.3 (109.0)	82.8 (111.0)	83.9 (112.5)
2430 RPM	Mixture Distribution Δ Fuel Flow Kg/Hr (Lb/Hr)	2.3 (5)	1.4 (3)	1.4 (3)
	BSFC @ 20 Kg/Hr (44 Lb/Hr) FF $\frac{Kg}{Kw\text{-}Hr}$ $\left(\frac{Lb}{BHP\text{-}Hr}\right)$	.296 (.485)	.299 (.490)	.314 (.515)
78.5 (105) Kw (BHP)	Observed Kw (BHP) @ 20 Kg/Hr (44 Lb/Hr) F.F.	67.1 (90.0)	67.5 (90.5)	64.1 (86.0)
2340 RPM	Mixture Distribution Δ Fuel Flow Kg/Hr (Lb/Hr)	0.9 (2)	.9 (2)	2.3 (5)
	BSFC @ 18.1 Kg/Hr (40 Lb/Hr)F.F. $\frac{Kg}{Kw\text{-}Hr}$ $\left(\frac{Lb}{BHP\text{-}Hr}\right)$	.299 (.490)	.303 (.498)	.311 (.510)
72.7 (97.5) Kw (BHP)	Observed Kw (BHP) @ 18.1 Kg/Hr (40 Lb/Hr)F.F.	60.4 (81.0)	59.7 (80.0)	58.5 (78.5)
2200 RPM	Mixture Distribution Δ Fuel Flow Kg/Hr (Lb/Hr)	0.9 (2)	0.9 (2)	1.4 (3)
	BSFC @ 16.3 Kg/Hr (36.6 Lb/Hr)F.F. $\frac{Kg}{Kw\text{-}Hr}$ $\left(\frac{Lb}{BHP\text{-}Hr}\right)$	.305 (.500)	.305 (.500)	.302 (.495)
61.5 (82.5) Kw (BHP)	Observed Kw (BHP) @ 16.3 Kg/Hr (36 Lb/Hr)F.F.	53.7 (72.0)	53.7 (73.0)	53.7 (73.0)

TABLE V

MIXTURE DISTRIBUTION RUNS COMPARISON, CARBURETOR S/N A-40-20036

NOMINAL SETTING	DATA TYPE	STANDARD ENGINE	PCA INSTALLED	PCA OPERATING
2700 RPM	Mixture Distribution △ Fuel Flow Kg/Hr (Lb/Hr)	2.3 (5)	4.5 (10)	4.5 (10)
Full Throttle	BSFC (Minimum) $\frac{Kg}{Kw\text{-}Hr}$ $\left(\frac{Lb}{BHP\text{-}Hr}\right)$	.281 (460)	.287 (.470)	.296 (.485)
	Observed Maximum Kw (BHP)	101.6 (136.2)	99.8 (133.8)	97.0 (130.1)
2430	Mixture Distribution △ Fuel Flow Kg/Hr (Lb/Hr)	6.8+ (15+)	5.9 (13)	5.0 (11)
89.5 (120) Kw (BHP)	BSFC @ 23.6 Kg/Hr (52 Lb/Hr)F.F. $\frac{Kg}{Kw\text{-}Hr}$ $\left(\frac{Lb}{BHP\text{-}Hr}\right)$	.299 (.490)	.299 (.490)	.293 (.480)
	Observed Kw (BHP) @ 23.6 Kg/Hr (52 Lb/Hr)F.F.	79.6 (106.8)	79.0 (106.0)	80.2 (107.5)
2430 RPM	Mixture Distribution △ Fuel Flow Kg/Hr (Lb/Hr)	2.3 (5)	0.9 (2)	.5 (1)
78.3 (105) Kw (BHP)	BSFC @ 20 Kg/Hr (44 Lb/Hr)F.F. $\frac{Kg}{Kw\text{-}Hr}$ $\left(\frac{Lb}{BHP\text{-}Hr}\right)$	.305 (.500)	.303 (.498)	.305 (.500)
	Observed Kw (BHP) @ 20 Kg/Hr (44 Lb/Hr)F.F.	65.6 (88.0)	67.1 (90.0)	66.4 (89.0)
2340 RPM	Mixture Distribution △ Fuel Flow Kg/Hr (Lb/Hr)	3.6 (8)	1.4 (3)	1.4 (3)
72.7 (97.5) Kw (BHP)	BSFC @ 18.1 Kg/Hr (40 Lb/Hr)F.F. $\frac{Kg}{Kw\text{-}Hr}$ $\left(\frac{Lb}{BHP\text{-}Hr}\right)$	.308 (.505)	.311 (.510)	.341 (.560)
	Observed Kw (BHP) @ 18.1 Kg/Hr (40 Lb/Hr)F.F.	59.6 (80.0)	57.8 (77.5)	53.7 (72.0)
2200 RPM	Mixture Distribution △ Fuel Flow Kg/Hr (Lb/Hr)	0.9 (2)	0.9 (2)	1.4 (3)
61.5 (82.5) Kw (BHP)	BSFC @ 16.3 Kg/Hr (36 Lb/Hr)F.F. $\frac{Kg}{Kw\text{-}Hr}$ $\left(\frac{Lb}{BHP\text{-}Hr}\right)$	.320 (.525)	.305 (.500)	.342 (.560)
	Observed Kw (BHP) @ 16.3 Kg/Hr (36 Lb/Hr)F.F.	51.5 (68.5)	53.7 (72.0)	49.6 (66.5)

TABLE VI

EXHAUST EMISSION SURVEY ENGINE TEST PARAMETERS

MODE	ENGINE SPEED	OBSERVED POWER Kw - HP	MANIFOLD PRESSURE	COOLING AIR Δ P-KPa (In H_2O)
Take-Off	3200	Maximum	Full Throttle	1.5 (6)
Climb	2880	119.3 (160) (80%)	As Required	1.5 (6)
Approach	2780	78.3 (105)	As Required	1.5 (6)
Taxi	1200	-	As Required	None
Idle	600	-	As Required	None

TABLE VII - SUMMARY OF OPTIMUM PERFORMANCE RESULTS

ENGINE CONDITIONS	STANDARD CAM STANDARD TIMING		STANDARD CAM OPTIMUM TIMING		SHORT DURATION CAM OPTIMUM TIMING		LONG DURACTION CAM OPTIMUM TIMING	
	Kw Kg/Kw-Hr	HP LB/BHP-Hr	Kw Kg/Kw-Hr	HP LB/BHP-Hr	Kw Kg/Kw-Hr	HP Lb/BHP-Hr	Kw Kg/Kw-Hr	HP Lb/BHP-Hr
3200 RPM, F.T.	153 .299	205 .49 (0,0)	153 .299	205 .490 (0,0)	155 .322	208 .520 (0,0)	154 .299	206 .490 (0,0)
2800 RPM, F.T.	134 .311	180 (0,0) .51	139 .295	187 (2,-1) .485	141 .287	189 (3,-2) .470	144 .287	193 (2,-1) .470
2800 RPM, 81 KPa M.P. (24 In. Hg)	101 .341	135 (0,0) .56	101 .341	135 (0,0) .560	110 .299	147 (2,-1) .490	99 .299	133 (2,-1) .490
2000 RPM, F.T.	94 .290	126 (0,0) .475	101 .287	135 (5,0) .470	106 .268	142 (5,0) .440	100 .287	134 (5,0) .470
1500 RPM, 51 KPa M.P. (15 In. Hg)	- .549	- (0,0) .900	- .397	- (3,8) .650	- .329	- (5,2) .54	- .415	- (4,9) .68
TOTAL PERCENT PERFORMANCE IMPROVEMENT		-		11		25		17
TOTAL PERCENT BSFC IMPROVEMENT		-		5		23		20

NOTE: BSFC'S SHOWN ARE FOR BEST POWER FOR ALL CONDITIONS EXCEPT 1500 RPM (WHICH WAS MINIMUM OBTAINABLE)

$$\text{BSFC} \sim \underset{\text{METRIC UNITS}}{\frac{\text{Kg (F.F.)}}{\text{Kw-Hr}}} \sim \underset{\text{S.I. UNITS}}{\frac{\text{Lbs (F.F.)}}{\text{Hp-Hr}}}$$

(Continued)

TABLE VII - SUMMARY OF OPTIMUM PERFORMANCE RESULTS - (Cont'd.)

ENGINE CONDITIONS	STANDARD CAM-28" INTAKES OPTIMUM TIMING Kw $\frac{Kg}{Kw\text{-}Hr}$	HP $\frac{Lb}{BHP\text{-}Hr}$	STAND. CAM-1-3/4 D.INT. OPTIMUM TIMING Kw $\frac{Kg}{Kw\text{-}Hr}$	HP $\frac{Lb}{BHP\text{-}Hr}$	STAND. CAM-28" INTAKES (0,0) TIMING Kw $\frac{Kg}{Kw\text{-}Hr}$	HP $\frac{Lb}{BHP\text{-}Hr}$	
3200 RPM, F.T.	163 .293	218 (0,0) .480	158 .305	212 (-2,1) .530	163 .293	218 (0,0) .480	
2800 RPM, F.T.	147 .287	197 (5,0) .470	147 .305	197 (2,1) .500	142 .305	191 (0,0) .500	
2800 RPM, 81 KPa M.P. (24 In. Hg)	109 .299	146 (0,0) .490	110 .311	147 (0,0) .510	109 .299	146 (0,0) .490	
2000 RPM, F.T.	106 .275	142 (5,0) .450	110 .281	148 (5,0) .460	97 .287	130 (0,0) .470	
1500 RPM, 51 KPa M.P. (15 In. Hg)							
TOTAL PERCENT PERFORMANCE IMPROVEMENT	-	36	-	38	-	23	
TOTAL PERCENT BSFC IMPROVEMENT	-	27	-	12	-	14	

NOTE: BSFC'S SHOWN ARE FOR BEST POWER FOR ALL CONDITIONS EXCEPT 1500 RPM (WHICH WAS MINIMUM OBTAINABLE).

$$BSFC = \frac{Kg\ (Fuel)}{Kw - Hr} \approx \frac{Lb\ (Fuel)}{BHP - Hr}$$

TABLE VIII

STANDARD AND SHORT DURATION HC EMISSIONS

Kg/MODE / Kw (LBS/MODE / BHP) AT STANDARD VALVE TIMING

	TAKE-OFF .09 F/A	CLIMB .09 F/A	APPROACH .08 F/A	TAXI .11 F/A	IDLE .13 F/A
Standard Cam	.26 (.438)	4.4 (7.3)	3.5 (5.8)	.24 (.40)	.08 (.125)
Short Duration Cam	.31 (.51)	6.1 (.10)	4.3 (7.1)	.14 (.23)	.03 (.050)

FIG. 1 - SPARKPLUG CONFIGURATIONS

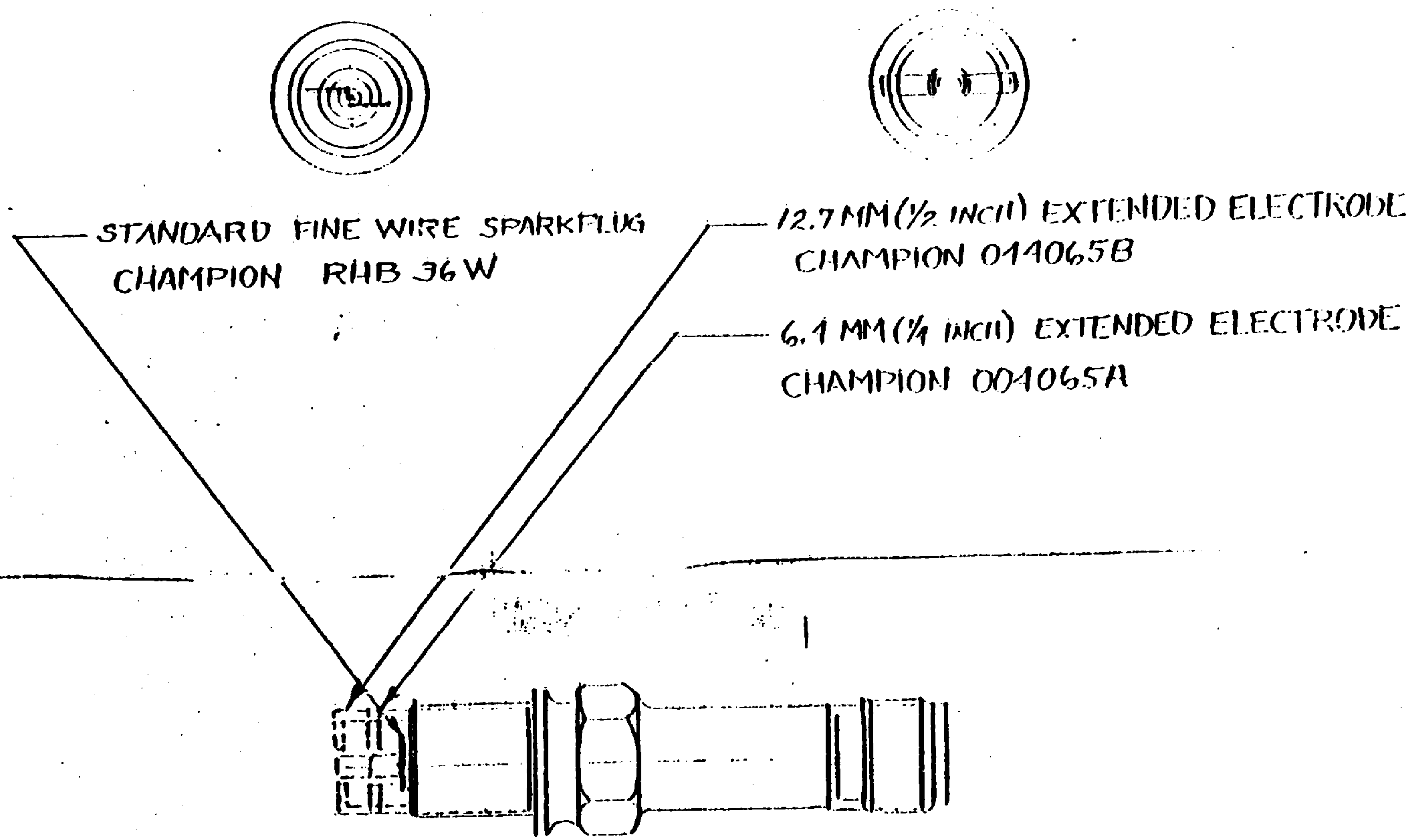

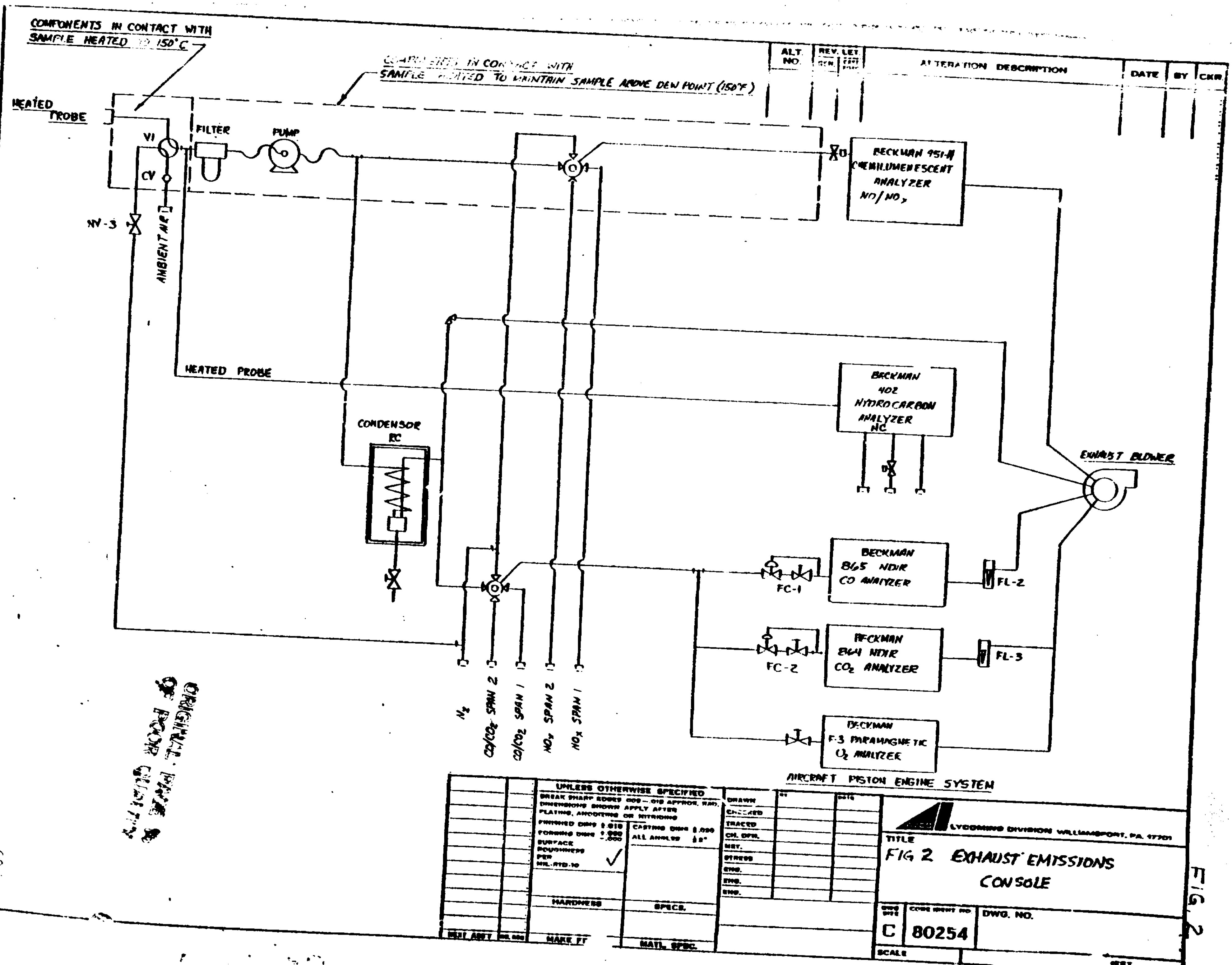

COMPONENTS IN CONTACT WITH SAMPLE HEATED TO 150°C
COMPONENTS IN CONTACT WITH SAMPLE HEATED TO MAINTAIN SAMPLE ABOVE DEW POINT (150°F)
HEATED PROBE
VI
CV
NV-3
AMBIENT AIR
FILTER
PUMP
HEATED PROBE
CONDENSOR
RC
BECKMAN 951-A CHEMILUMENESCENT ANALYZER NO/NOx
BECKMAN 402 HYDROCARBON ANALYZER HC
EXHAUST BLOWER
BECKMAN 865 NDIR CO ANALYZER
BECKMAN 864 NDIR CO2 ANALYZER
BECKMAN F-3 PARAMAGNETIC O2 ANALYZER
FC-1
FC-2
FL-2
FL-3
N2
CO/CO2 SPAN 2
CO/CO2 SPAN 1
NOx SPAN 2
NOx SPAN 1
AIRCRAFT PISTON ENGINE SYSTEM
ALT. NO.
REV. LET.
ALTERATION DESCRIPTION
DATE
BY
CKR
UNLESS OTHERWISE SPECIFIED
DRAWN
CHECKED
TRACED
HARDNESS
SPECS.
MAKE FT
MATL. SPEC.
LYCOMING DIVISION WILLIAMSPORT, PA. 17701
TITLE
FIG 2 EXHAUST EMISSIONS CONSOLE
C
80254
DWG. NO.
SCALE

FIG. 2

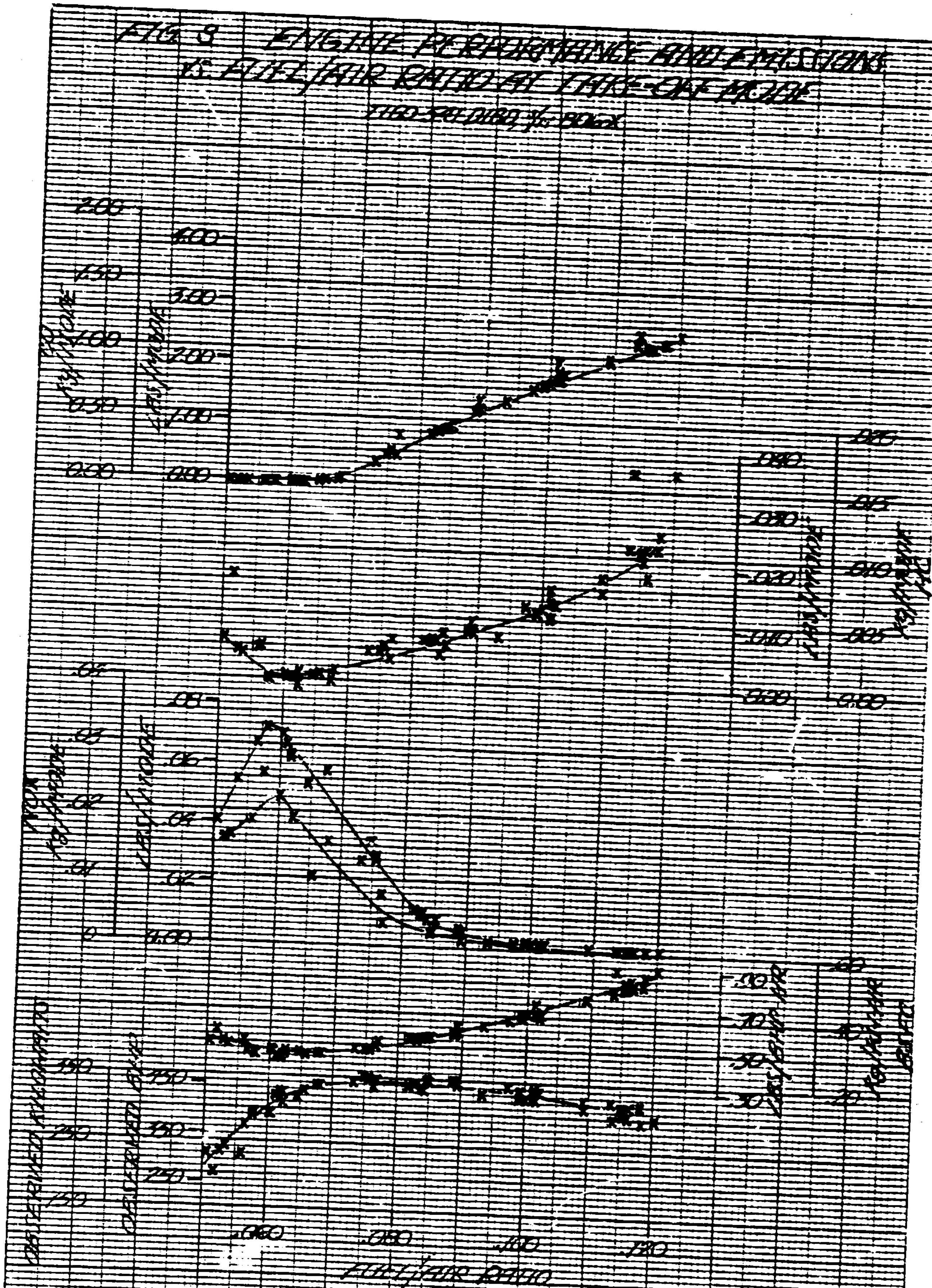
FIG. 8 ENGINE PERFORMANCE AND EMISSIONS
VS FUEL/AIR RATIO AT TAKE-OFF MODE
FUEL/AIR RATIO
OBSERVED KILOWATTS
OBSERVED BHP

FIG. 4 ENGINE PERFORMANCE AND EMISSIONS vs FUEL/AIR RATIO AT CLIMB MODE

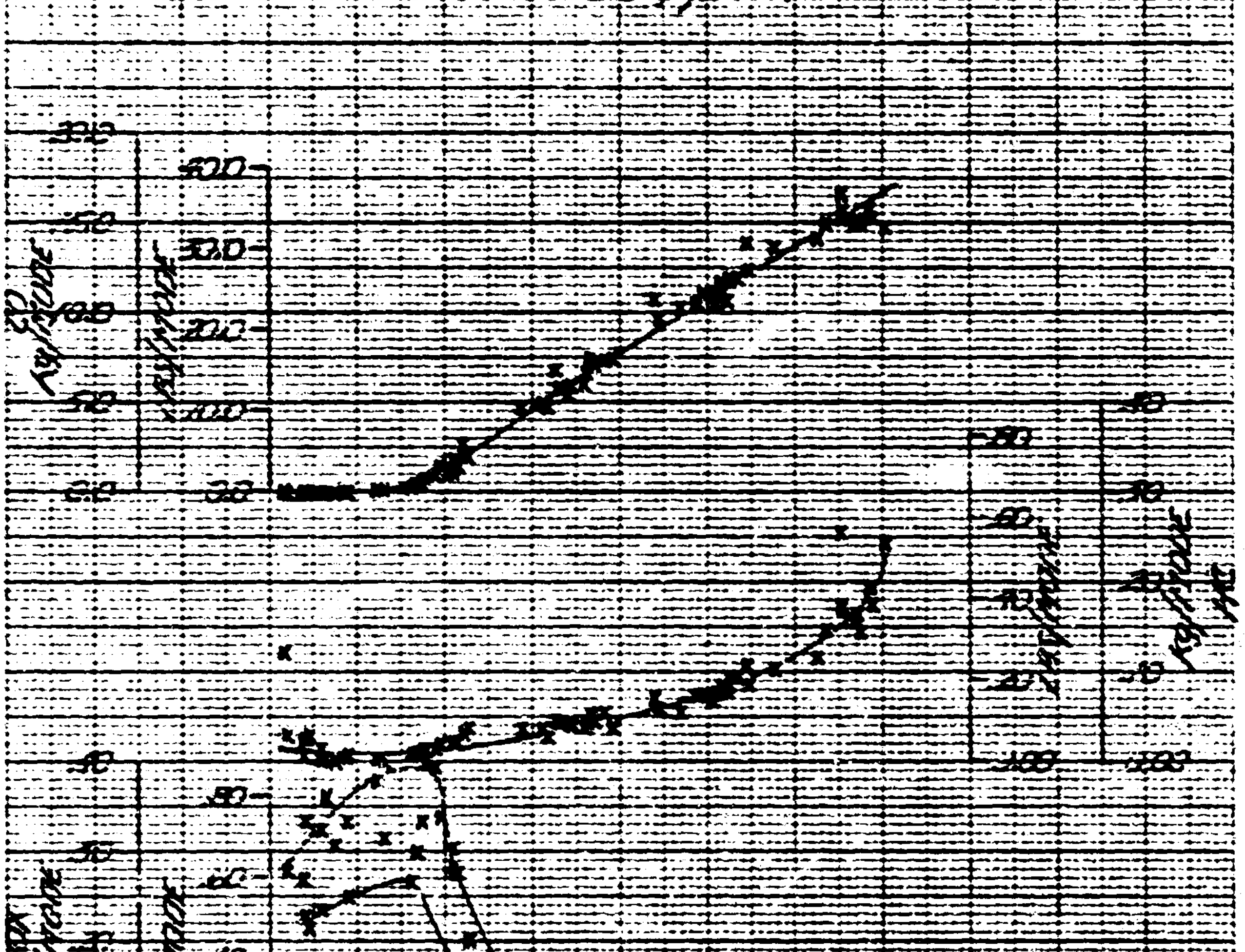

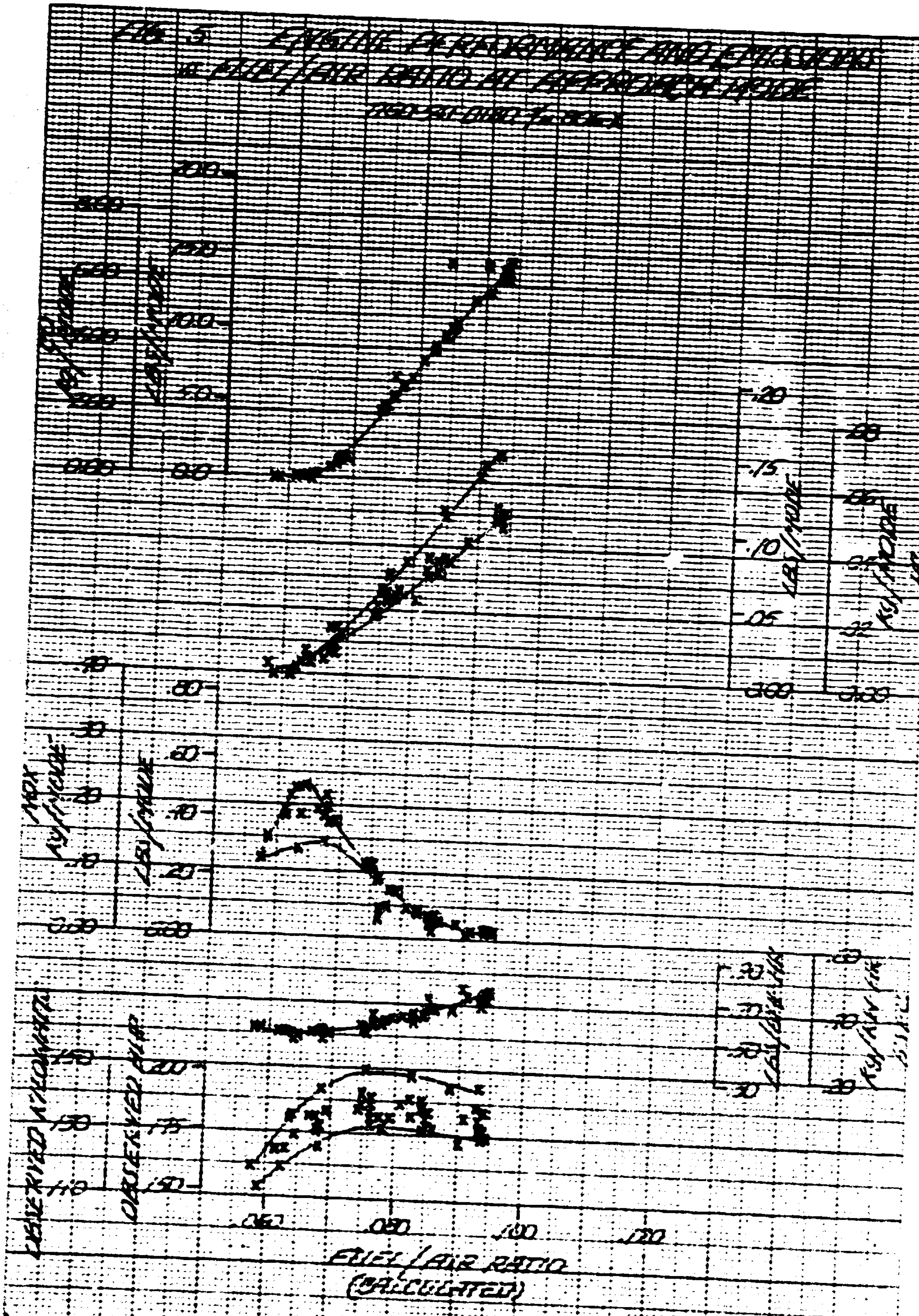
FIG. 5 ENGINE PERFORMANCE AND EMISSIONS
vs FUEL/AIR RATIO AT APPROACH MODE
FUEL/AIR RATIO
(CALCULATED)

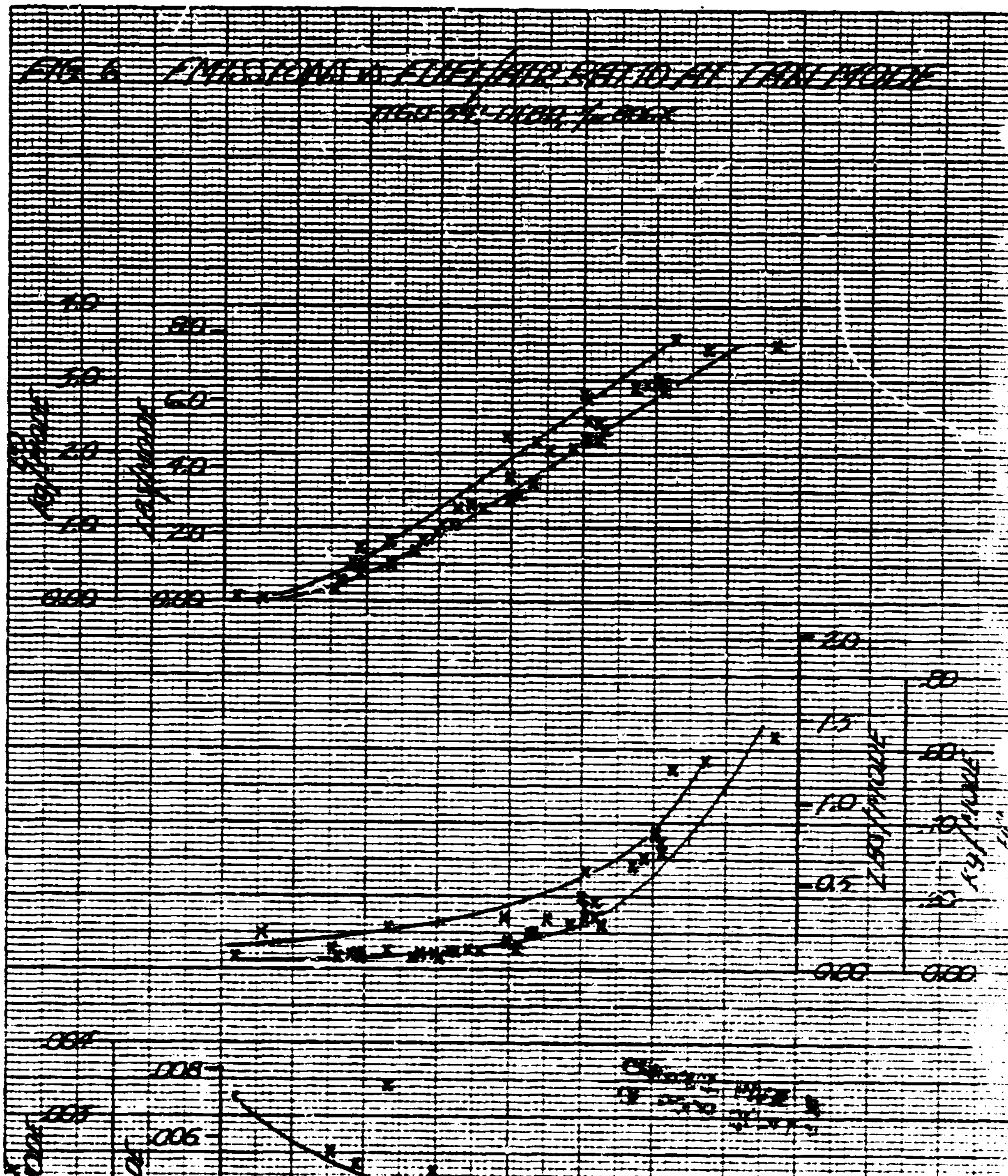
FIG. 6 EMISSIONS vs FUEL/AIR RATIO AT TAXI MODE
LBS/MODE
.050
.070
.090
.110
.130
FUEL/AIR RATIO

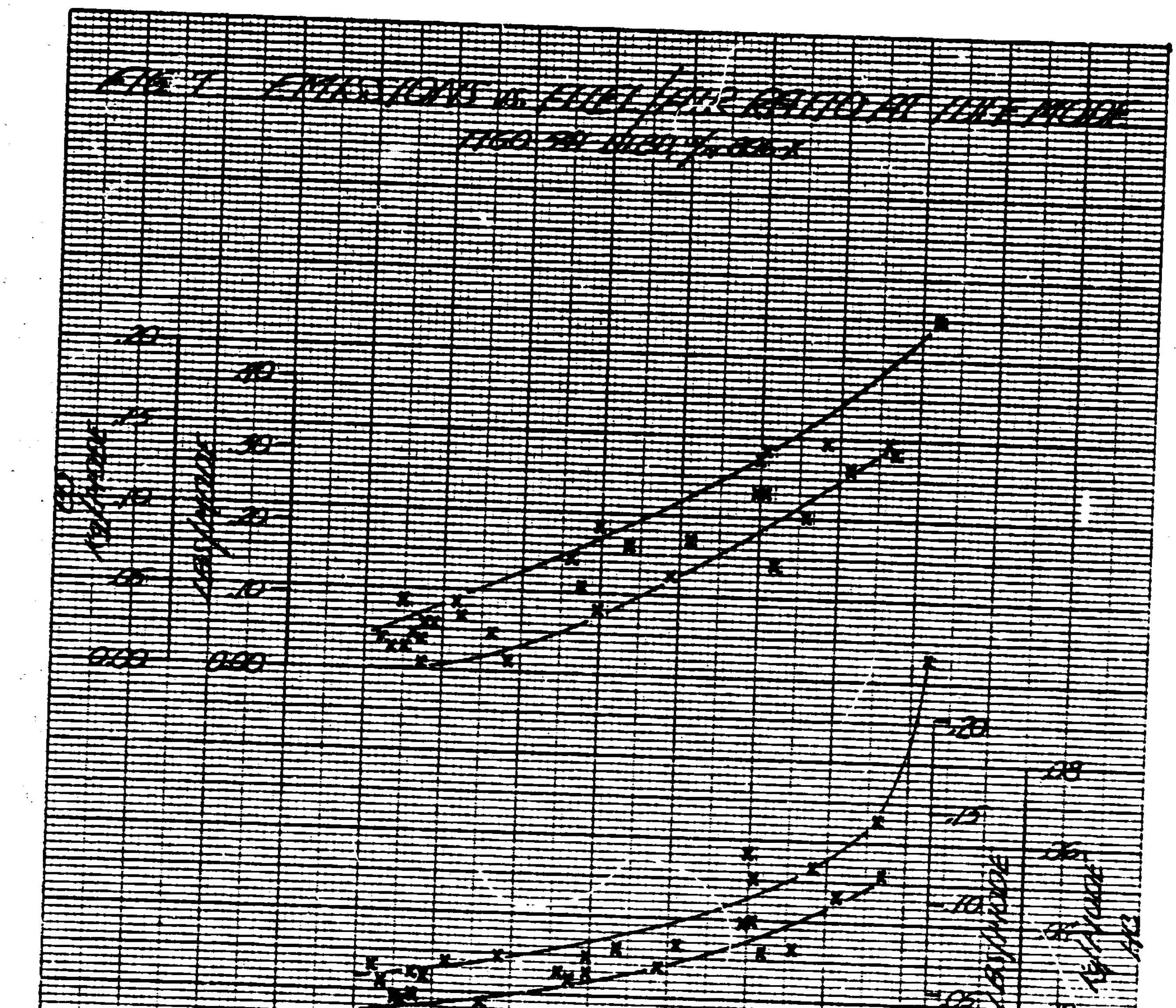
FIG. 7 EMISSIONS vs. FUEL/AIR RATIO AT IDLE MODE
FUEL/AIR RATIO
.050
.070
.090
.110
.130
CO LBS/MODE
CO KG/MODE
HC LBS/MODE
HC KG/MODE
NOX LBS/MODE
NOX KG/MODE

FIG. 8 - SPARKPLUG VOLTAGE vs TIME
CONF. 6.4 MM EXTENDED ELECTRODE

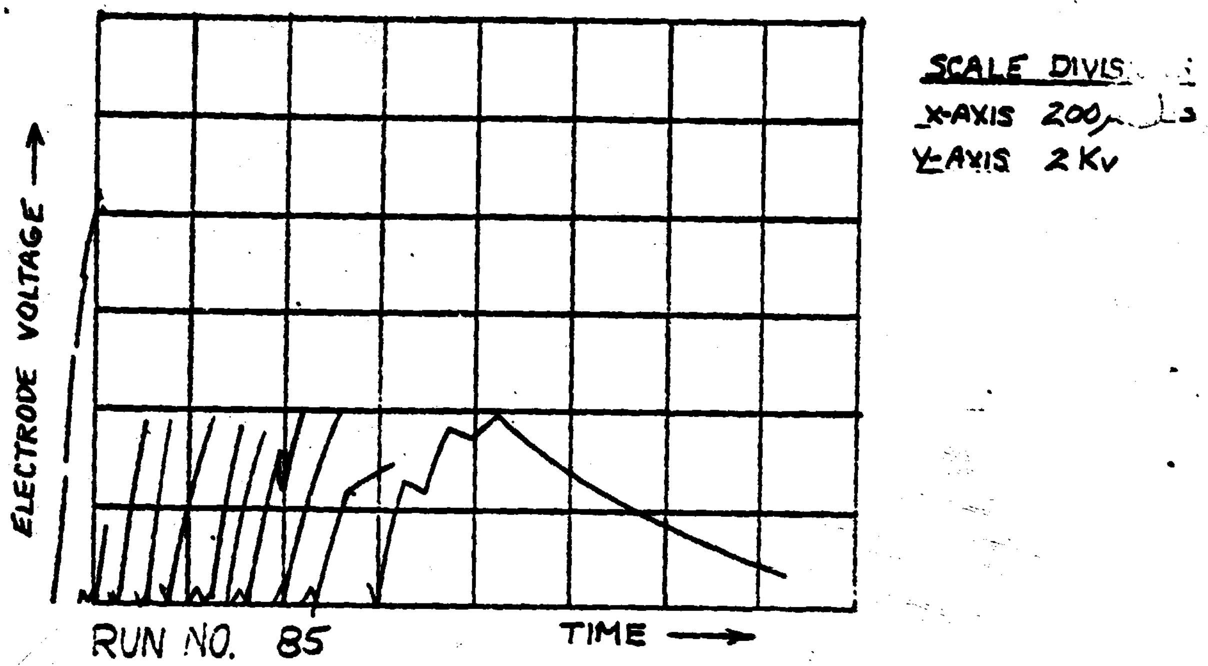

RUN NO. 85
CYLINDER NO. 6 TOP PLUG
MODE CLIMB

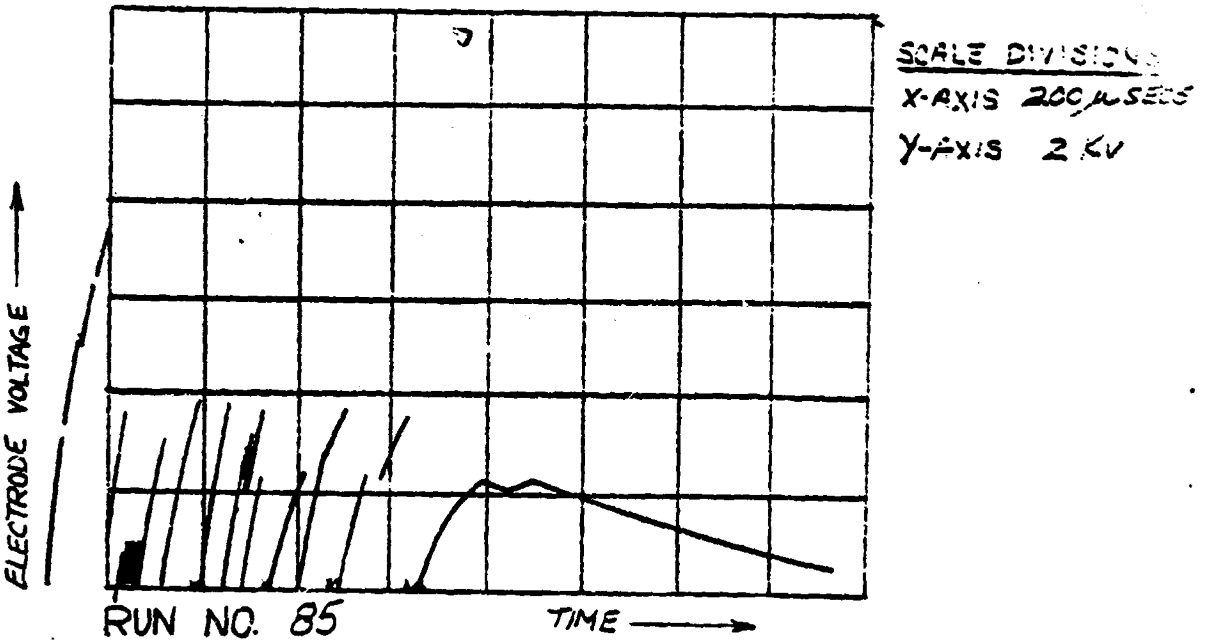

RUN NO. 85
CYLINDER NO. 6 BOTTOM PLUG
MODE CLIMB

FIG. 9 SPARKPLUG VOLTAGE vs. TIME

CONF. 6.4MM EXTENDED ELECTRODE

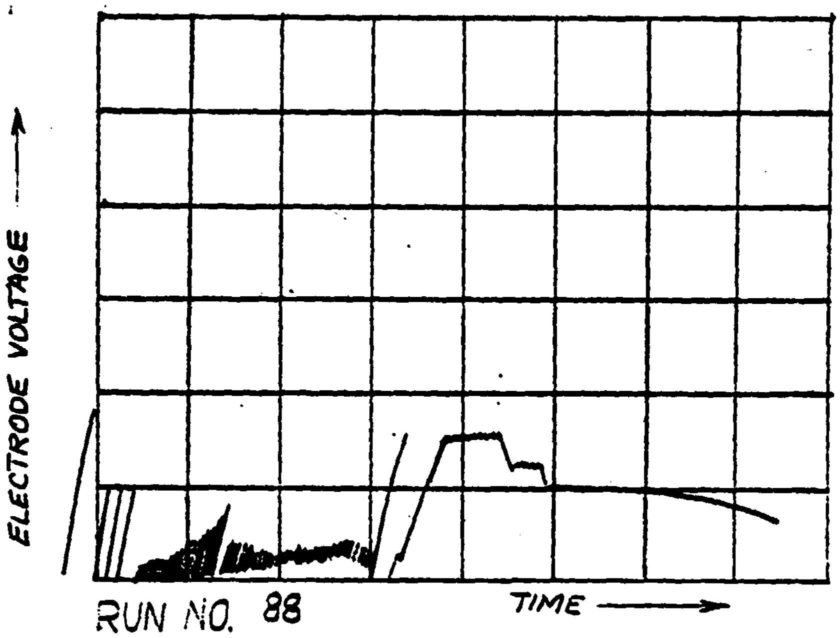

SCALE DIVISIONS
X-AXIS 500 μSECS
Y-AXIS 2 KV

RUN NO. 88
CYLINDER NO. 6 TOP PLUG
MODE TAXI

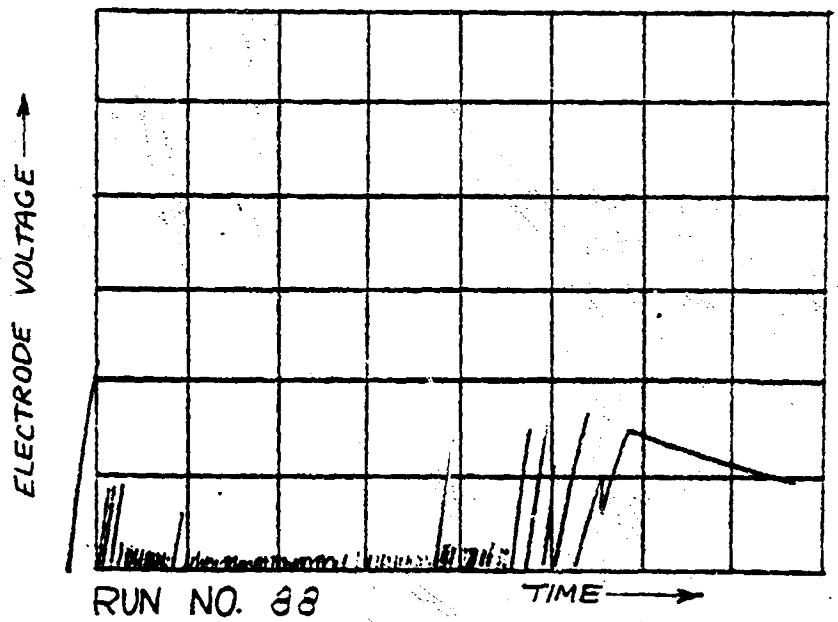

SCALE DIVISIONS
X-AXIS 500 μSECS
Y-AXIS 2 KV

RUN NO. 88
CYLINDER NO. 6 BOTTOM PLUG
MODE TAXI

FIG. 10 SPARKPLUG VOLTAGE vs. TIME

CONF. 6.4MM EXTENDED ELECTRODE

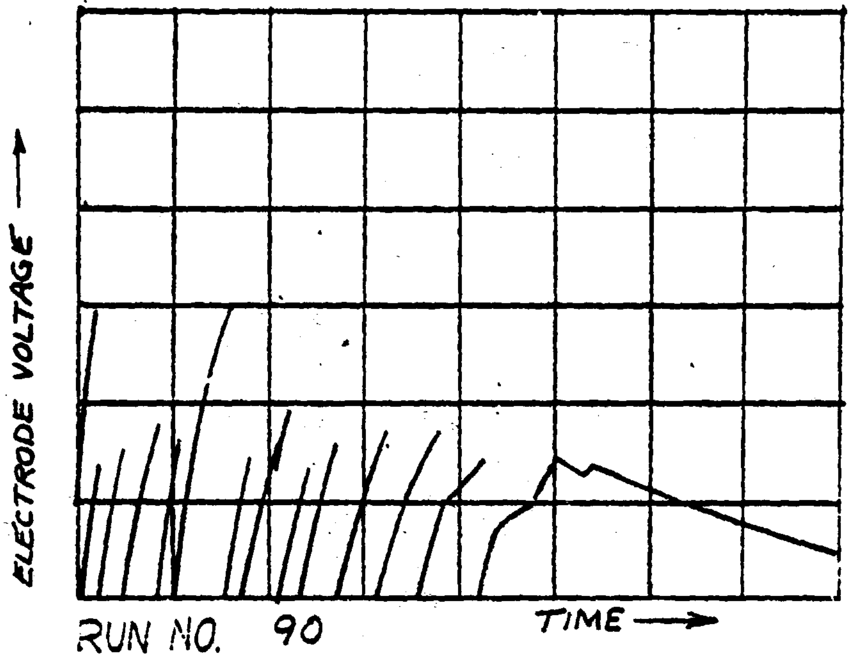

SCALE DIVISIONS
X-AXIS 200μ SECS
Y-AXIS 2 KV

RUN NO. 90
CYLINDER NO. 6 TOP PLUG
MODE APPROACH

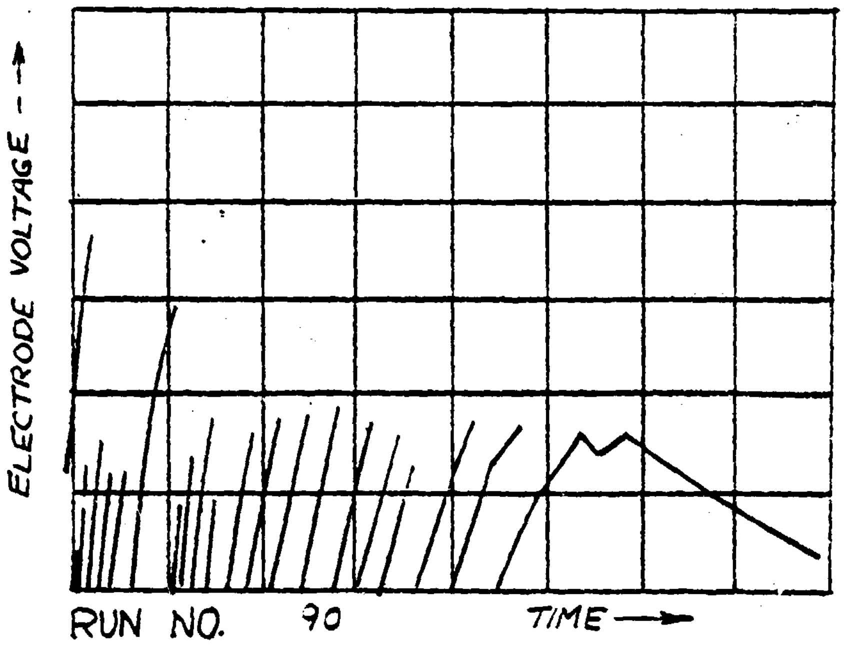

SCALE DIVISIONS
X-AXIS 200μ SECS
Y-AXIS 2 KV

RUN NO. 90
CYLINDER NO. 6 BOTTOM PLUG
MODE APPROACH

FIG. 11. SPARKPLUG VOLTAGE vs. TIME

CONF. STAGGERED, TOP 15° BTC, BOTTOM 25° BTC

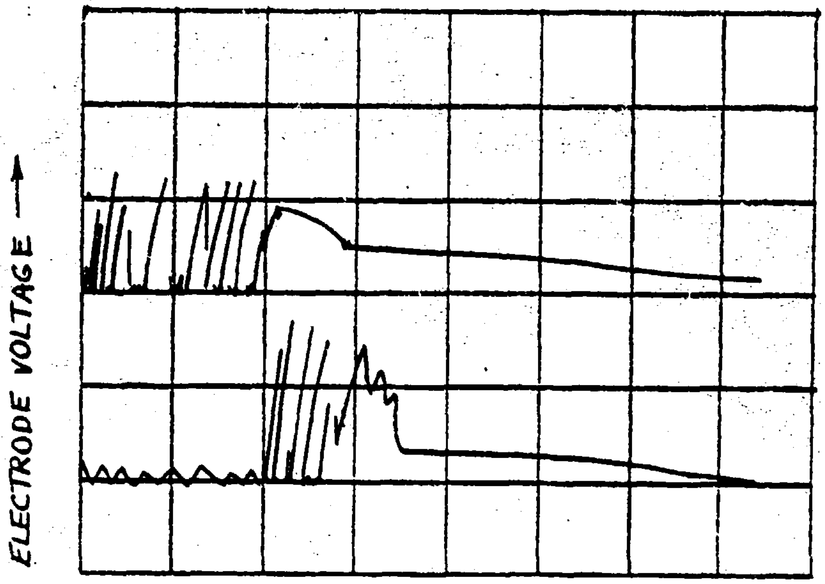

SCALE DIVISIONS
X-AXIS 500 μ Secs
Y-AXIS 5 Kv

RUN NO. 348 TIME →
CYLINDER NO. 6 TOP & BOTTOM
MODE CLIMB

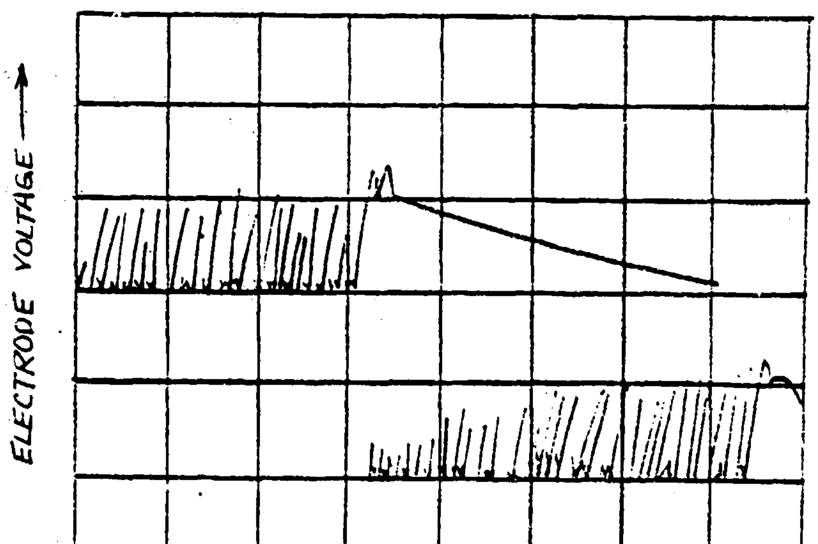

SCALE DIVISIONS
X-AXIS 500 μ Sec
Y-AXIS 2 Kv

RUN NO. 351 TIME →
CYLINDER NO. 6 TOP & BOTTOM
MODE TAXI

FIG. 12 SPARKPLUG VOLTAGE vs. TIME

– – CONF. CAPACITIVE DISCHARGE IGNITION
LONG DURATION COILS

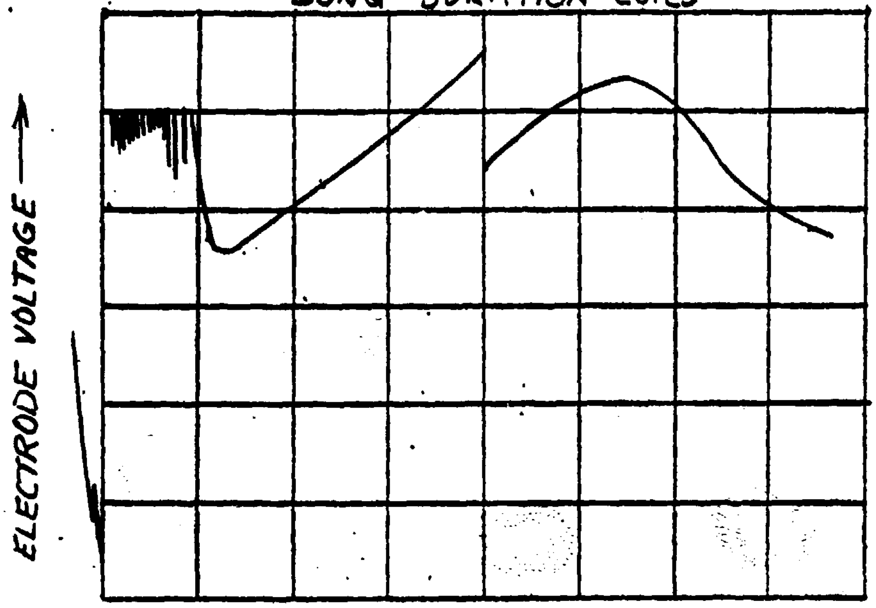

SCALE DIVISIONS
X-AXIS 200 μ Secs
Y-AXIS 2 KV

RUN NO. 415 TIME →
CYLINDER NO. 4 TOP PLUG
MODE APPROACH

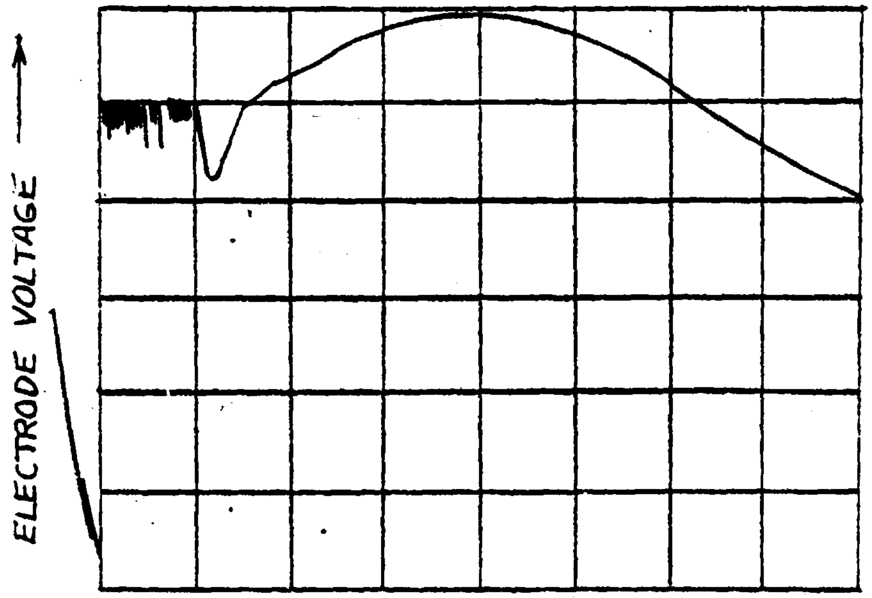

SCALE DIVISIONS
X-AXIS 200 μ Secs
Y-AXIS 2 KV

RUN NO. 415 TIME →
CYLINDER NO. 4 BOTTOM PLUG
MODE APPROACH

FIG. 13 SPARKPLUG VOLTAGE vs. TIME

CONF. MULTIPLE SPARK IGNITION

20° DURATION

SCALE DIVISIONS

X-AXIS 200μ SECS

Y-AXIS 5 KV

RUN NO. 479

CYLINDER NO. 6 TOP PLUG

MODE APPROACH

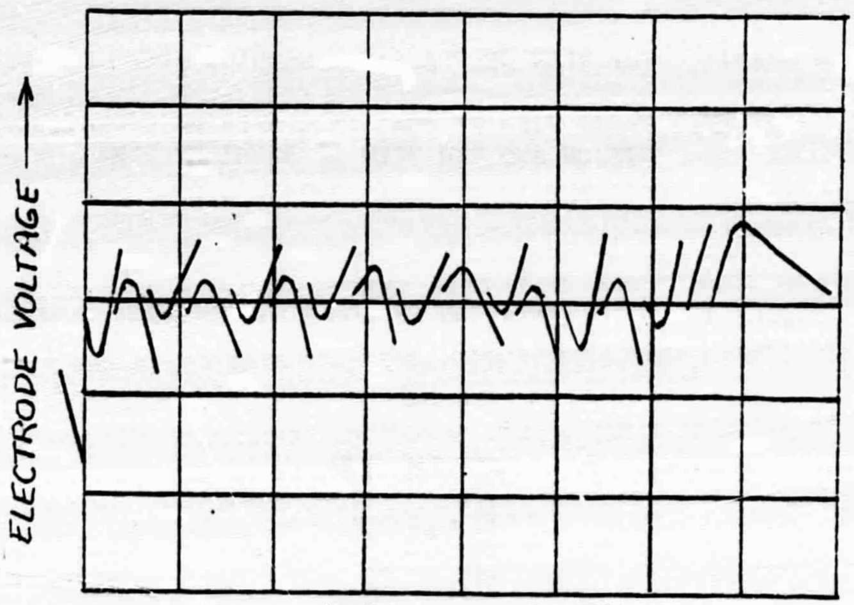

SCALE DIVISIONS

X-AXIS 200μ SECS

Y-AXIS 5 KV

RUN NO. 479

CYLINDER NO. 6 BOTTOM PLUG

MODE APPROACH

ORIGINAL PAGE IS OF POOR QUALITY

FIG. 13 SPARKPLUG VOLTAGE vs. TIME

CONF. MULTIPLE SPARK IGNITION

20° DURATION

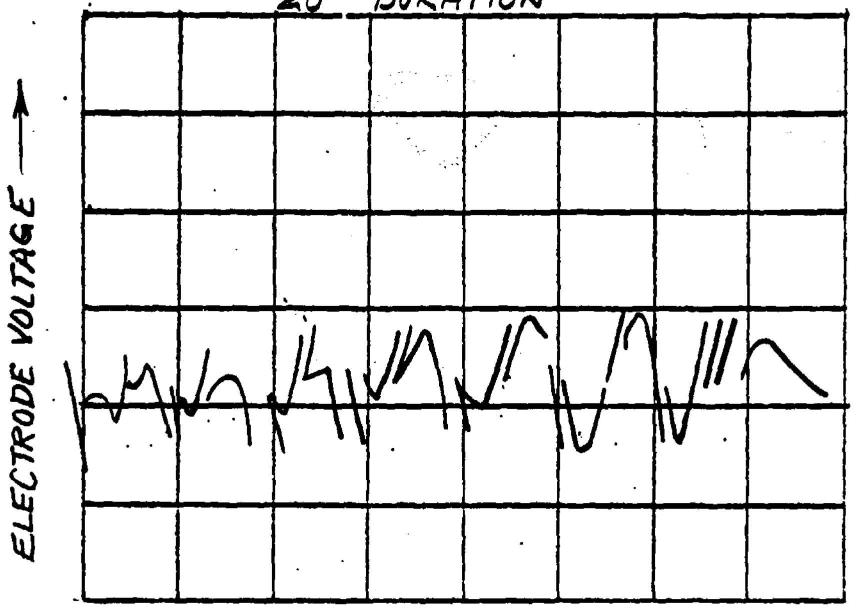

SCALE DIVISIONS

X-AXIS 200μ Secs

Y-AXIS 5 KV

RUN NO. 479 TIME →

CYLINDER NO. 6 TOP PLUG

MODE APPROACH

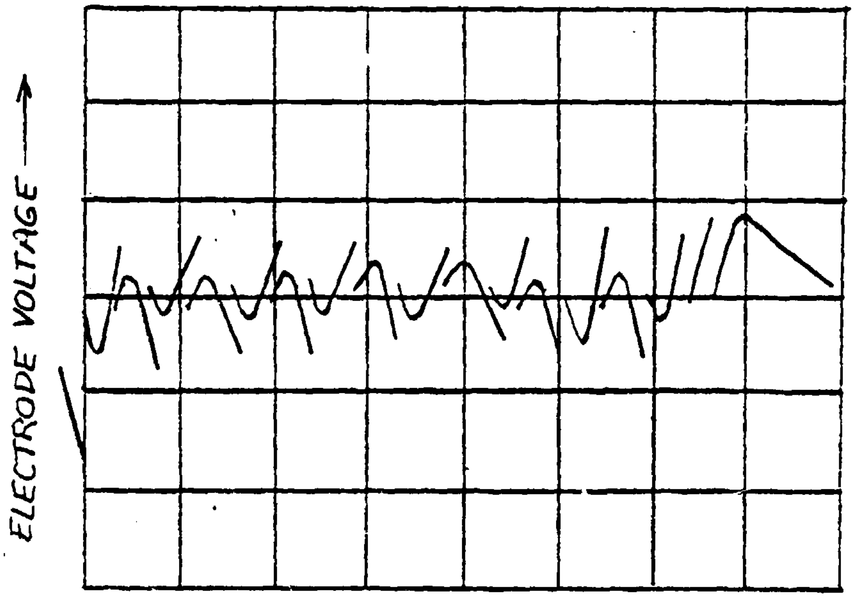

SCALE DIVISIONS

X-AXIS 200μSECS

Y-AXIS 5 KV

RUN NO. 479 TIME →

CYLINDER NO. 6 BOTTOM PLUG

MODE APPROACH

ORIGINAL PAGE IS OF POOR QUALITY

Lycoming
Avco CORPORATION

REPORT NO.

FIGURE 14

POST CARBURETOR ATOMIZER PHOTOGRAPH

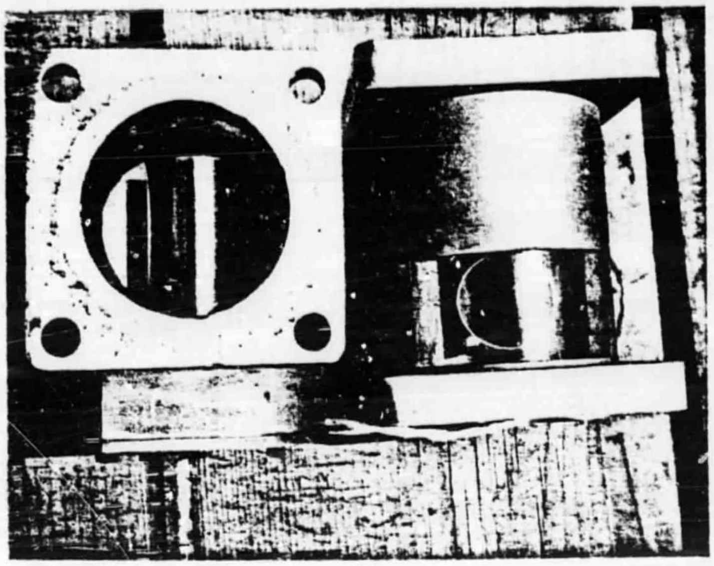

LEFT: TOP VIEW OF PCA S/N 1 SHOWING ATOMIZER TUBE

RIGHT: FRONT VIEW OF PCA S/N 2 SHOWING OBSERVATION WINDOW AND END VIEW OF ATOMIZER TUBE

FIGURE 15 - ORIENTATION OF PCA TO CARBURETOR (STANDARD)

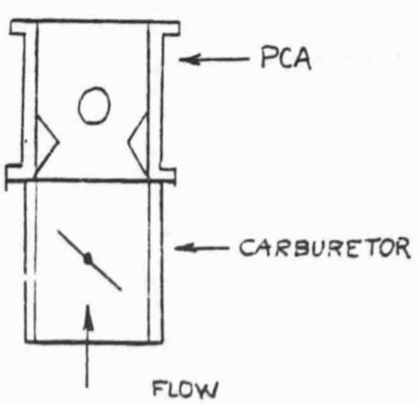

Lycoming
Avco CORPORATION

REPORT NO.

FIGURE 14

POST CARBURETOR ATOMIZER PHOTOGRAPH

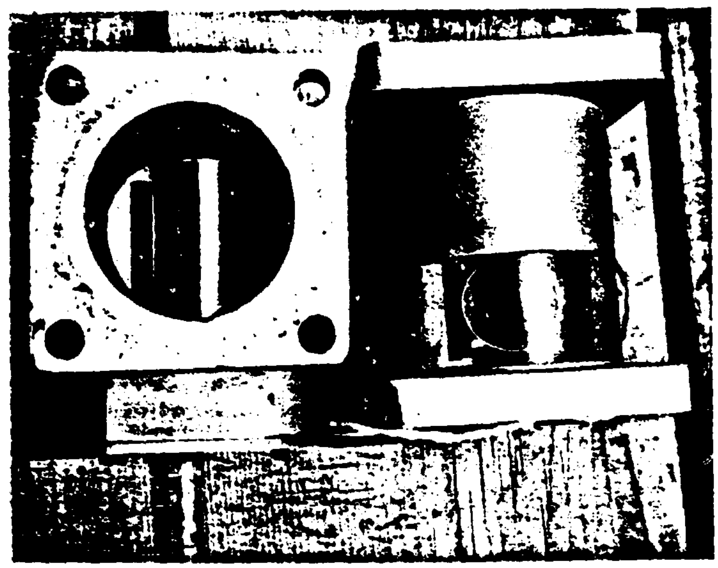

LEFT: TOP VIEW OF PCA S/N 1 SHOWING ATOMIZER TUBE

RIGHT: FRONT VIEW OF PCA S/N 2 SHOWING OBSERVATION WINDOW AND END VIEW OF ATOMIZER TUBE

FIGURE 15 - ORIENTATION OF PCA TO CARBURETOR (STANDARD)

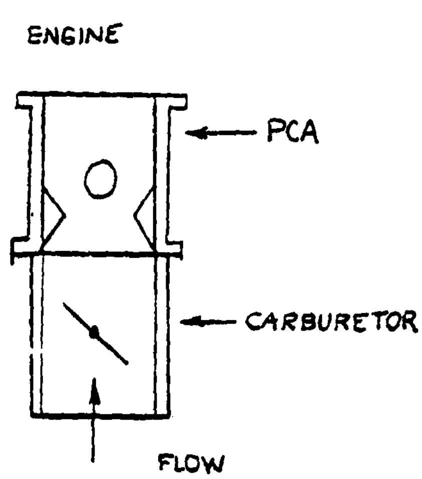

Lycoming
Avco CORPORATION

FIGURE 16

EXHAUST SAMPLING SYSTEM

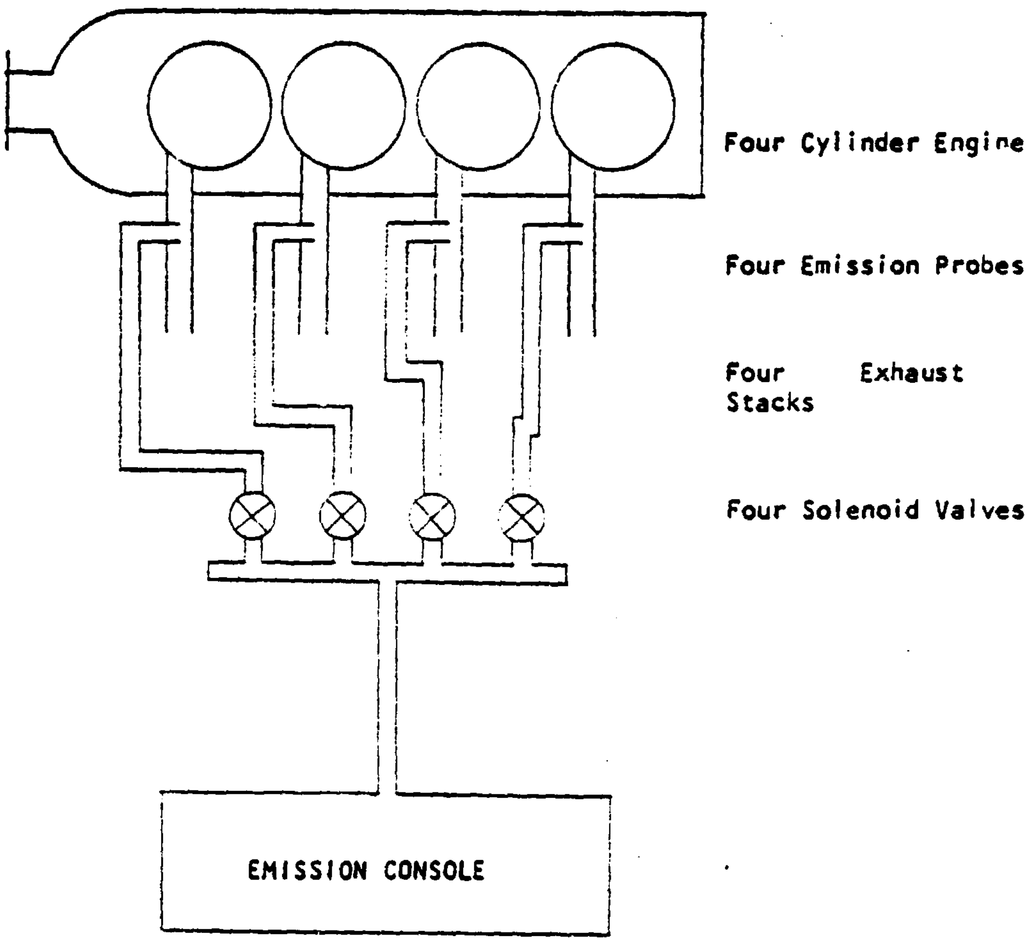

SCHEMATIC OF SELECTIVE EXHAUST SAMPLING SYSTEM

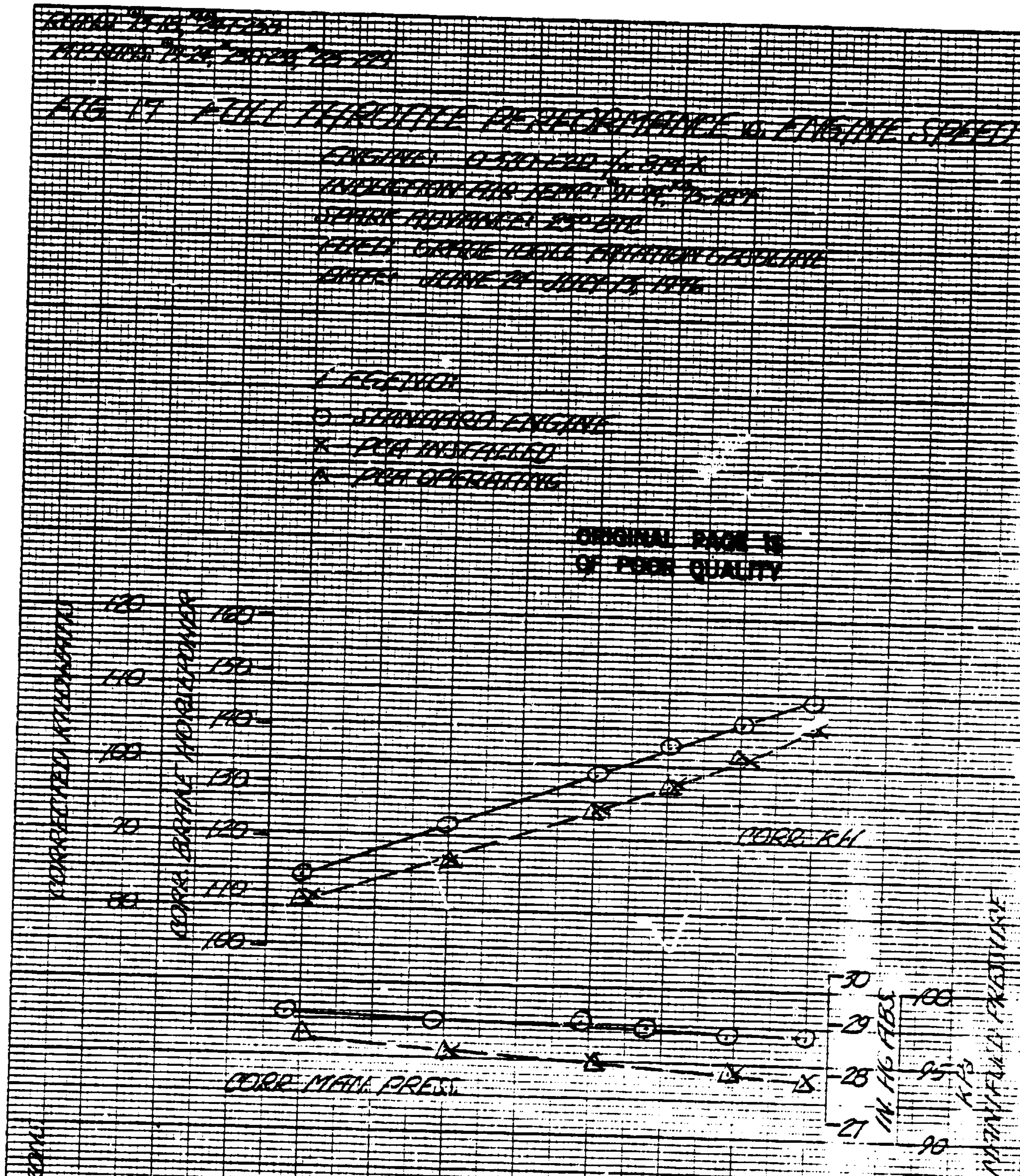
FIG 17 FULL THROTTLE PERFORMANCE vs ENGINE SPEED
LEGEND
STANDARD ENGINE
PCA INSTALLED
PCA OPERATING
CORRECTED KILOWATTS
CORR BRAKE HORSEPOWER
120
110
100
90
80
160
150
140
130
120
110
100
CORR KW
CORR MAN PRESS
IN. HG ABS
30
29
28
27
100
95
90
CORR MANIFOLD PRESSURE
BRAKE SPEC FUEL CONS
BSFC
40
35
30
.60
.50
2000
2200
2400
2600
2800
ENGINE SPEED RPM

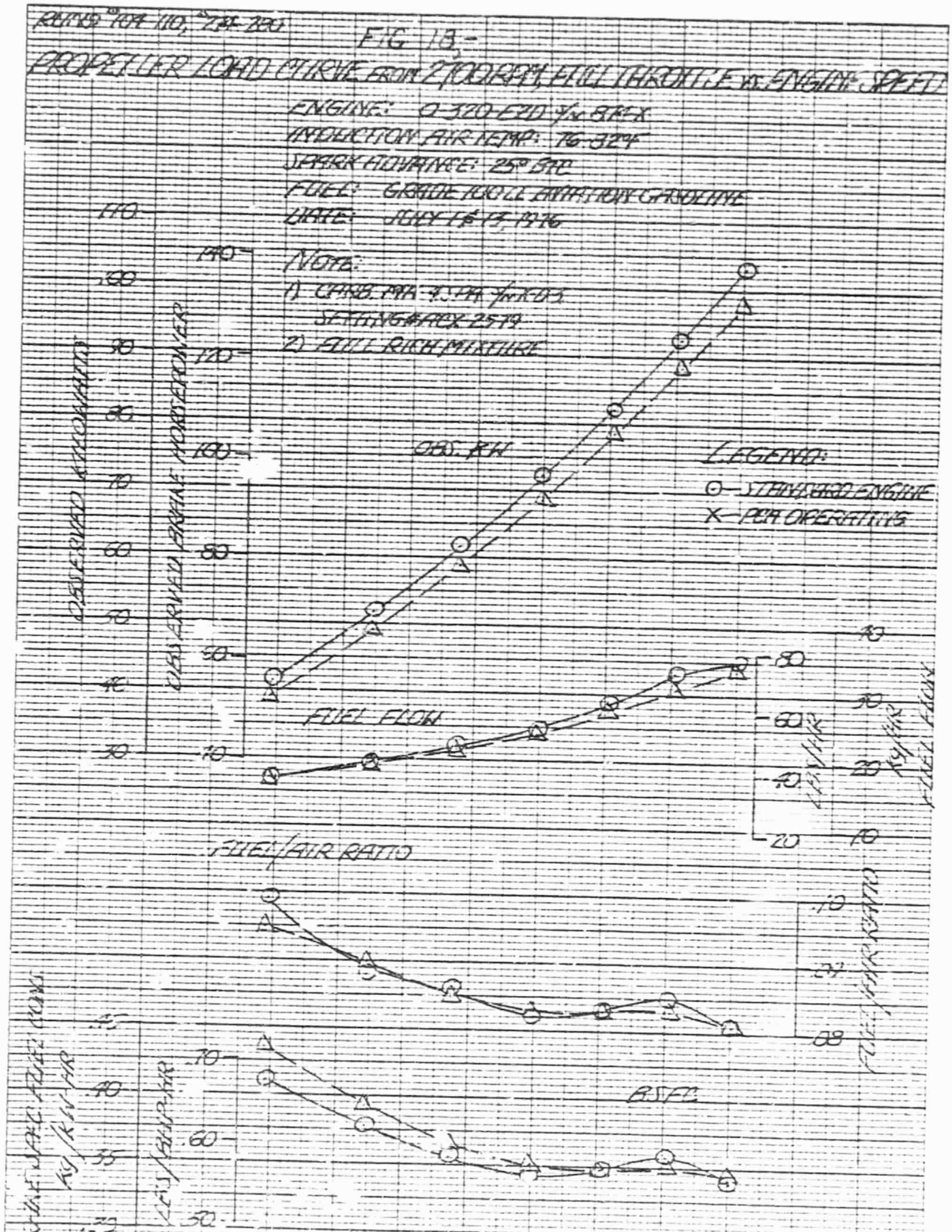
FIG 18
PROPELLER LOAD CURVE FROM 2700 RPM, FULL THROTTLE vs. ENGINE SPEED
ENGINE: O-320-E2D
SPARK ADVANCE: 25° BTC
FUEL: GRADE 100LL AVIATION GASOLINE
NOTE:
1) CARB. MA-4SPA
2) FULL RICH MIXTURE
OBS. BH
LEGEND:
O—STANDARD ENGINE
X—PCR OPERATING
OBSERVED BRAKE HORSEPOWER
OBSERVED KILOWATTS
FUEL FLOW
FUEL/AIR RATIO
BSFC
1900
2100
2300
2500
2700
ENGINE SPEED - RPM

FIGURE 19 - ULTRASONIC FUEL VAPORIZATION PROGRAM

TAKE OFF EMISSIONS (.075 F/A)

DIFFERENCES IN CYLINDER TO CYLINDER EMISSION LEVELS

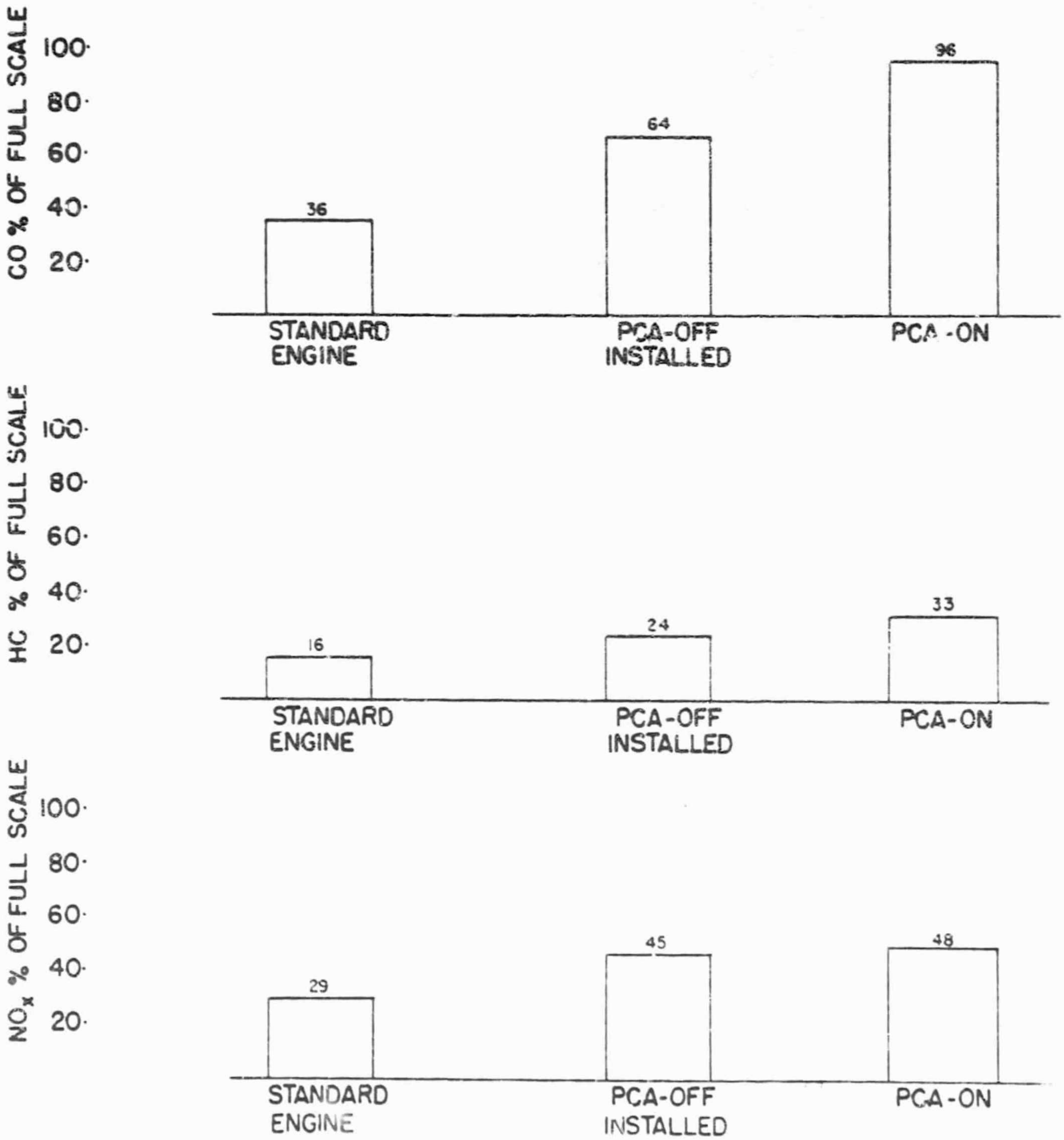

FIGURE 20 - **ULTRASONIC FUEL VAPORIZATION PROGRAM**

CLIMB EMISSIONS (.075 F/A)

DIFFERENCES IN CYLINDER TO CYLINDER EMISSION LEVELS

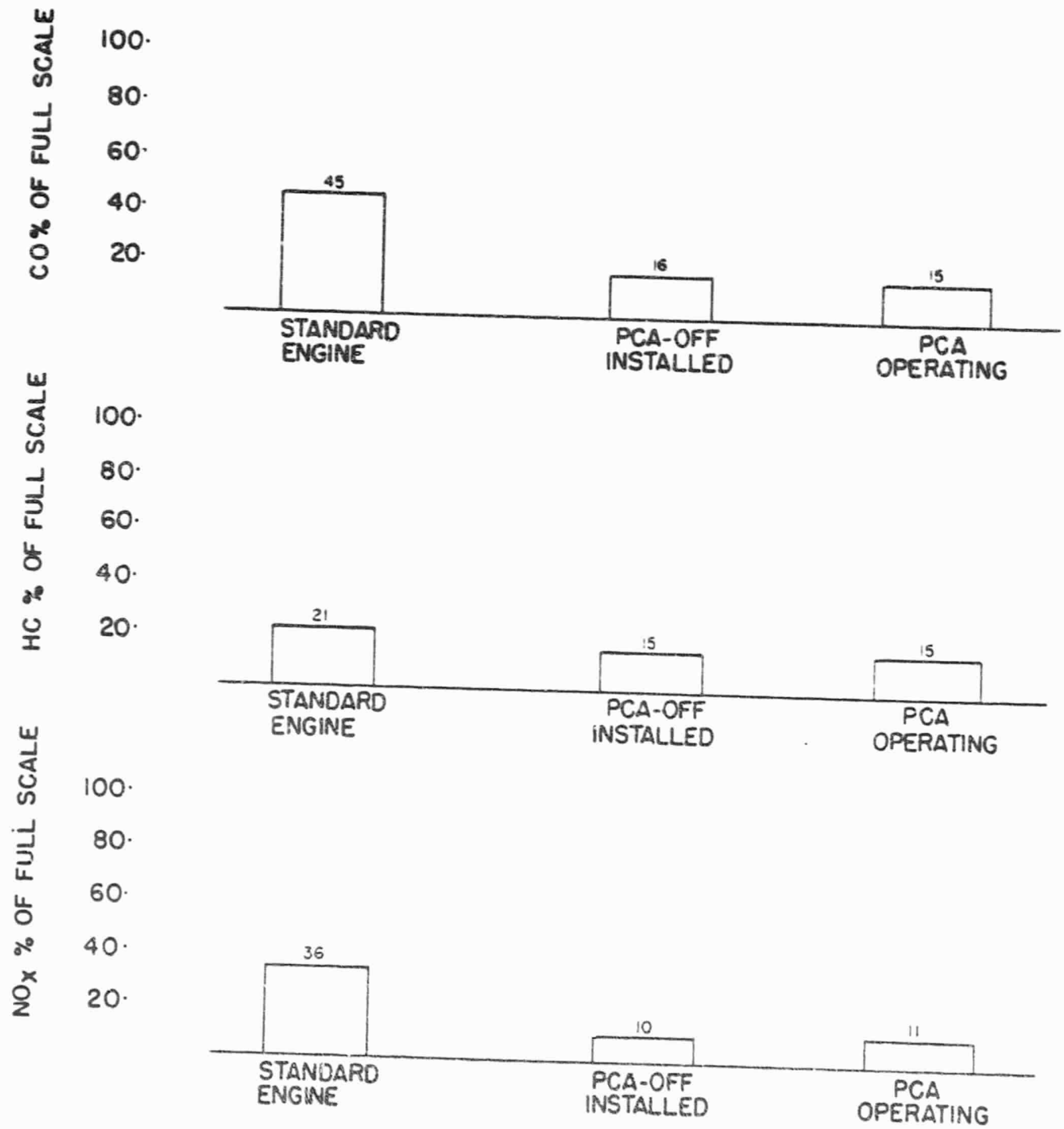

FIGURE 21 - **ULTRASONIC FUEL VAPORIZATION PROGRAM**

APPROACH EMISSIONS (.075 F/A)

DIFFERENCES IN CYLINDER TO CYLINDER EMISSION LEVELS

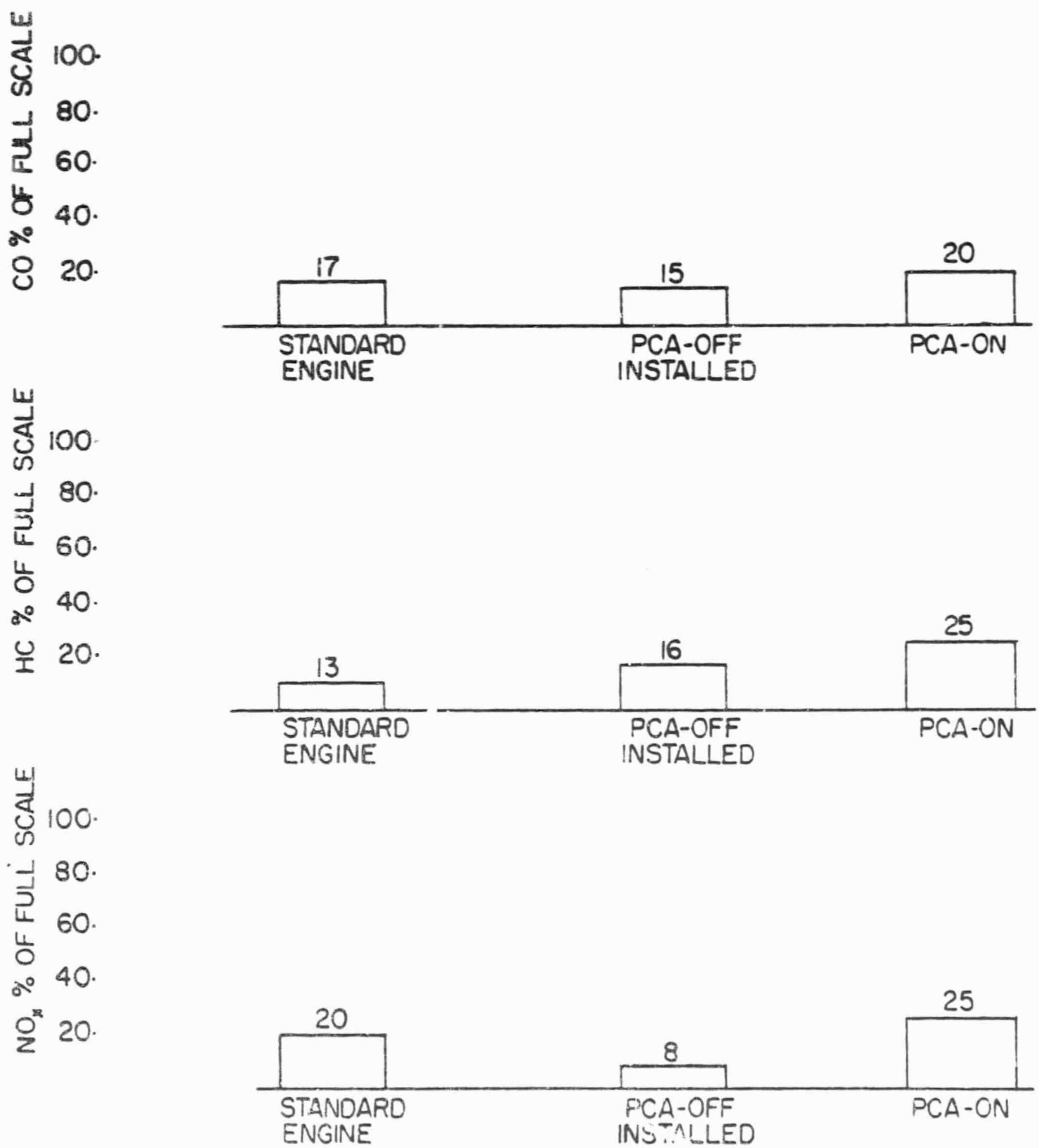

FIGURE 22 - **ULTRASONIC FUEL VAPORIZATION PROGRAM**

TAXI EMISSIONS (.090 F/A)

DIFFERENCES IN CYLINDER TO CYLINDER EMISSION LEVELS

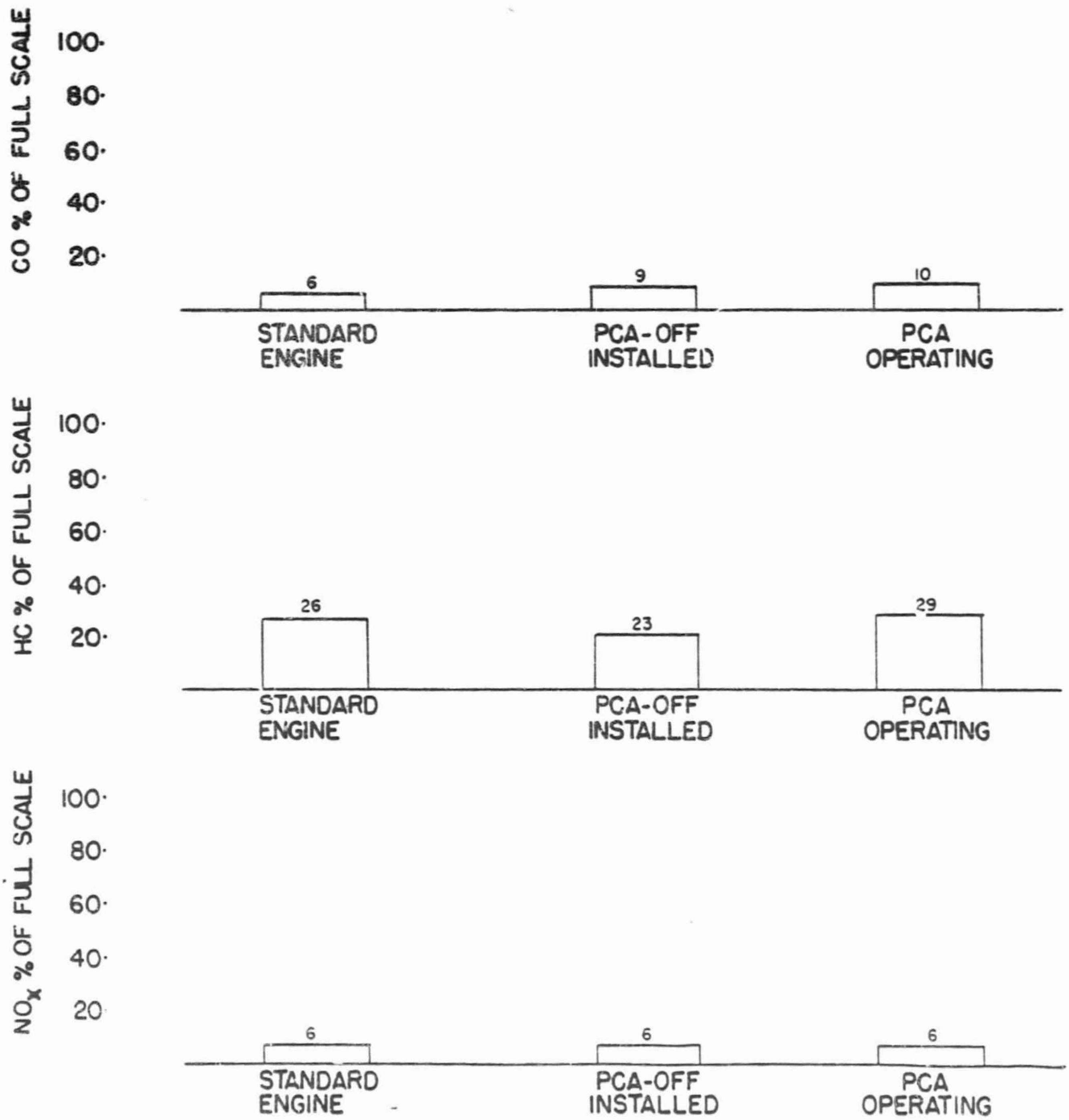

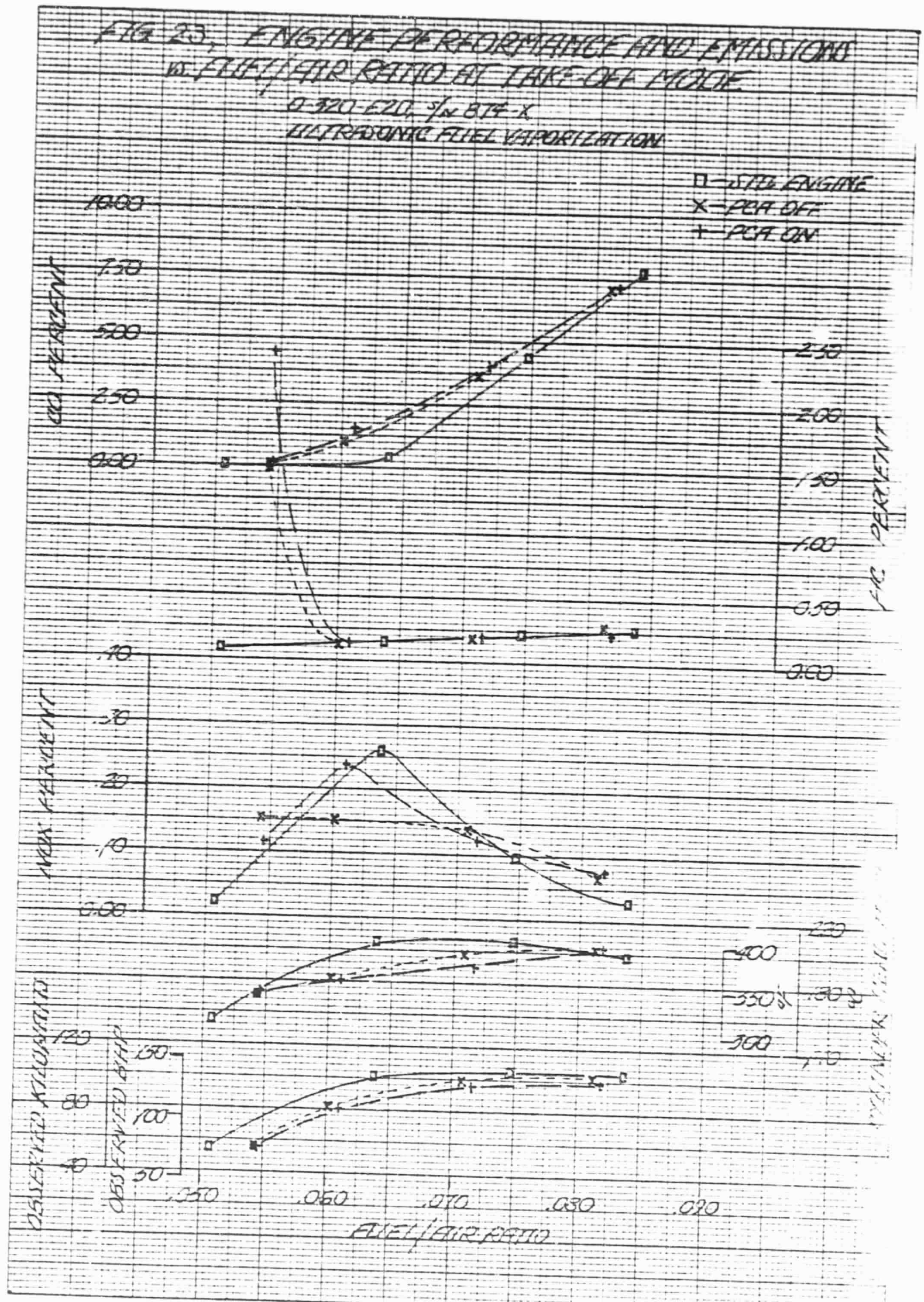
FIG 23, ENGINE PERFORMANCE AND EMISSIONS
vs FUEL/AIR RATIO AT TAKE-OFF MODE
O-320-E2D, S/N 874-X
ULTRASONIC FUEL VAPORIZATION
□ - STD ENGINE
X - PCA OFF
+ - PCA ON
CO PERCENT
10.00
7.50
5.00
2.50
0.00
HC PERCENT
2.50
2.00
1.50
1.00
0.50
0.00
NOX PERCENT
.40
.30
.20
.10
0.00
OBSERVED KILOWATTS
120
80
40
OBSERVED BHP
150
100
50
400
350
300
2.0
1.50
1.0
.050
.060
.070
.080
.090
FUEL/AIR RATIO

FIG. 24 ENGINE PERFORMANCE AND EMISSIONS vs. FUEL/AIR RATIO AT CLIMB MODE

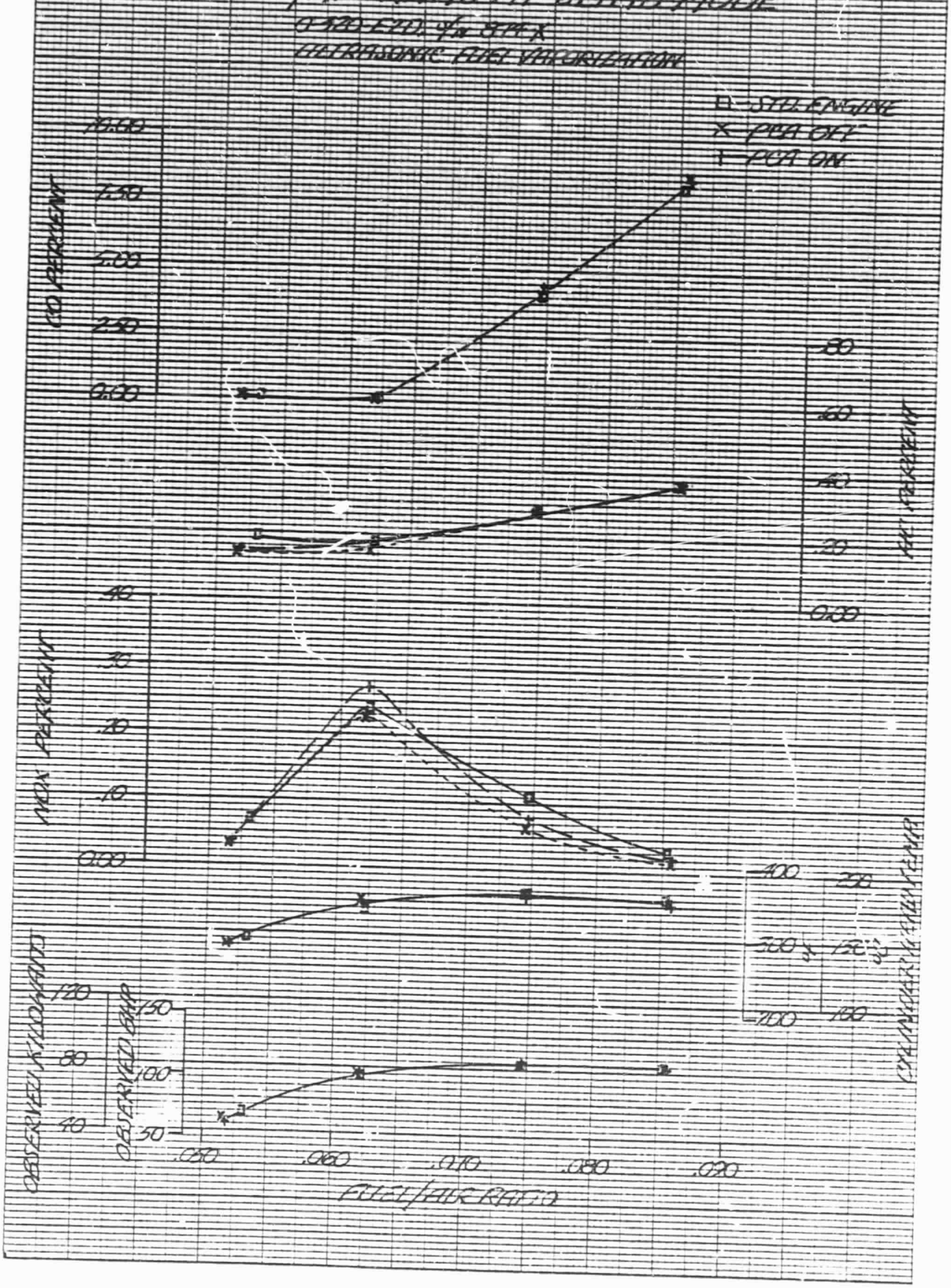

FIG. 25 ENGINE PERFORMANCE AND EMISSIONS vs FUEL/AIR RATIO AT APPROACH MODE

O-320 E2D S/N 514X

ULTRASONIC FUEL VAPORIZATION

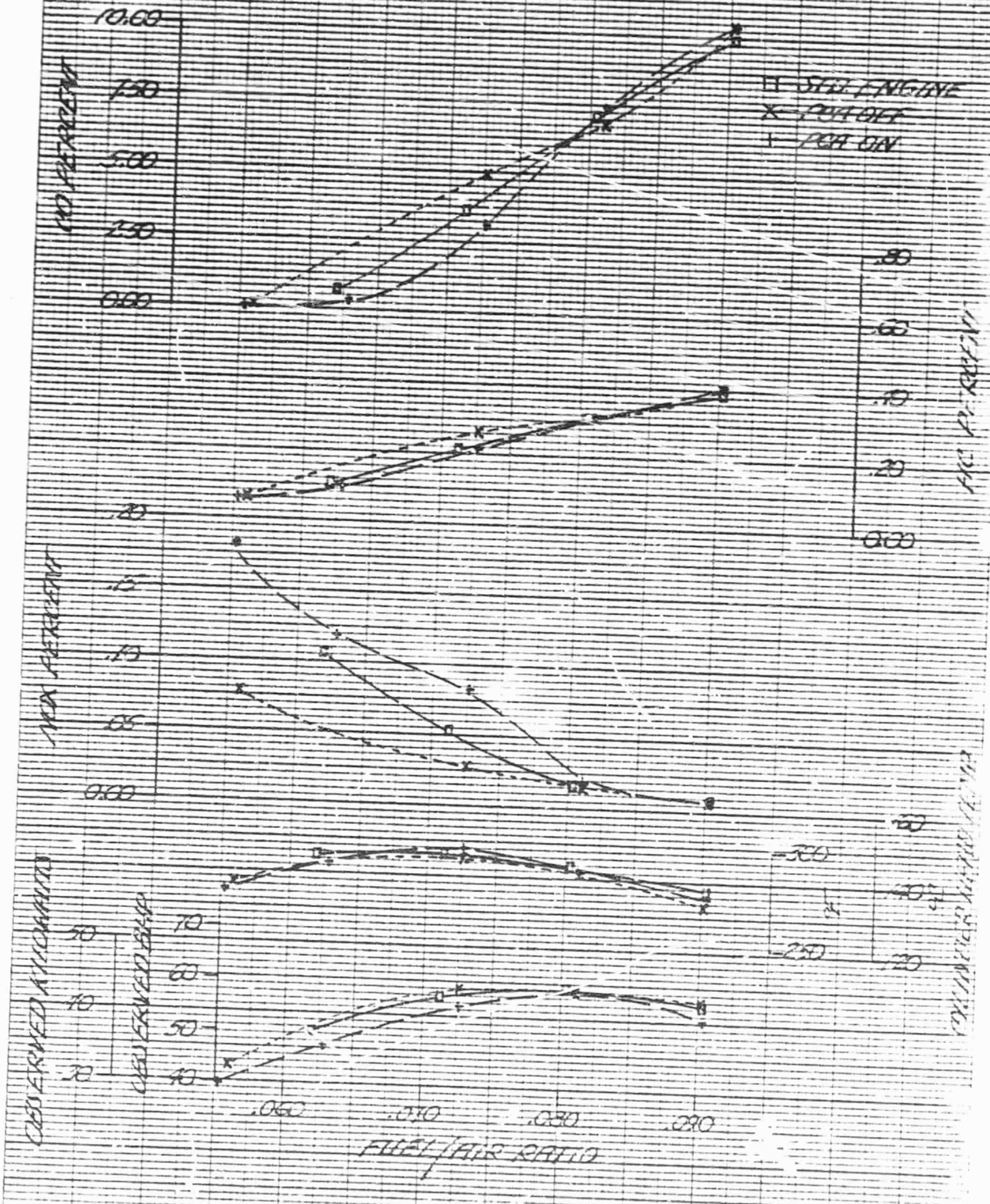

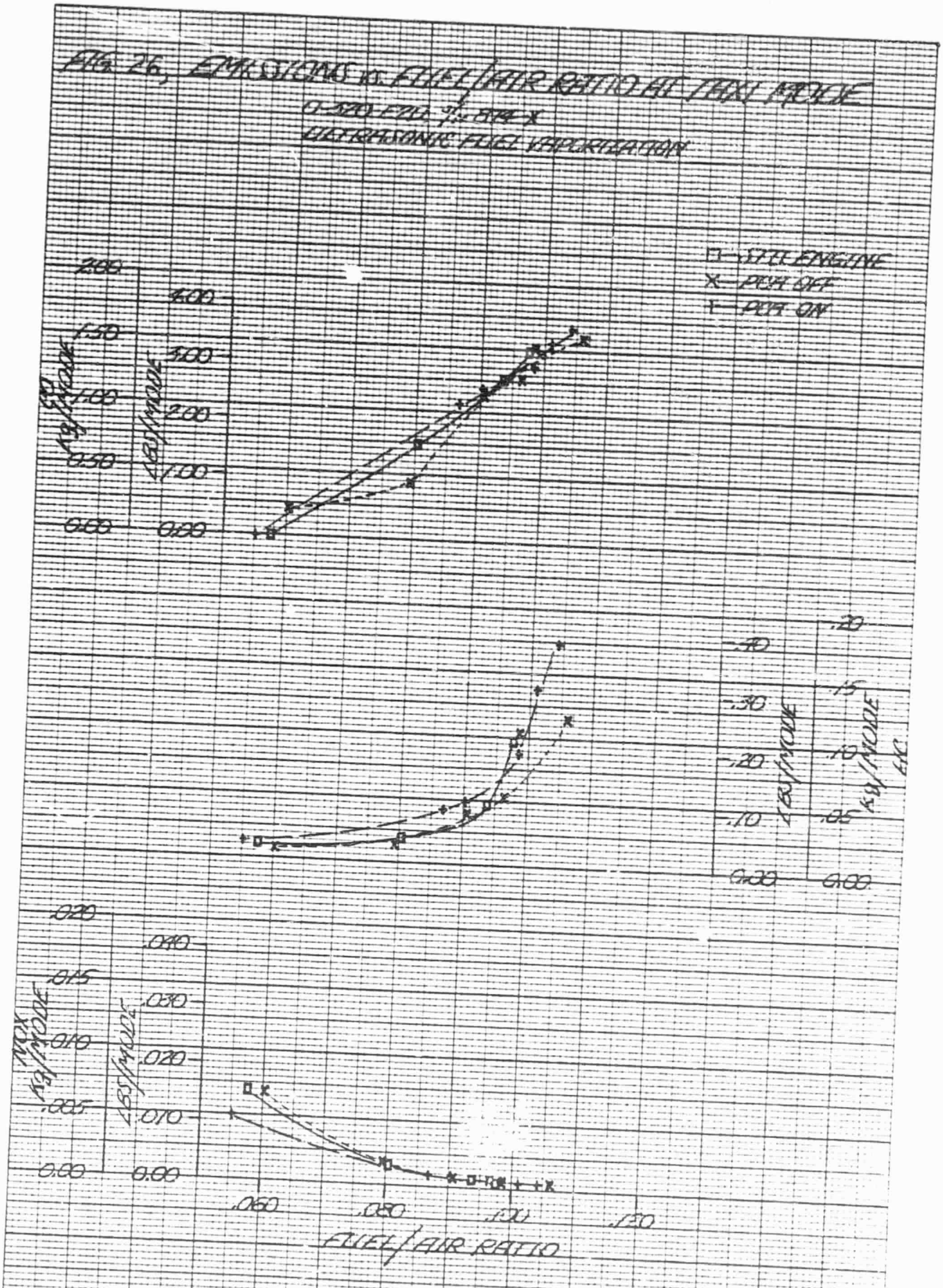
FIG 26, EMISSIONS vs FUEL/AIR RATIO AT TAXI MODE
O-320-E2D ⅞ 884 X
ULTRASONIC FUEL VAPORIZATION
□ STD ENGINE
X PER OFF
+ PER ON
CO
KG/MODE
LBS/MODE
HC
KG/MODE
LBS/MODE
NOX
KG/MODE
LBS/MODE
FUEL/AIR RATIO

FIG. 27, ENGINE PERFORMANCE AND EMISSIONS vs. FUEL/AIR RATIO AT CLIMB MODE

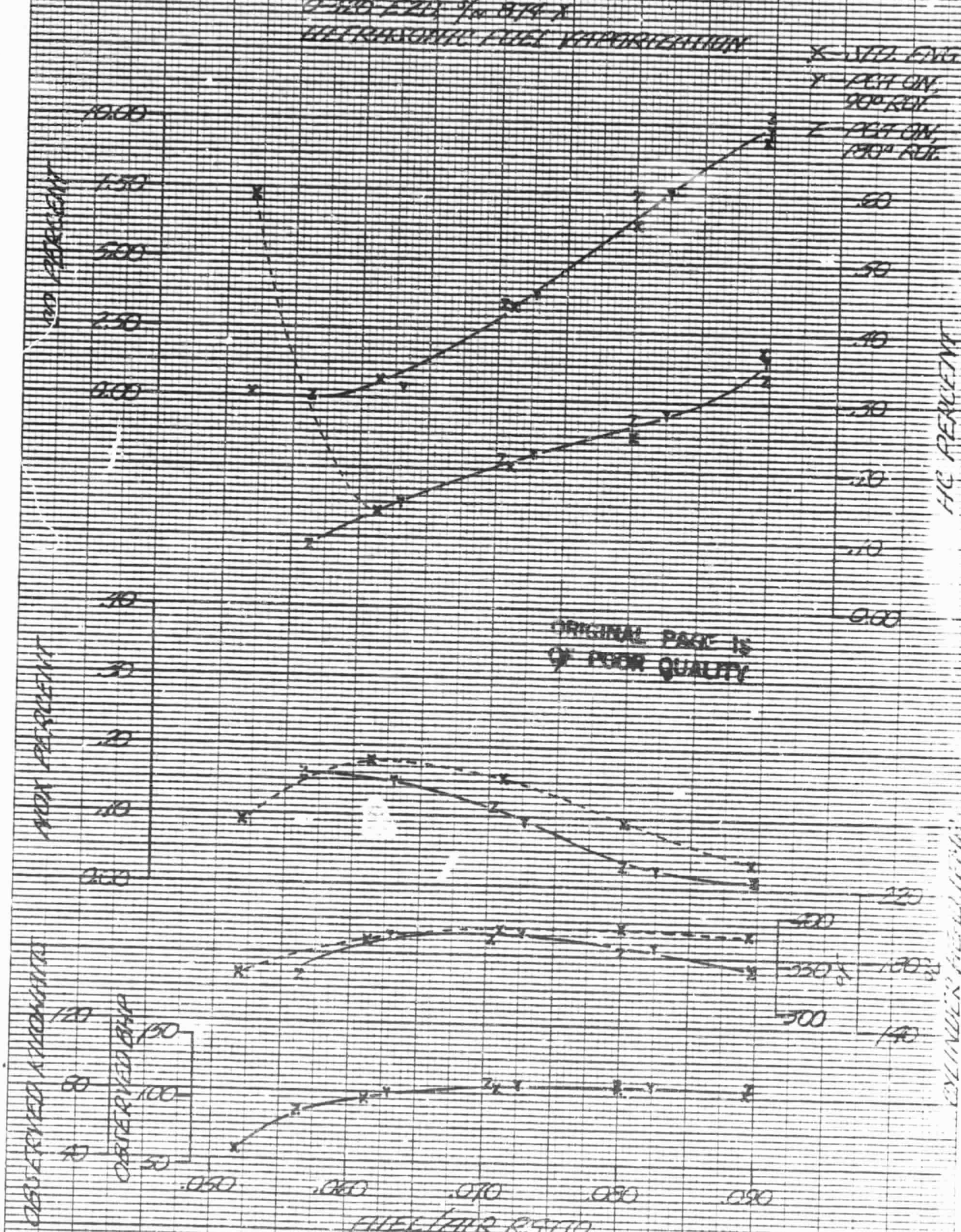

FIGURE 28

REPRESENTATIVE EFFECT OF LEANING ON CYLINDER HEAD TEMPERATURE, E G T (EXHAUST GAS TEMPERATURE) ENGINE POWER AND SPECIFIC FUEL CONSUMPTION AT CONSTANT ENGINE RPM AND MANIFOLD PRESSURE

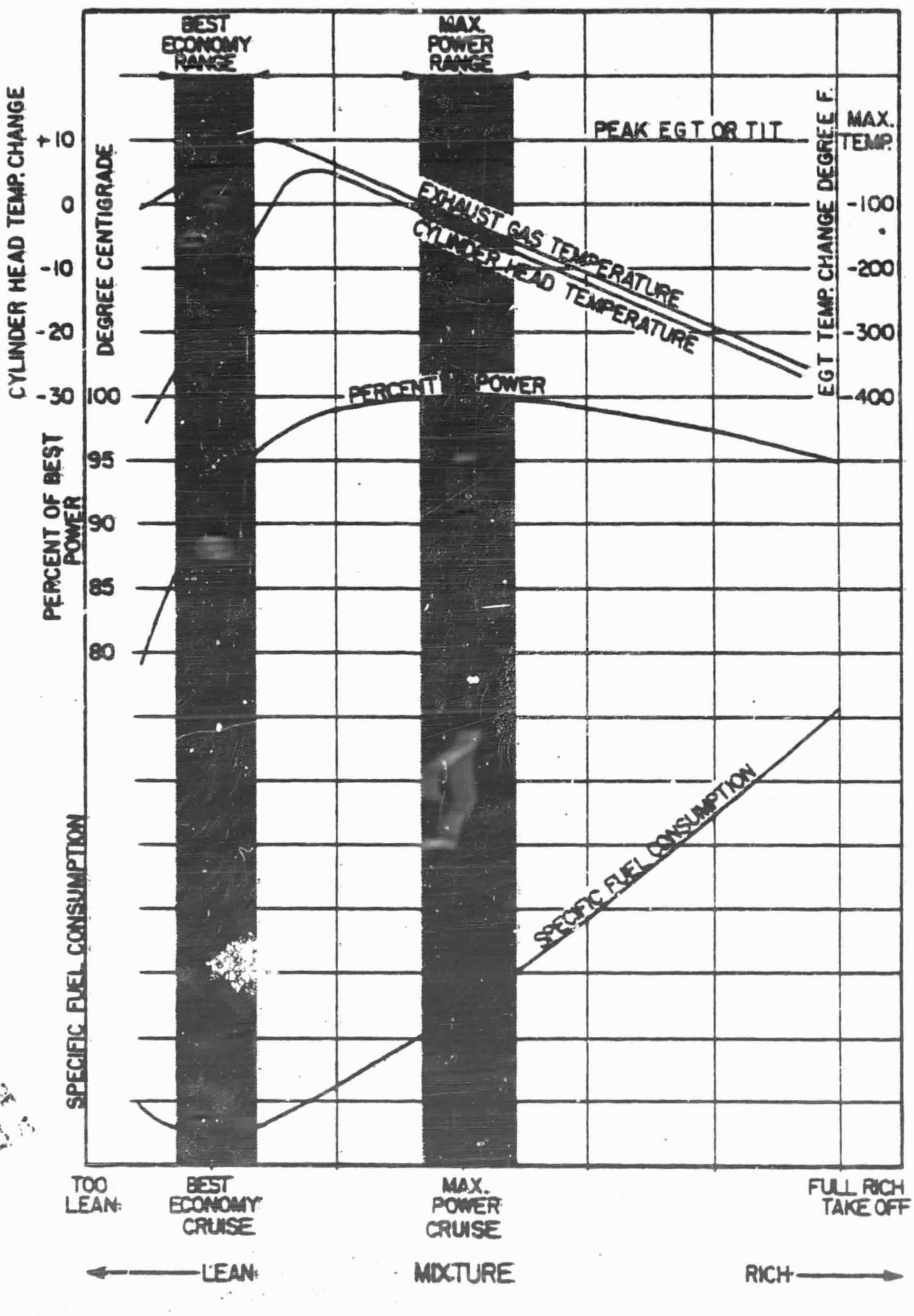

RUNS 340-341

FIG 29, MIXTURE DISTRIBUTION @ 2340 RPM, 80 KW vs FUEL FLOW

ENGINE: O-320-E2D S/N 8194X
INDUCTION AIR TEMP: 94-97°F
SPARK ADVANCE: 25° BTC
FUEL: GRADE 100LL AVIATION GASOLINE
DATE: JULY 19, 1976

Note:

1) CARB. MA-4SPA S/N A-40-20036
SETTING NO. 10-3678-32
2) STANDARD ENGINE

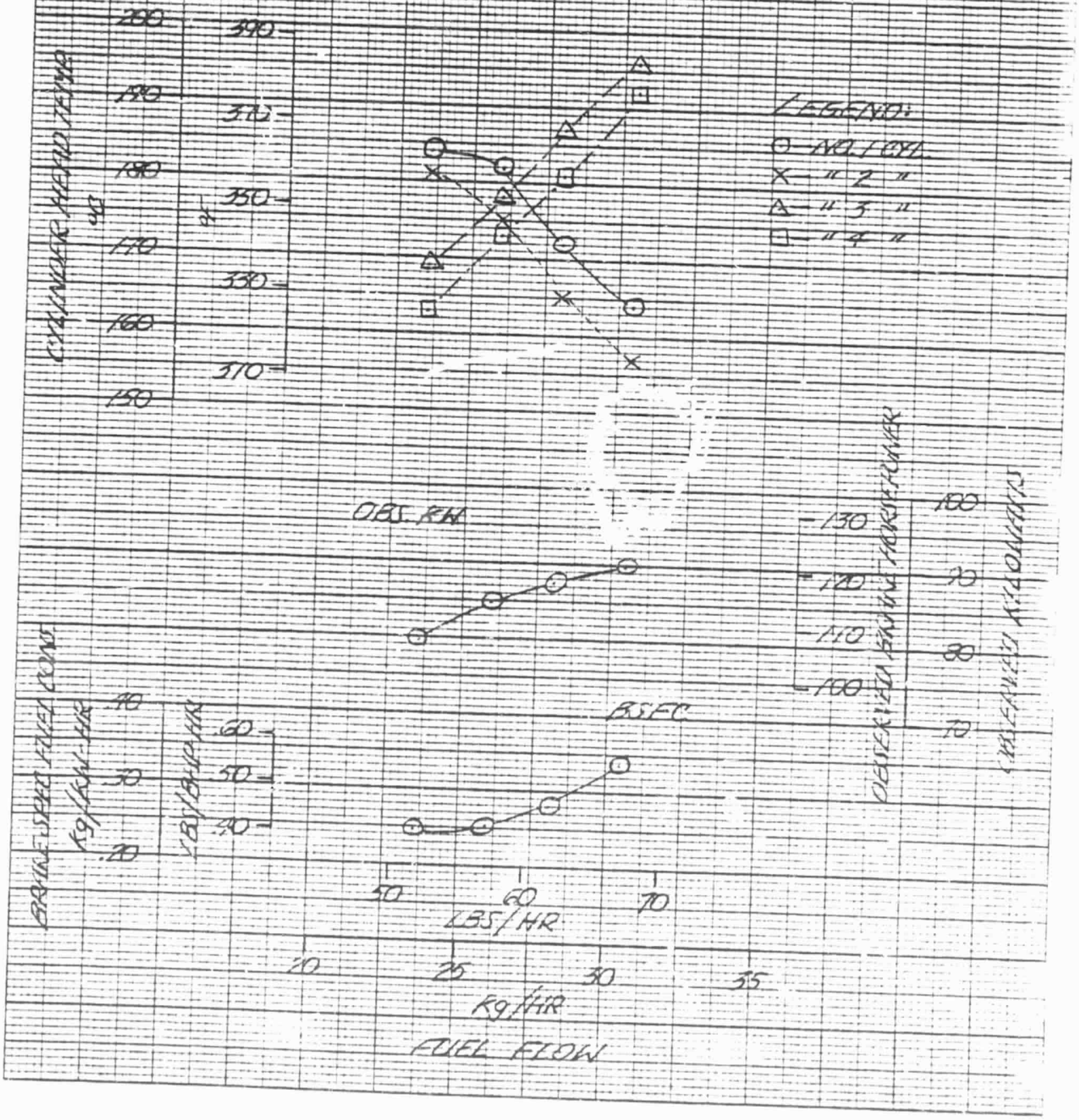

Lycoming
Avco CORPORATION

FIGURE 30

STANDARD ENGINE CONFIGURATION
AT FULL THROTTLE

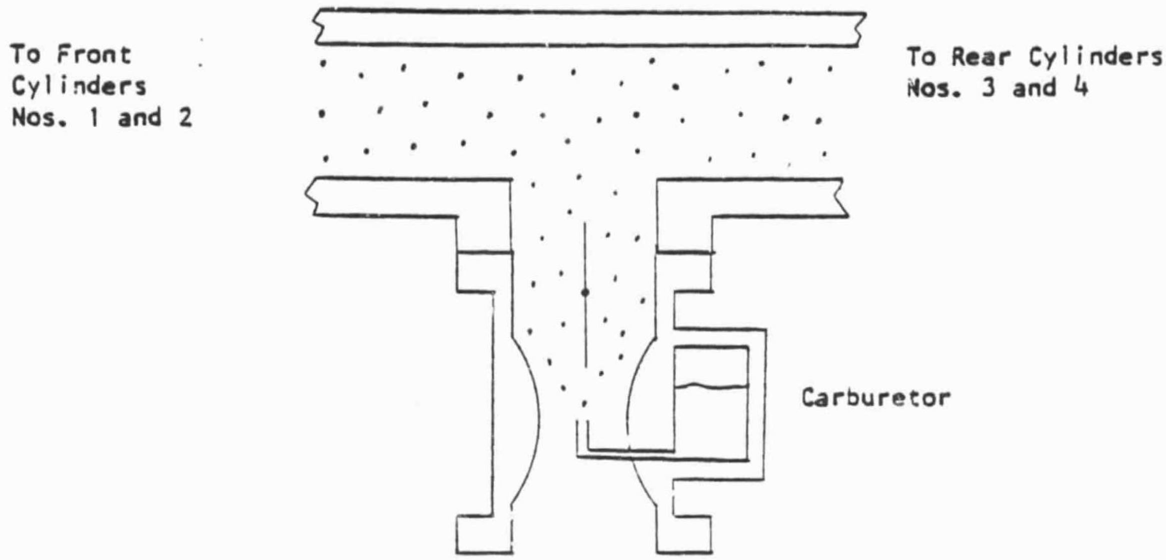

Left Side View

Dramatization of even mixture distribution

FIGURE 31

STANDARD ENGINE CONFIGURATION AT 80% POWER

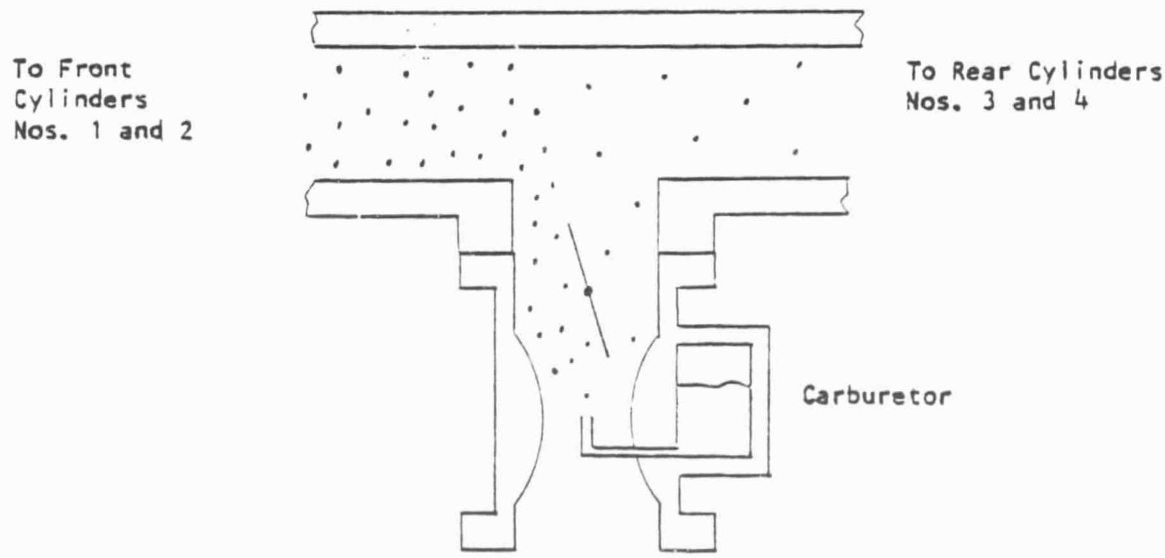

Left Side View

Dramatization of rich fuel/air mixture to the front cylinders

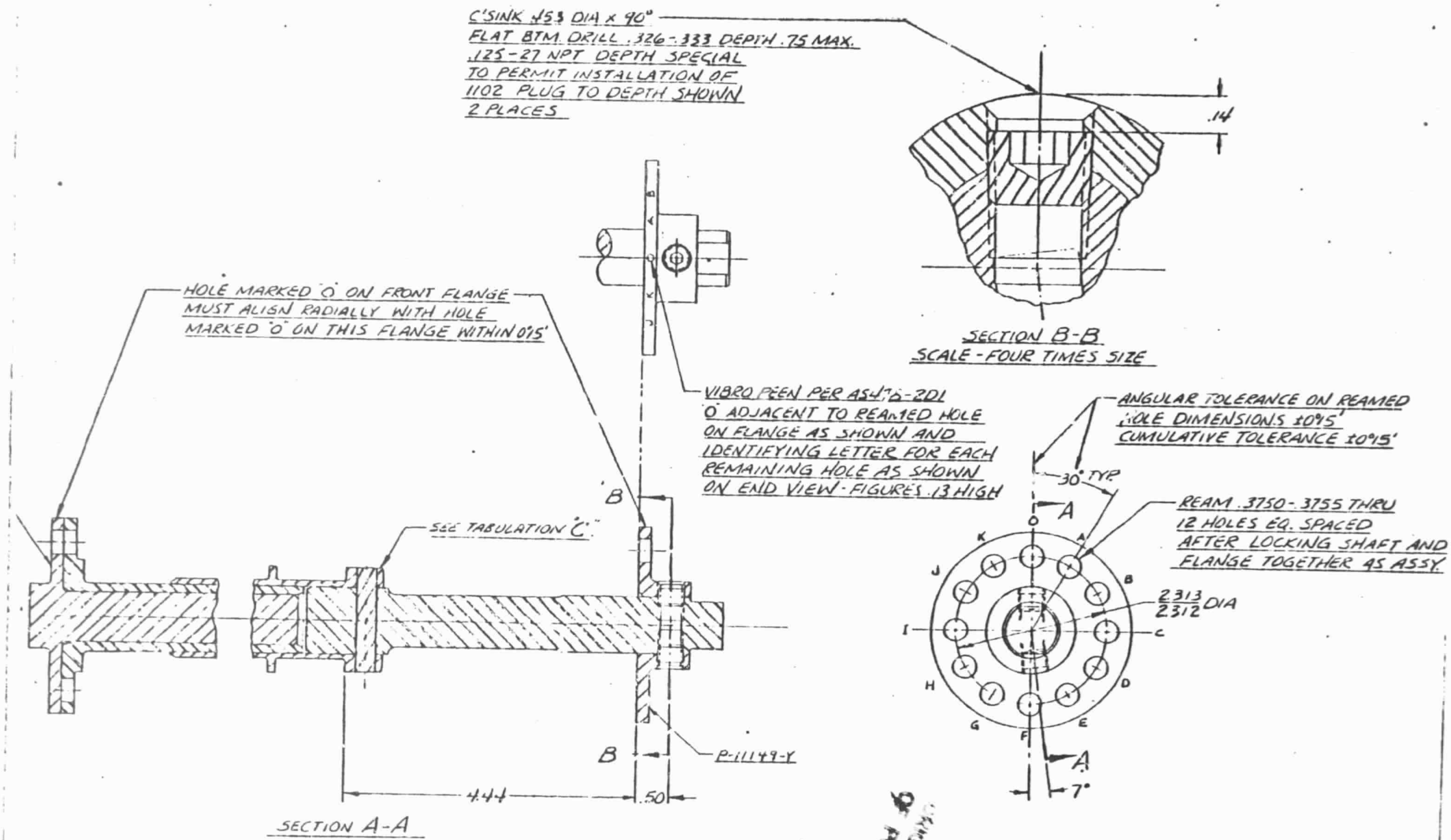

FIGURE 32 - CROSS SECTION VARIABLE TIMING CAMSHAFT

FIG. 33, VARIABLE VALVE TIMING CONFIGURATIONS

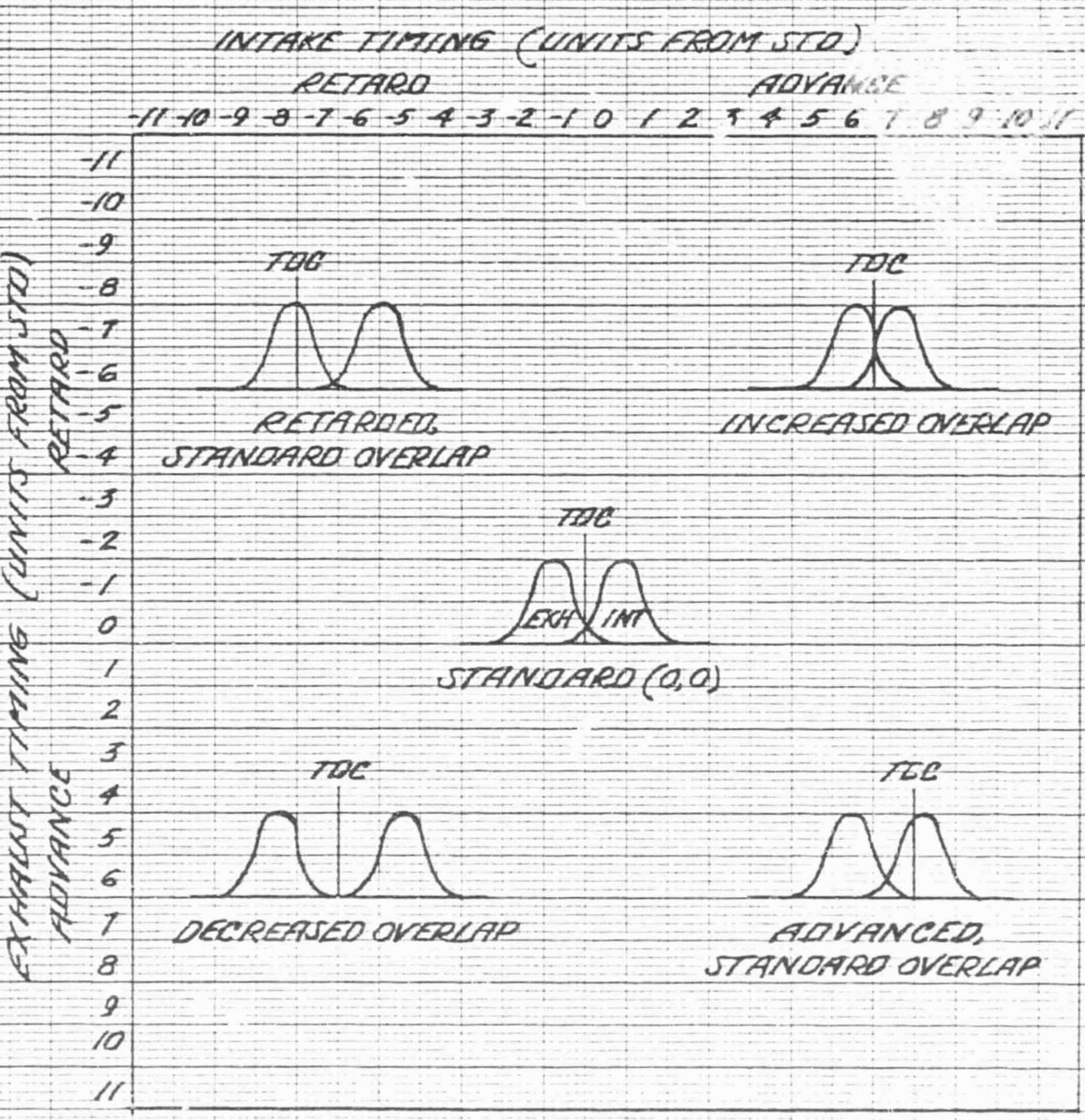

ONE TIMING UNIT = 2° 18' 28" CAMSHAFT DEG.

FIG. 33, VARIABLE VALVE TIMING CONFIGURATIONS

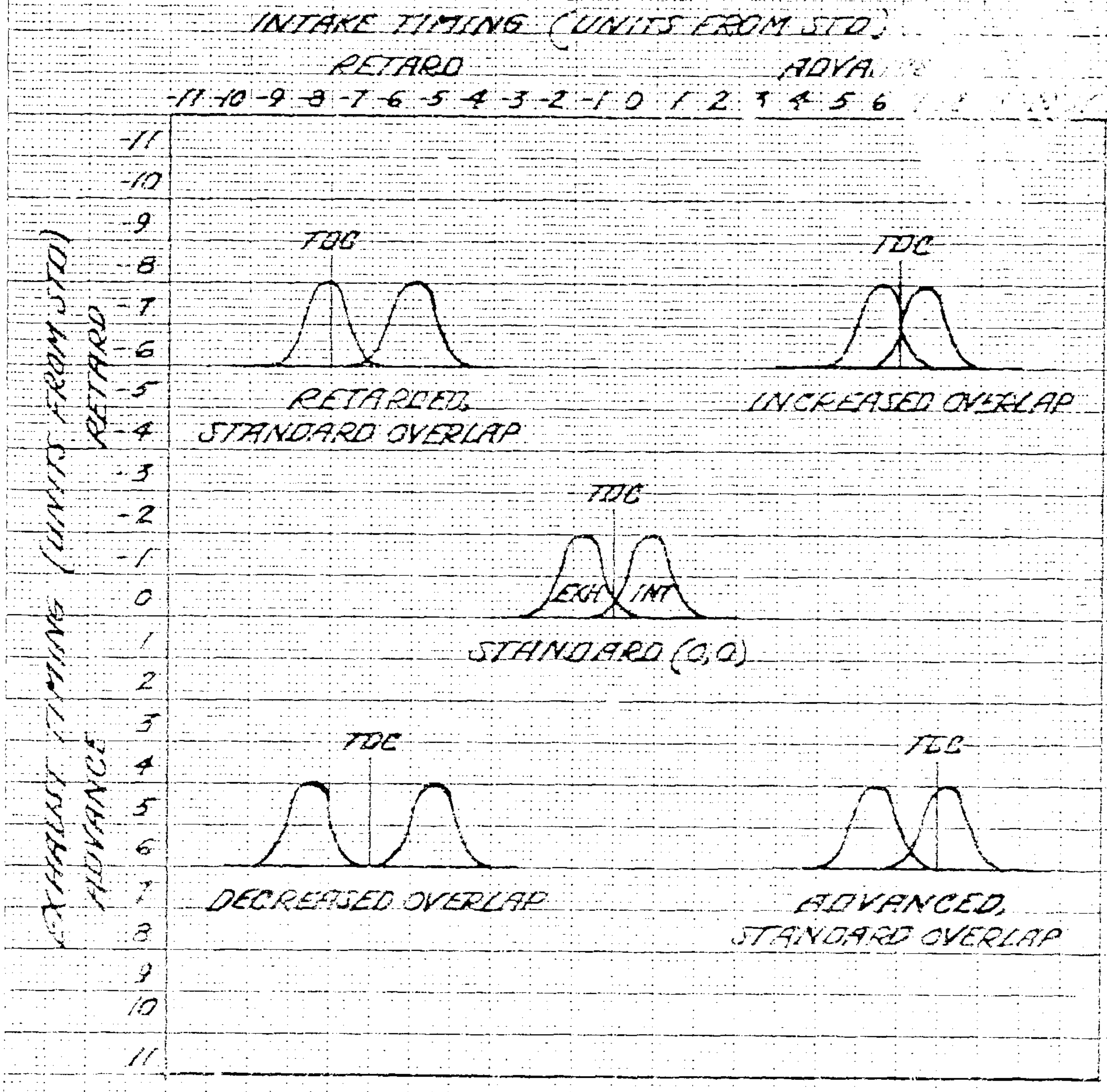

ONE TIMING UNIT = 2° 13' 28" CAMSHAFT DEG.

FIG. 34, ENGINE PERFORMANCE (CORR. KW) vs. CAMSHAFT TIMING AT 3200 RPM, FULL THROTTLE

STD. CAMSHAFT

STD. TIMING

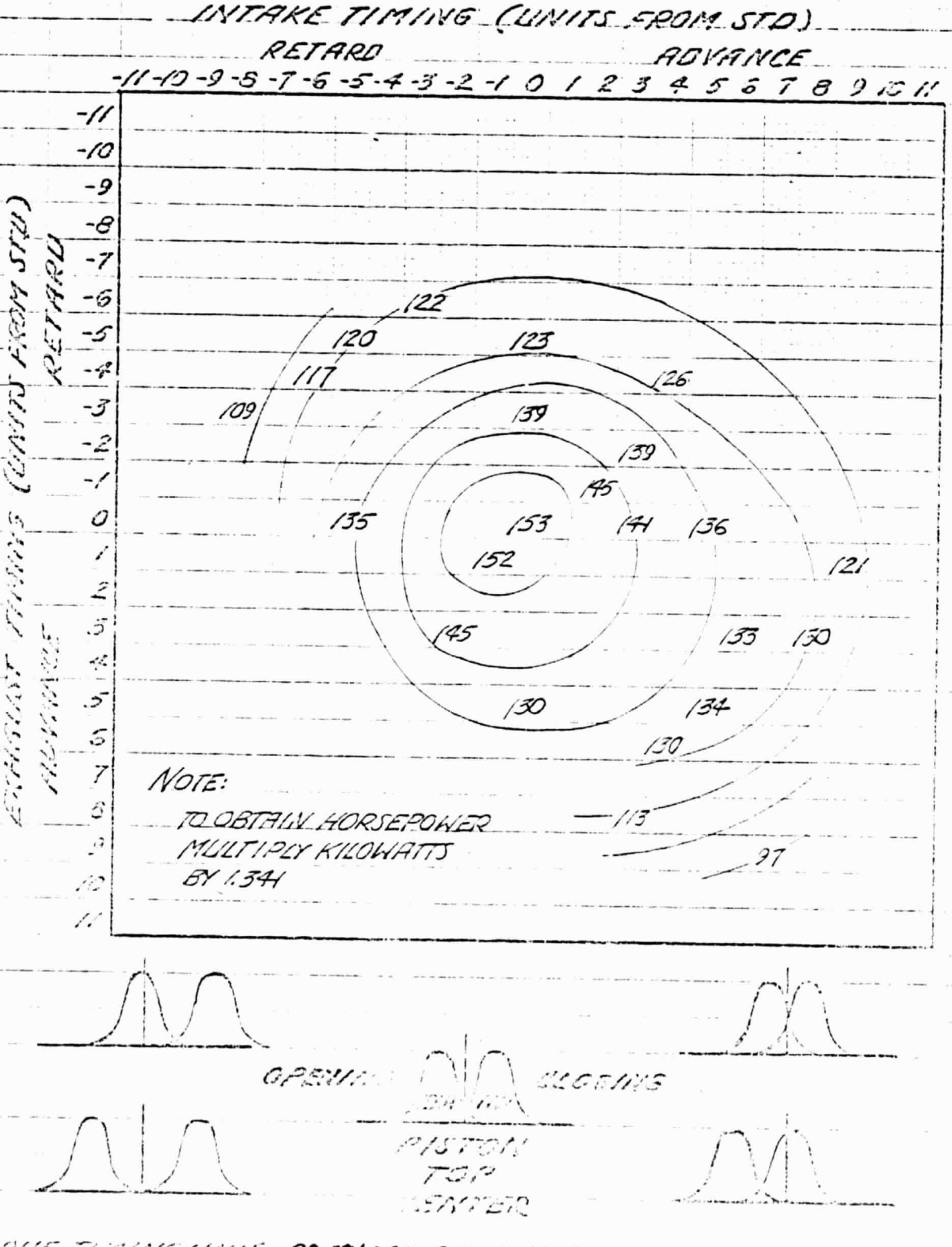

ONE TIMING UNIT = 2° 18' 28" CAMSHAFT DEG.

FIG. 34, ENGINE PERFORMANCE (CORR. KW) vs. CAMSHAFT TIMING AT 3200 RPM, FULL THROTTLE

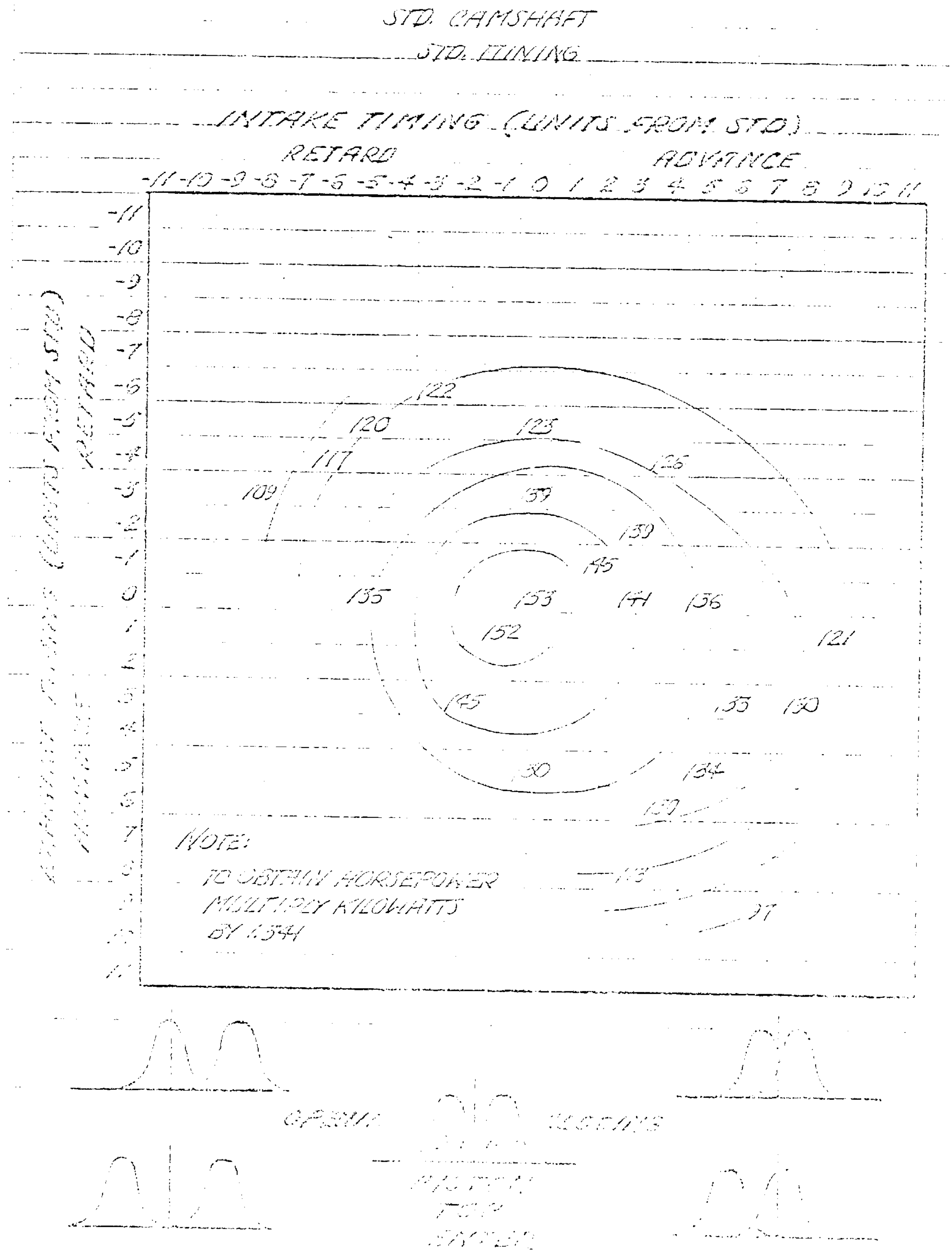

ONE [illegible] = 2° 13' 28" CAMSHAFT DEG.

FIG. 35, ENGINE PERFORMANCE (CORR KW) vs. CAMSHAFT TIMING AT 2800 RPM, FULL THROTTLE

STD. CAMSHAFT

STD TUNING

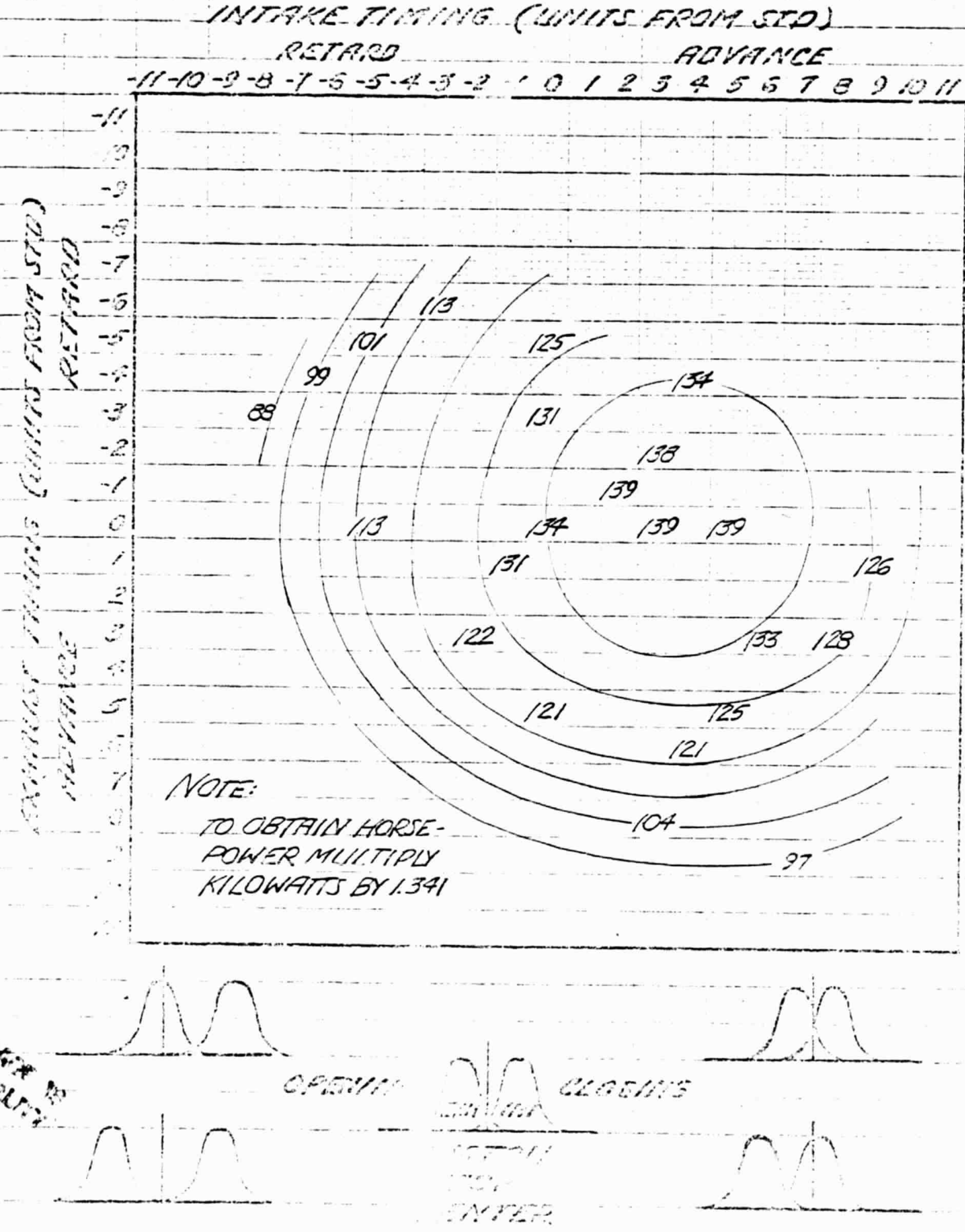

FIG. 36, ENGINE PERFORMANCE (CORR. KW) VS. CAMSHAFT TIMING AT 2400 RPM, FULL THROTTLE

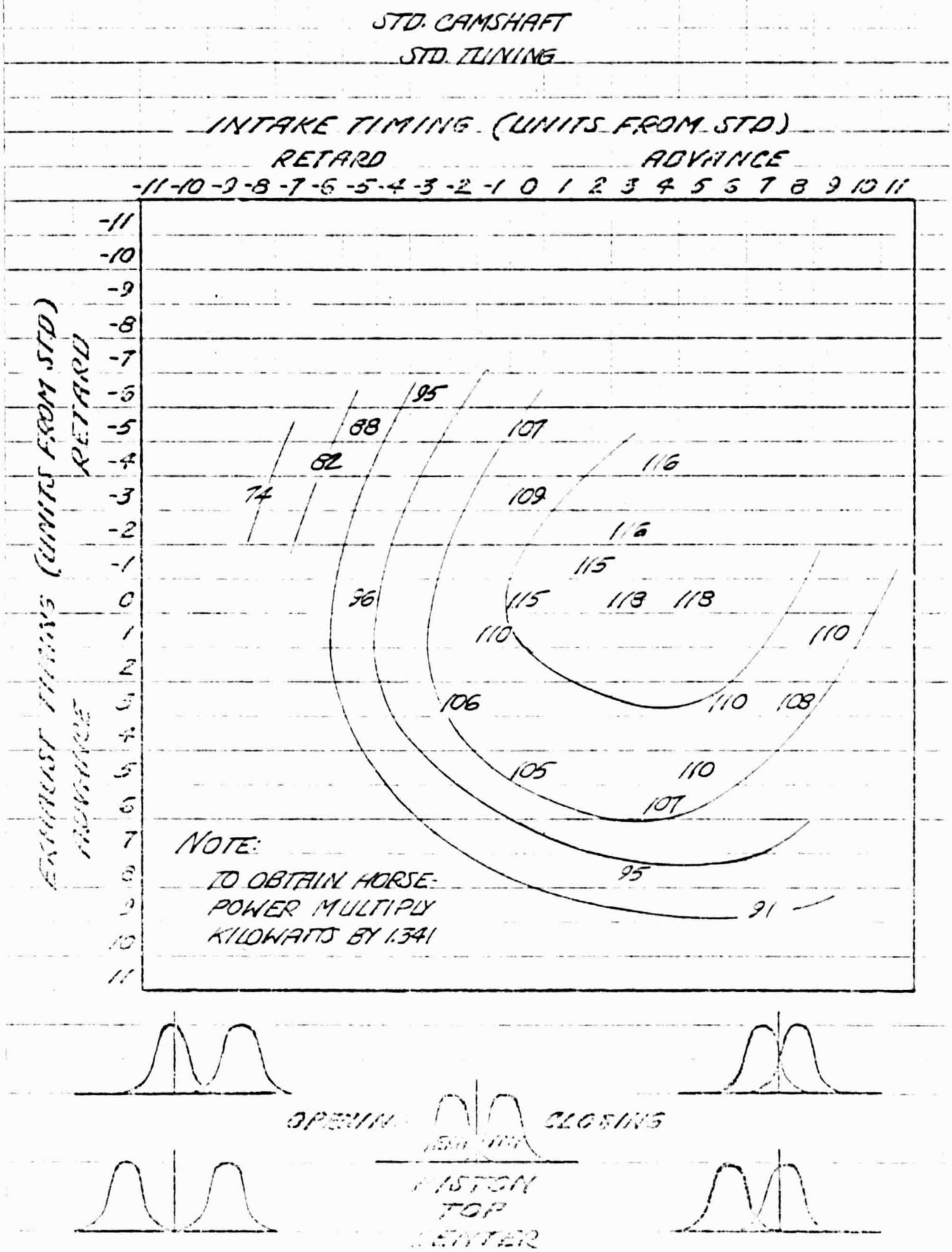

ONE TIMING UNIT = 2° 18' 28" CAMSHAFT DEG.

FIG. 37, ENGINE PERFORMANCE (CORR. kW) vs. CAMSHAFT TIMING AT 2000 RPM, FULL THROTTLE

STD. CAMSHAFT

STD. TUNING

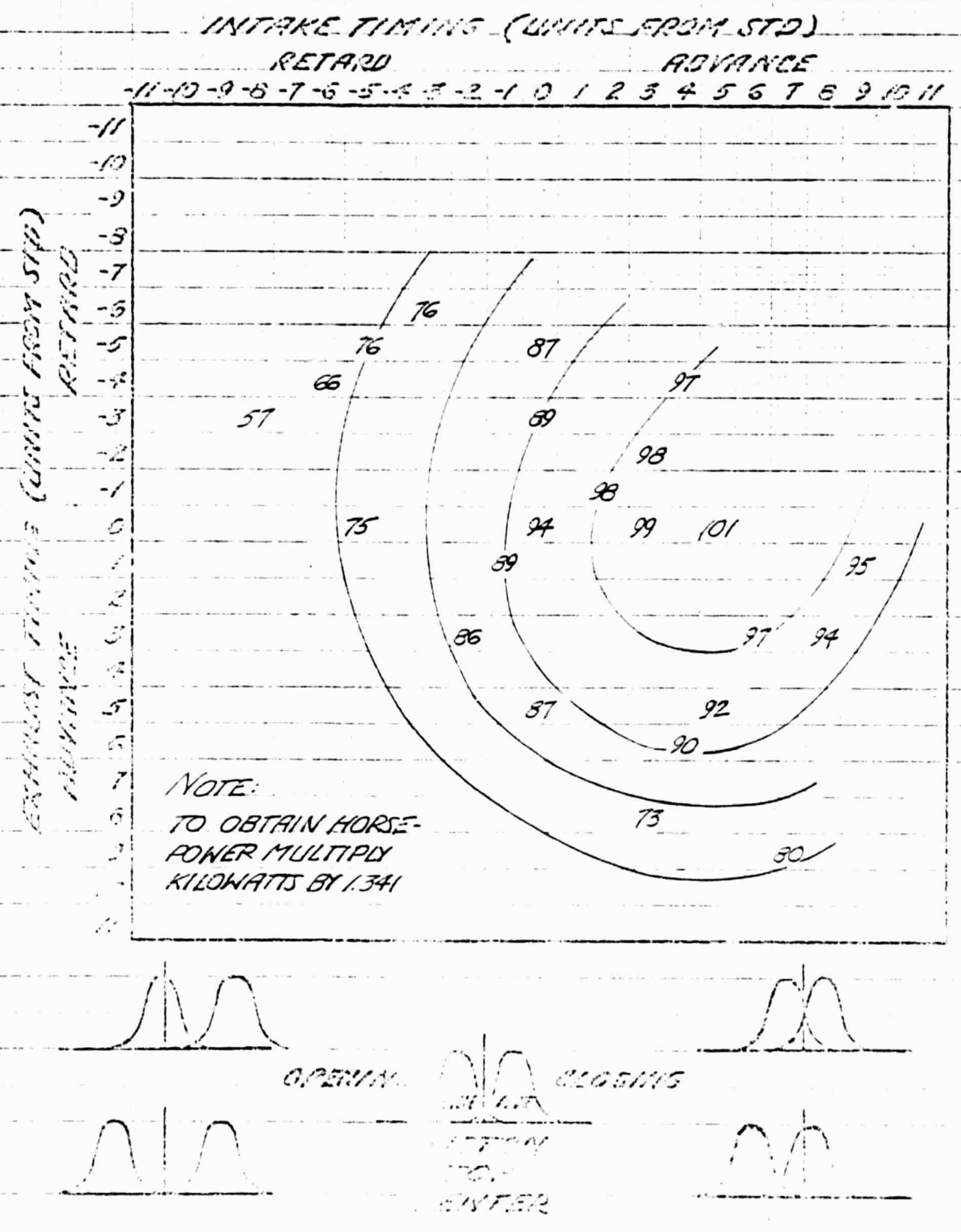

FIG. 38. ENGINE PERFORMANCE (CORR. kW) vs. CAMSHAFT TIMING AT 2800 RPM, 88 kPa MANIFOLD PRESSURE

STD. CAMSHAFT

STD. TUNING

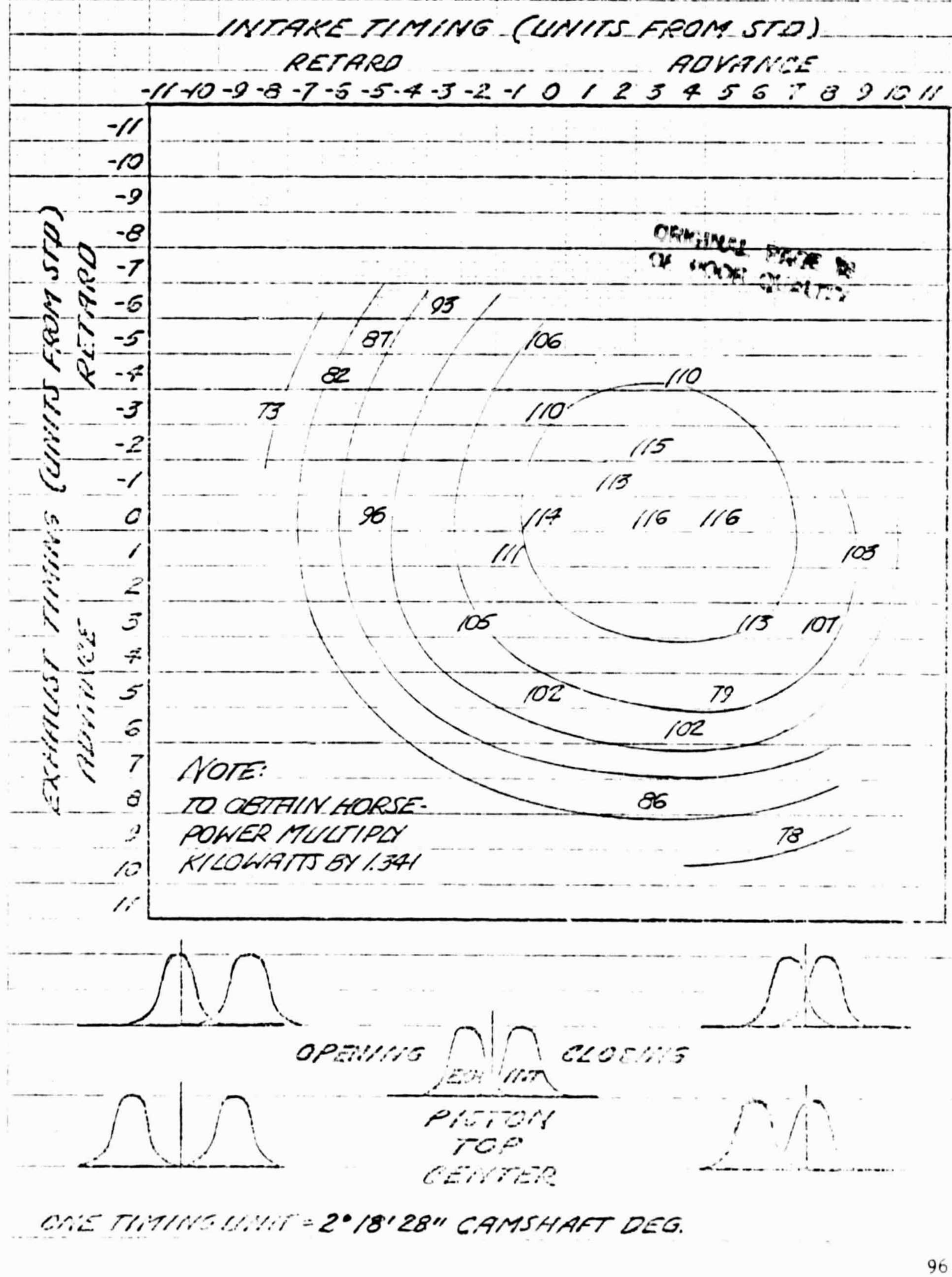

ONE TIMING UNIT = 2° 18' 28" CAMSHAFT DEG.

FIG. 39, ENGINE PERFORMANCE (CORR. kW) vs CAMSHAFT TIMING
AT 2800 RPM, 74 kPa MANIFOLD PRESSURE

STD. CAMSHAFT
STD. TUNING

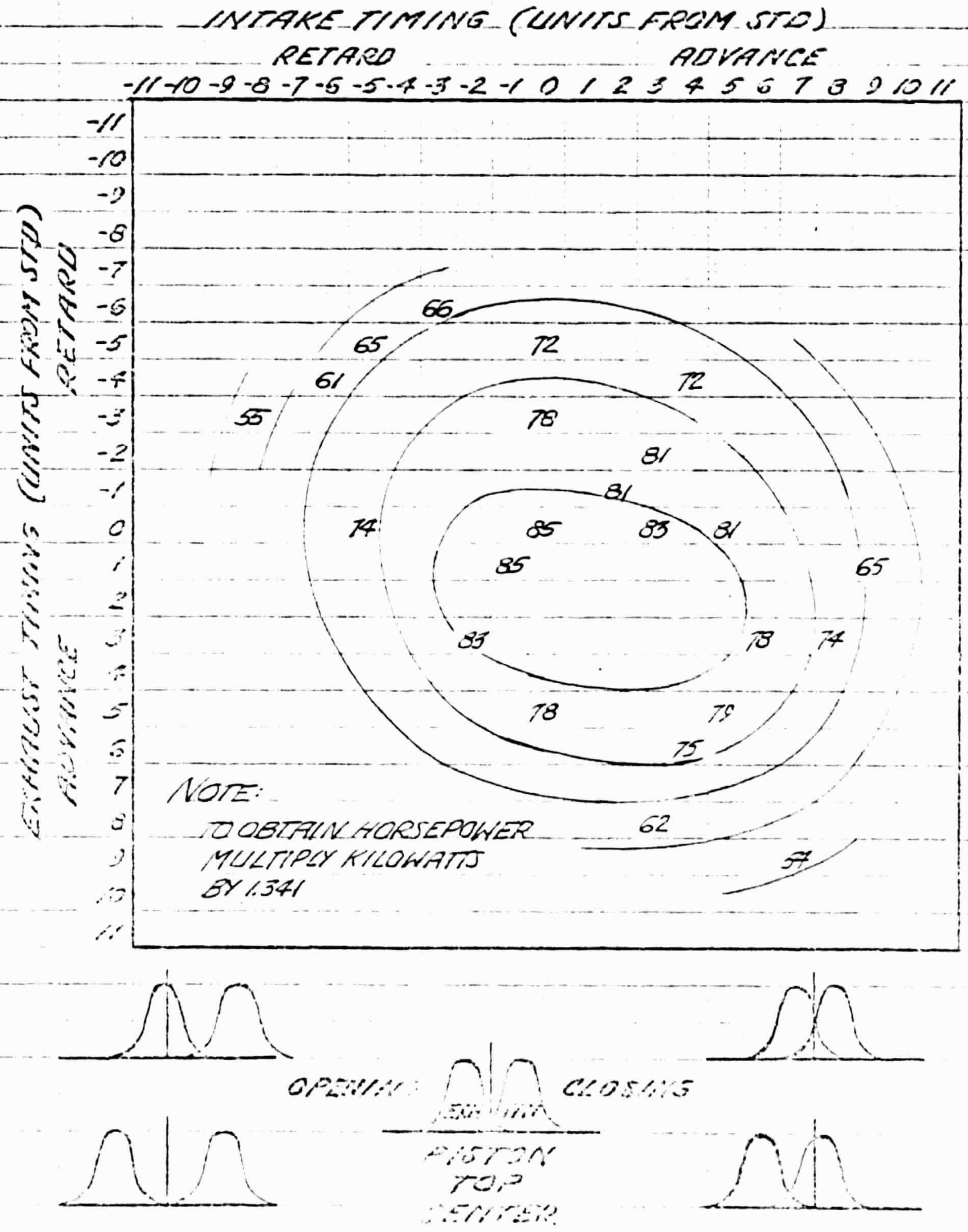

ONE TIMING UNIT = 2° 18' [illegible] CAMSHAFT DEG.

FIG. 40, ENGINE PERFORMANCE (CORR. kW) vs. CAMSHAFT TIMING
AT 2800 RPM, 61 kPa MANIFOLD PRESSURE

STD. CAMSHAFT
STD. TUNING

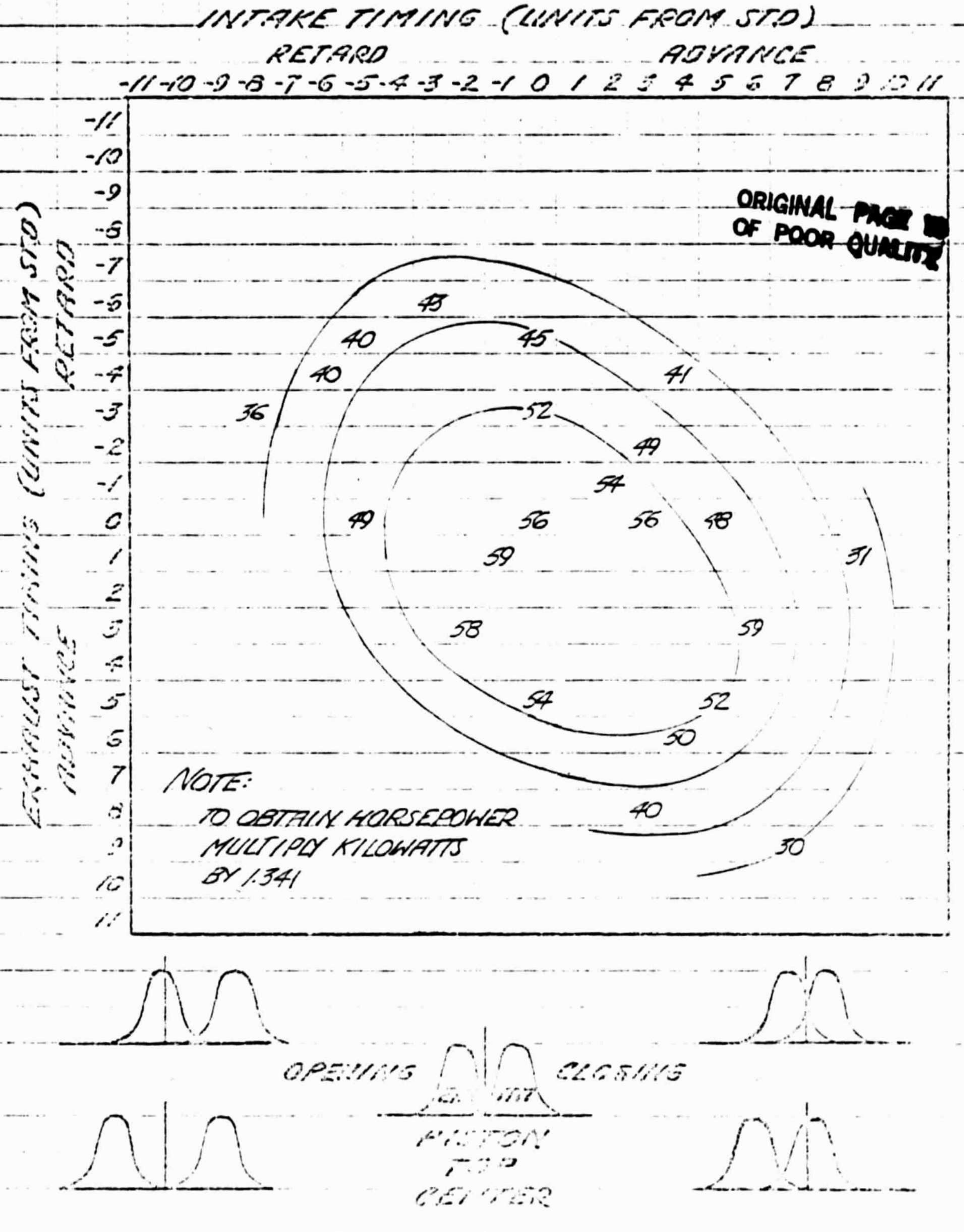

ONE TIMING UNIT = 2° 18' 28" CAMSHAFT DEG.

FIG. 41, MINIMUM BSFC vs. CAMSHAFT TIMING
AT 1500 RPM, 51 kPa MANIFOLD PRESSURE
STD. CAMSHAFT, STD. TIMING

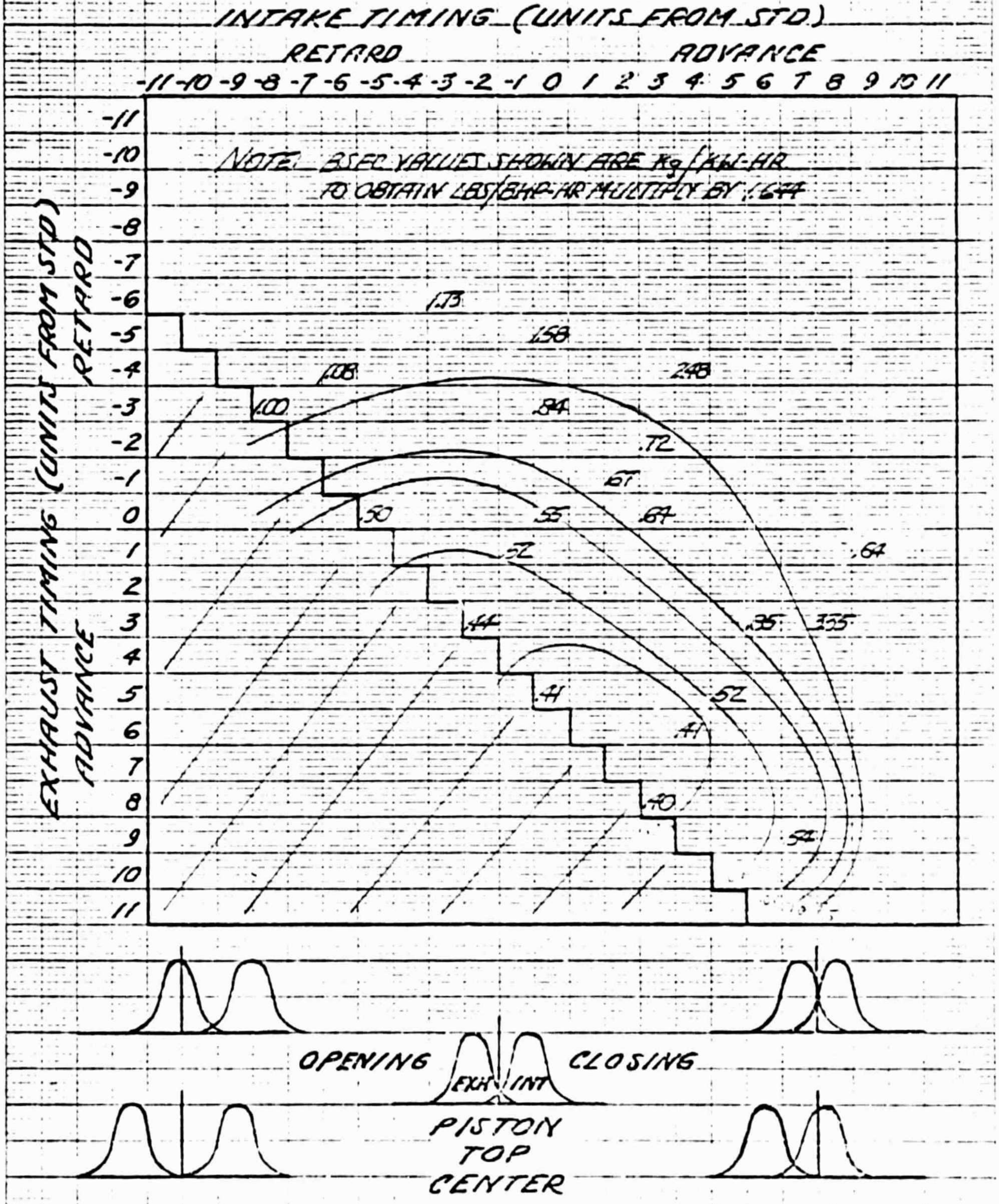

ONE TIMING UNIT = 2° 18' 28" CAMSHAFT DEG.

FIG 42, MINIMUM BSFC vs CAMSHAFT TIMING
AT 1500 RPM, 51 kPa MANIFOLD PRESSURE

8° LONGER DURATION CAMSHAFT

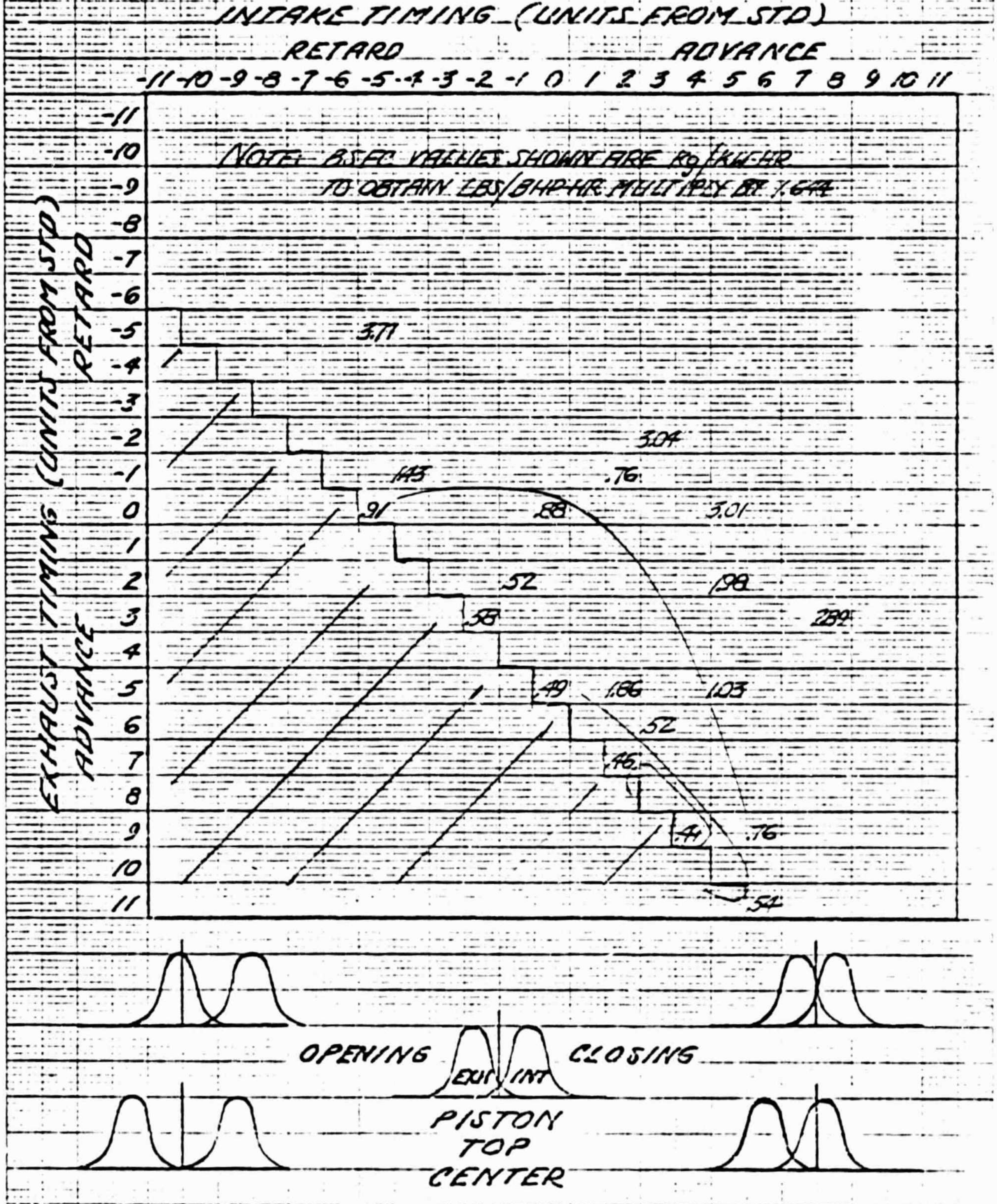

ONE TIMING UNIT = 2° 18' 28" CAMSHAFT DEG.

FIG. 43, MINIMUM BSFC vs. CAMSHAFT TIMING
AT 1500 RPM, 51kPa MANIFOLD PRESSURE
30° SHORTER DURATION CAMSHAFT

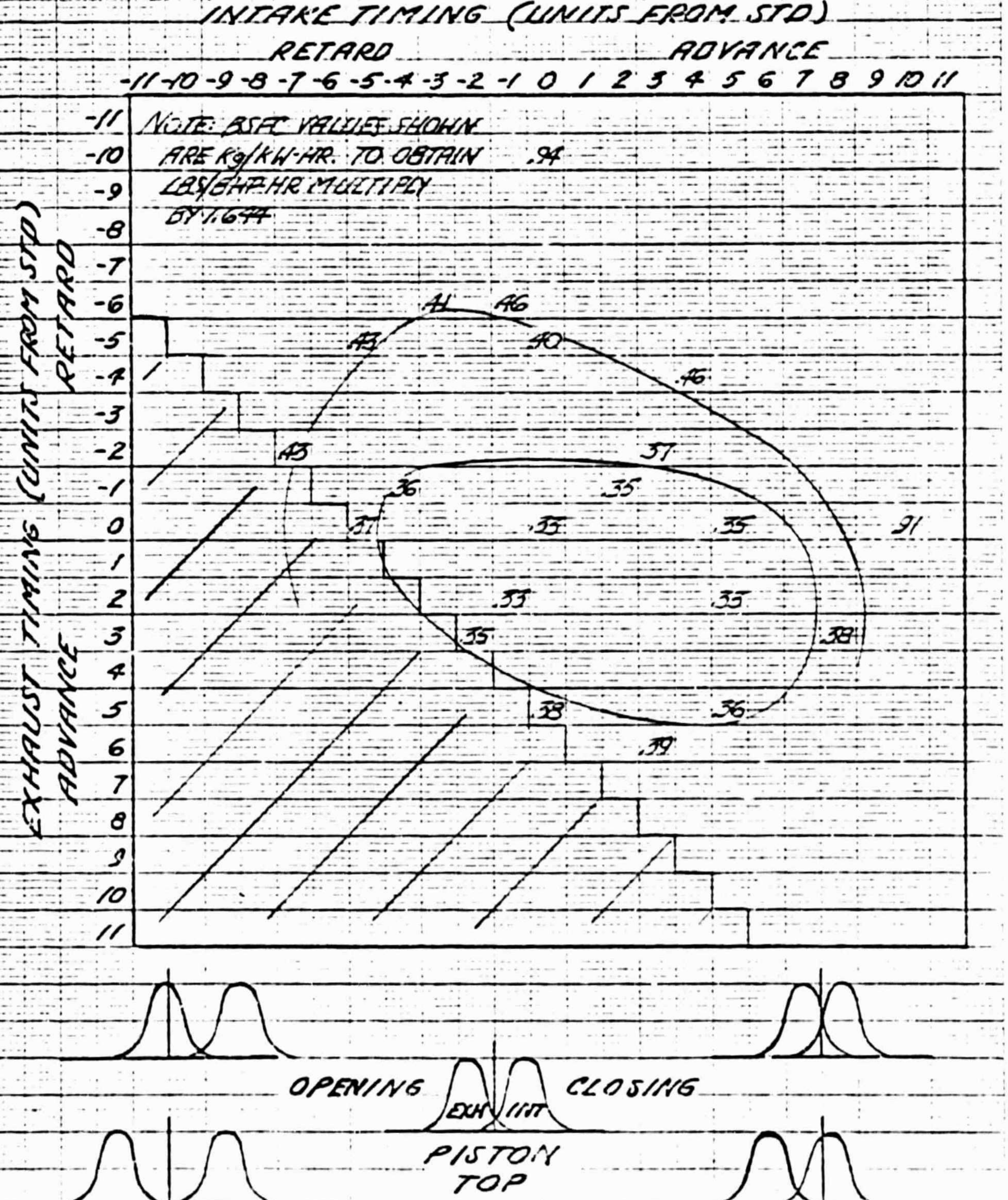

ONE TIMING UNIT = 2° 18' 28" CAMSHAFT DEG.

RUNS: ⊙29-35, ×2493-2499, △2708-2714
M.P. RUNS: ⊙93-99, △2308-2314

FIG. 44 - FULL THROTTLE PERFORMANCE vs ENGINE SPEED

ENGINE: IO-360-SPL S/N 959-X
DATE: OCT. 22, 1976; MAY 26 & 28, 1978

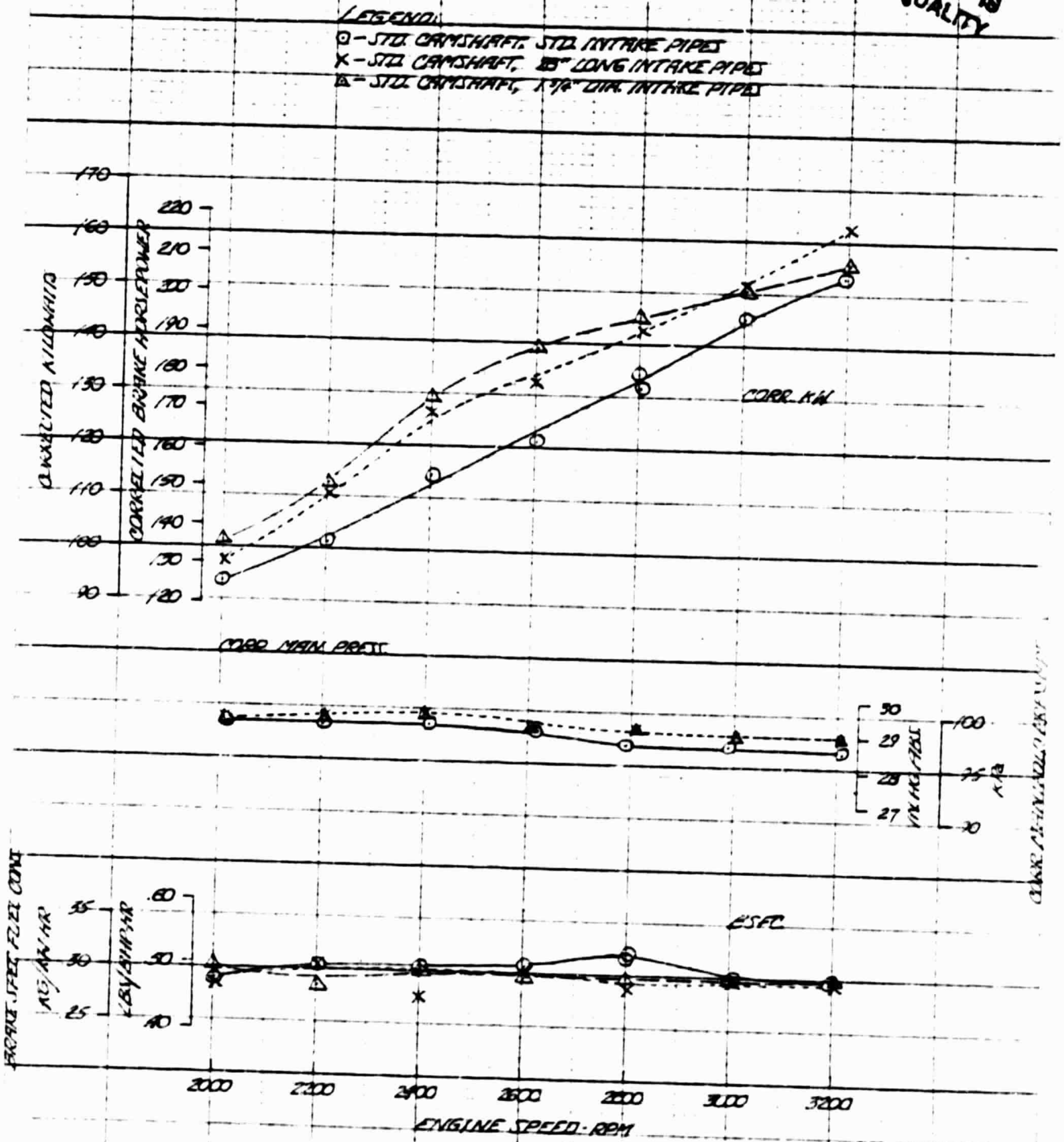

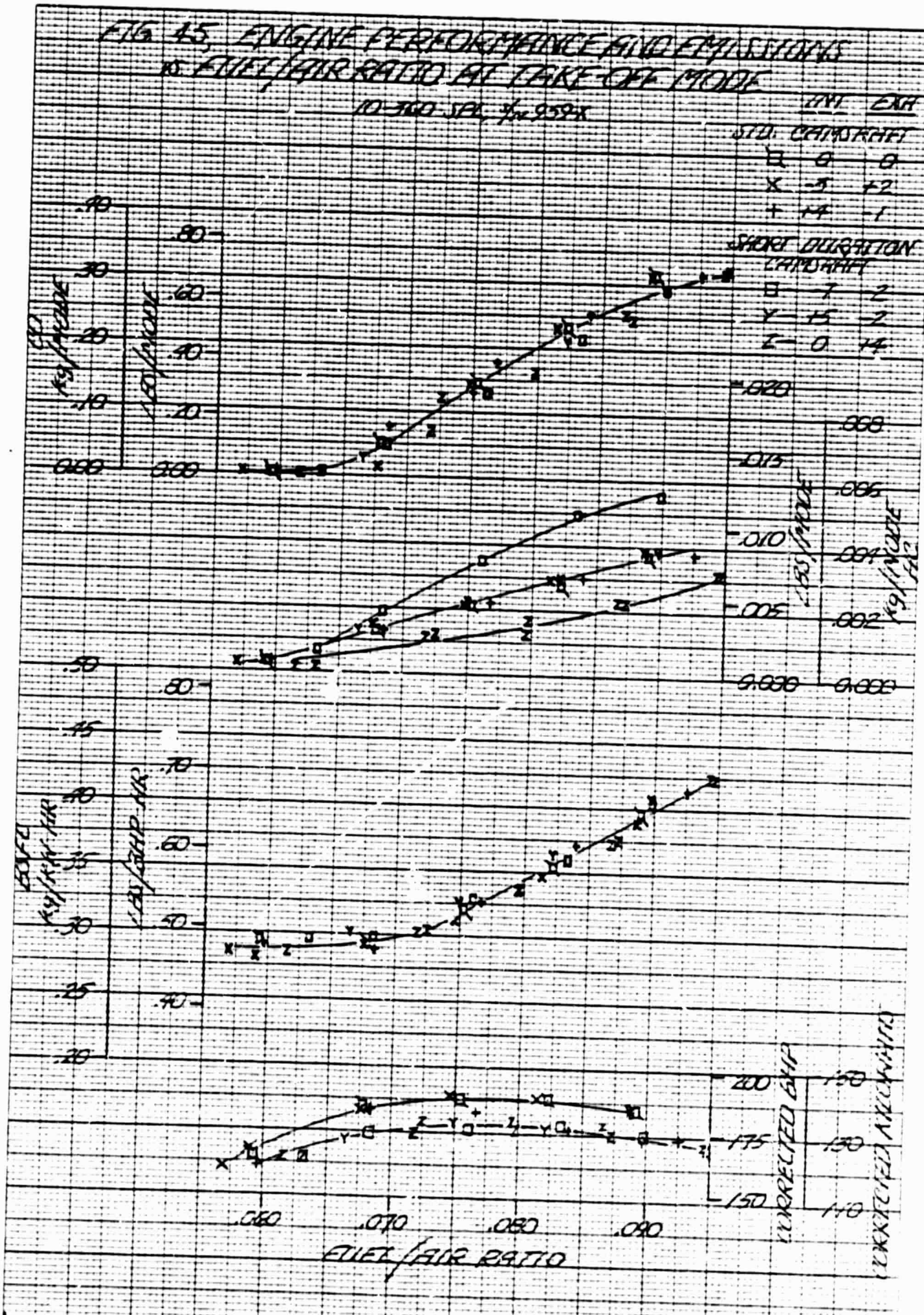
FIG. 45, ENGINE PERFORMANCE AND EMISSIONS
vs FUEL/AIR RATIO AT TAKE-OFF MODE
IO-360 SBL S/N 9594
INT. EXH
STD. CAMSHAFT
□ 0 0
X -5 +2
+ +4 -1
SHORT DURATION CAMSHAFT
□ -7 -2
Y +5 -2
Z 0 +4
CO KG/MODE
LBS/MODE
LBS/MODE
KG/MODE HC
BSFC KG/KW HR
LB/BHP HR
CORRECTED BHP
CORRECTED KILOWATTS
FUEL/AIR RATIO
.060
.070
.080
.090

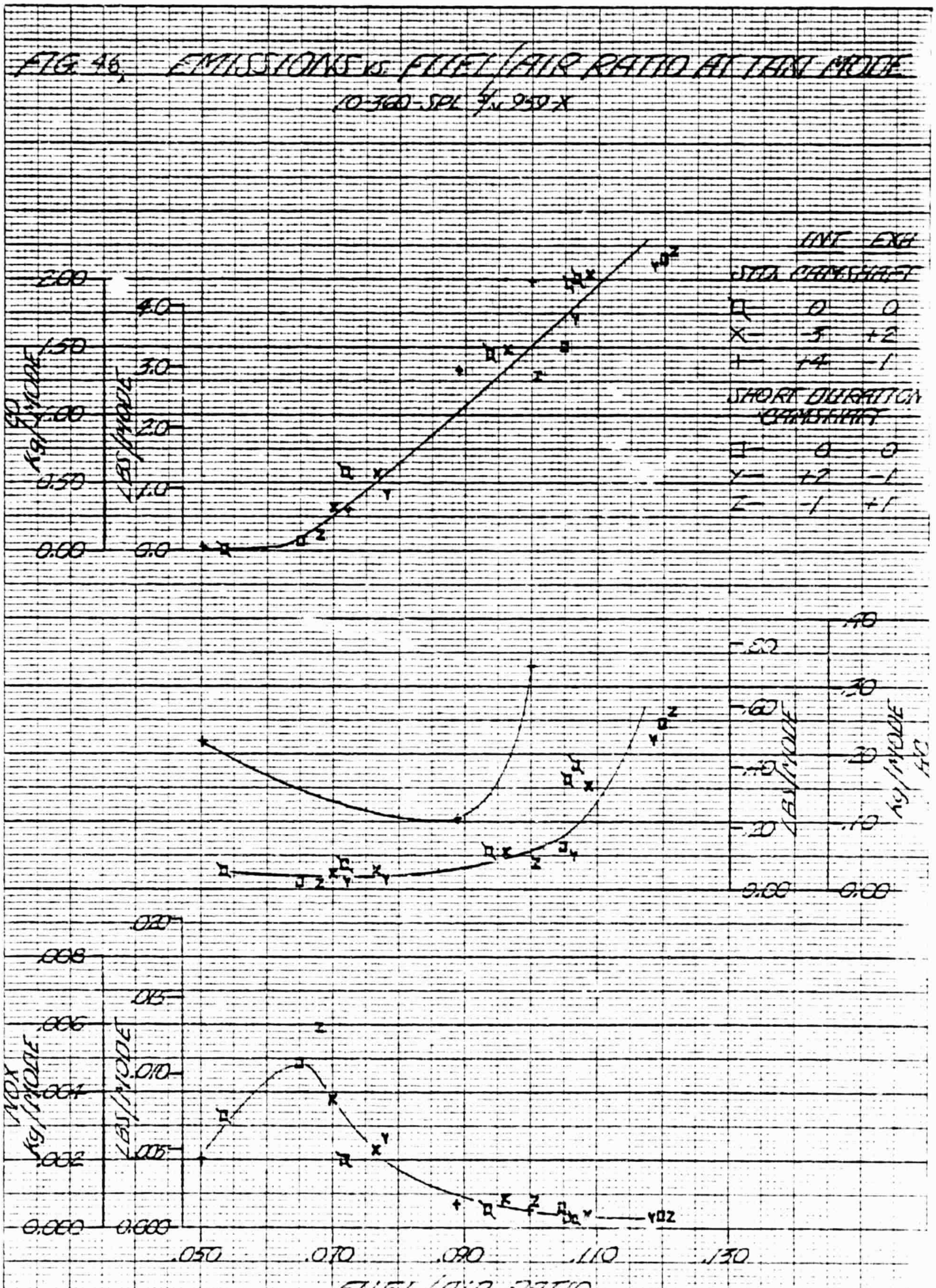
FIG. 46, EMISSIONS vs. FUEL/AIR RATIO AT TAXI MODE
IO-360-SPL S/N 959-X
CO
Kg/MODE
LBS/MODE
INT EXH
STD. CAMSHAFT
□ 0 0
X -3 +2
+ +4 -1
SHORT DURATION CAMSHAFT
□ 0 0
Y +2 -1
Z -1 +1
LBS/MODE
Kg/MODE
HC
NOX
Kg/MODE
LBS/MODE
.050
.070
.090
.110
.130
FUEL/AIR RATIO

FIGURE 47 - PISTON ENGINE VALVE SEQUENCING

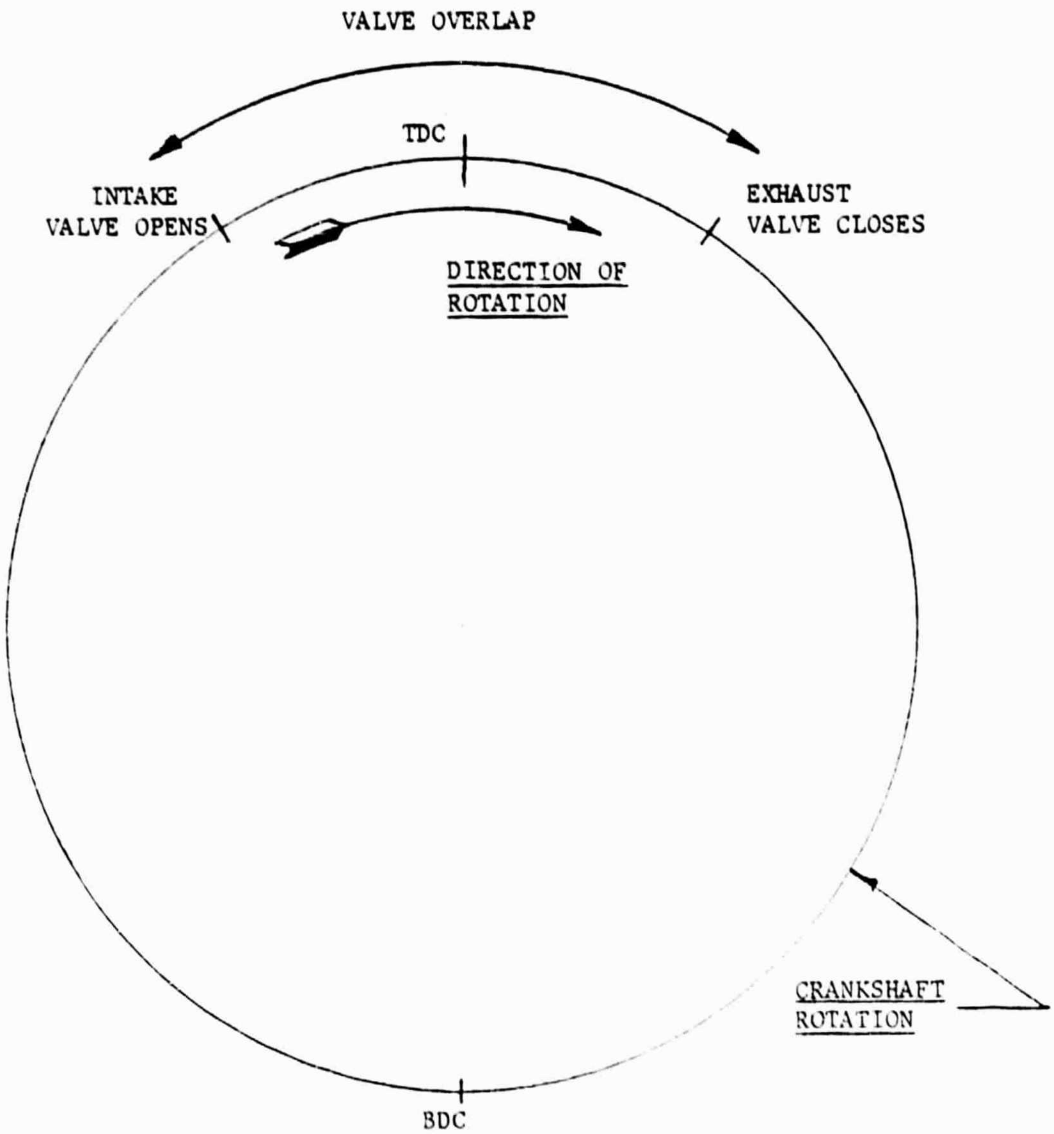

FIGURE 48 - BEST POWER VALVE TIMING